ELECTROCHEMICAL INVESTIGATIONS IN SUPERCRITICAL FLUIDS AND OTHER NON-POLAR MEDIA

John Harper

University of Leicester
Leicester
England
LE1 7RH

Sept. 1998

This thesis is submitted for the degree of

Doctor of Philosophy

ProQuest LLC
789 East Eisenhower Parkway
P.O. Box 1346
Ann Arbor, MI 48106-1346

ELECTROCHEMICAL INVESTIGATIONS IN SUPERCRITICAL FLUIDS AND OTHER NON-POLAR MEDIA

JOHN HARPER
UNIVERSITY OF LEICESTER
1998

ABSTRACT

This thesis describes the use of novel electrolytes in media of extremely low relative permittivity. Double layer capacitance, conductivity and voltammetric experiments are presented and attempts are made to elucidate the ionic entities in solution and at the electrode / solution interface. Charge is found to be predominantly carried by triple ions and these have a surprisingly appreciable influence on the double layer structure.
Voltammetric responses are presented in dichloroethane (DCE), anisole (Anis) and cyclohexane (cHex) and it is shown that the reversibility of a process is affected by the length of the tetraalkylammonium chain of the electrolyte. Reversible responses are only observed at very slow sweep rates and this is a result of the slow electrode desorption kinetics of the electrolyte ions. This has profound consequences for electrochemical studies made in non-aqueous media using quaternary ammonium electrolytes.
Finally, bulk electrolysis experiments are performed in $scCO_2$/water mixtures. It is shown that formate and hydrogen are primarily formed on a platinum surface, whereas oxalate and hydrogen are the major products on lead. This is ascribed to a change in reaction pathway compared to such studies in aqueous media. Supercritical fluids are shown to have significant advantages over liquid solvents for the electrochemical reduction of CO_2.

Acknowledgements

I would like to begin by thanking my supervisor Dr. Andrew Abbott. His support and enthusiasm over the years has made sure that this work was completed in good time. I sincerely wish him great success in the future for which his work deserves.

Many thanks to Chris Eardley who provided many interesting discussions on the general subject area and on other important matters such as the premiership results at the weekend. A big thankyou to Gill Lonergan who not only thrashed me at fantasy football, but was always willing to make cups of tea with plenty of sugar when the high-pressure cell exploded (on several occasions).

I would also like to thank all those people who have analysed chemicals and built the apparatus for me. I would particularly like to acknowledge Keith Wilkinson and John Weale who would build and repair anything at a very short notice. Thanks also to Mick Lee who demonstrated the HPLC analysis.

I cannot finish without thanking all those at Keble Road and anyone else who has lived with me these past three years. Thanks to Raul for his incessant jungle drumming, Dean for having the same affliction as myself (originating from the South West!), Liam for not playing any tricks on me and helping with all the computer stuff and Chris for not knowing the meaning of the word 'prompt'! Also, the gang from 21, Dan, Nat and John who provided all of the tacky videos, G&T's and somewhere to escape to during the final months! Mr (soon to be Doctor) O'Beirne deserves special attention because he blocked my computer account with leviathan e-mails of no importance (and he still listens to 80's Rock music). A big thankyou must go to Louise for simply being so like-minded!

Finally I'd like to thank my parents who've supported me throughout my university life.

" Scientists have proof without certainty. Creationists have certainty without any proof"

Ashley Montague

CONTENTS

	Page
CHAPTER I INTRODUCTION	1
1.1 Introduction	2
1.2 Supercritical Fluids	2
1.3 Electrochemistry in Non Polar Media	7
1.4 Electrochemistry in Supercritical Fluids	11
CHAPTER II EXPERIMENTAL	17
2.1 Materials	18
2.1.1 Electrolytes	18
2.1.2 Solvents	18
2.1.3 Preparation of complexes	19
2.2 Instrumentation	20
2.2.1 High Pressure Apparatus	20
2.2.2 High Pressure Bulk Electrolysis	22
2.2.3 Viscosity and Density Measurements	23
2.2.4 NMR and Crystallographic Methods	23
2.3 Electrochemical Methods	23
2.3.1 Linear Sweep Voltammetry	23
2.3.2 Microelectrodes	24
2.3.3 Capacitance Measurements	25
CHAPTER III ION ASSOCIATION AND MOBILITY	28
3.1 Introduction	29
3.1.1 Ion Association	29
3.1.2 Triple Ion Formation	30
3.1.3 Conductivity in Supercritical Fluids	33
3.2 Results and Discussion	36
3.2.1 Conductivity Measurements in Liquid Media	36
3.2.2 Conductivity Measurements in Supercritical Carbon Dioxide	57
3.2.3 Conclusions	66

CHAPTER IV ELECTROCHEMICAL INVESTIGATIONS IN SUPERCRITICAL CARBON DIOXIDE AND OTHER NON POLAR MEDIA 70

4.1 Introduction 71
4.1.1 The Metal Solution Interface 71
4.1.2 Methods of Double Layer Capacitance Measurements 75

4.2 Results and Discussion 80
4.2.1 Double Layer Capacitance Measurements in Non Polar Media 80
4.2.2 Voltammetry in Dichloroethane and Anisole 94
4.2.3 Voltammetry in Cyclohexane 99
4.2.4 Voltammetry in Supercritical Carbon Dioxide 103

4.3 Conclusions 105

CHAPTER V ELECTROCHEMICAL REDUCTION OF CARBON DIOXIDE IN SUPERCRITICAL FLUIDS 108

5.1 Introduction 109
5.1.1 Electrochemical Reduction of CO_2 109
5.1.2 Mechanism of CO_2 Reduction 112
5.1.3 Reduction of CO_2 at Elevated Temperatures and Pressures 113

5.2 Results and Discussion 116
5.2.1 Voltammetry 116
5.2.2 Bulk Electrolysis of Supercritical CO_2/H_2O Mixtures 121

5.3 Conclusions 122

CHAPTER VI SUMMARY AND FUTURE WORK 127

6.1 Summary 128
6.1.1 Conductivity 128
6.1.2 Double Layer Structure and Electrochemistry 129
6.1.3 Electrochemical Reduction of Carbon Dioxide 130

6.2 Future Work 131
6.2.1 Electrical Double Layer and Electrochemistry 131
6.2.2 Electrolysis 131

Appendix 133
X-ray data 133
NMR data 134

CHAPTER I

INTRODUCTION

1.1 Introduction

1.2 Supercritical Fluids

1.3 Electrochemistry in Supercritical Fluids

1.4 Electrochemistry in Non Polar Media

1.1 Introduction

The solvent often affects the kinetics, rate of mass transport and mechanism of an electrochemical reaction but its contribution to the process is often ignored.

The ideal properties of a solvent include

i) high conductivity by dissolution of inert supporting electrolyte

ii) low viscosity and hence high mass transport

iii) high electrochemical stability

iv) cheap and non-toxic

Supercritical carbon dioxide fulfills many of the criteria for an ideal solvent. It is the aim of this work to investigate electrochemical processes in supercritical carbon dioxide and other non-polar media and elucidate the effects of the solvent and electrolyte on electron transfer.

1.2 Supercritical Fluids

Above a certain critical temperature (T_c) and pressure (p_c), a supercritical fluid is formed.[1] Figure (1.1.1) shows the phase diagram of CO_2 [2] with the critical region shaded. The conditions for supercritical CO_2 are relatively mild (T_c = 31.4 °C, p_c = 72.3 bar).[3]

With the current environmental legislation, industry is seeking clean media for process control and synthetic reactions. Supercritical fluids offer potentially the best solution to this problem because they are often cheap and non-toxic. In this respect solvents like water and carbon dioxide have received by far the most attention.

There are other fundamental advantages of supercritical fluids that arise because they have properties of both liquids and gases. The motives for carrying out reactions in these media include the control of phase behavior, enhanced mass transport and

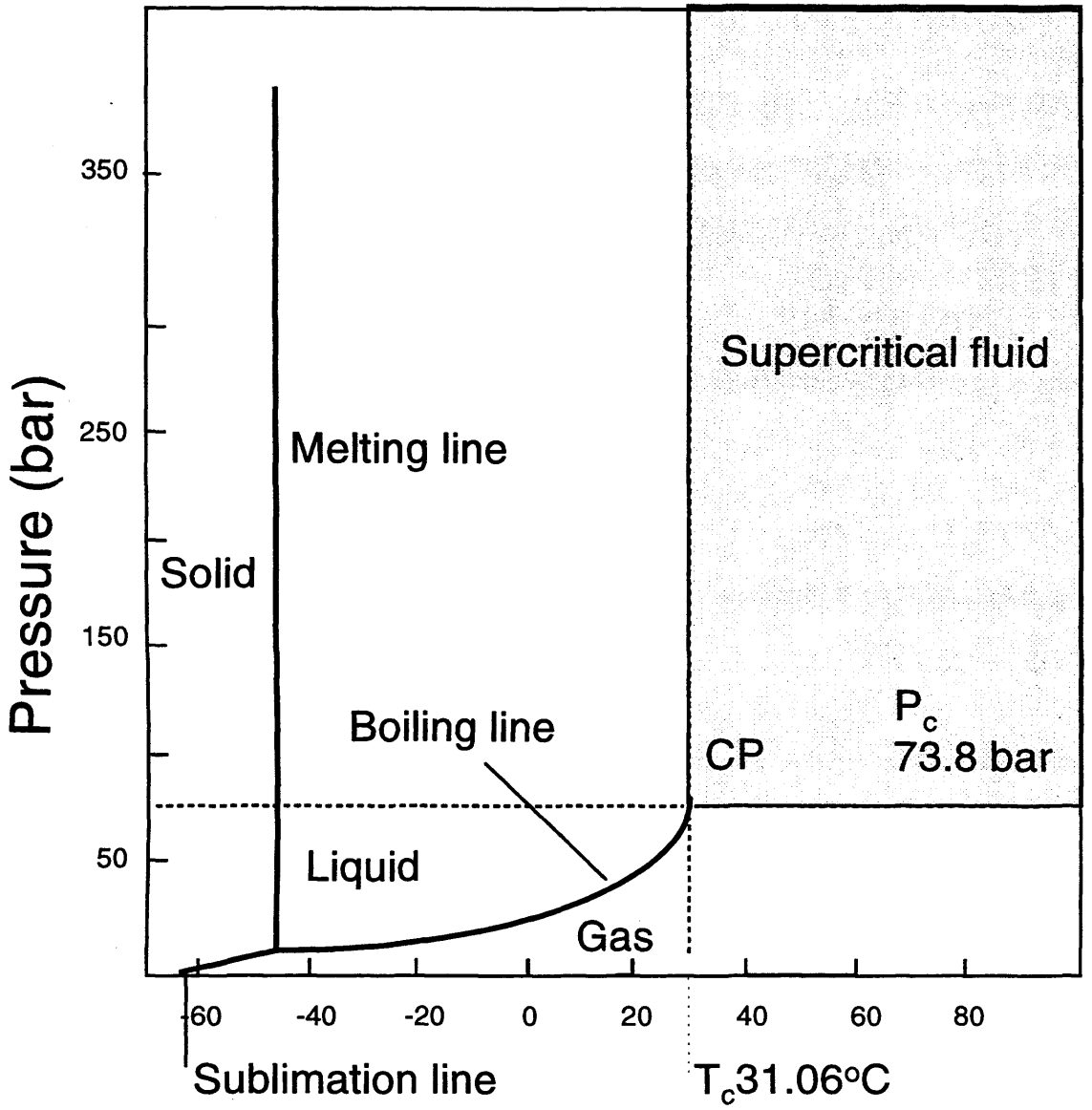

Figure (1.1.1) Phase diagram of carbon dioxide

product selectivity. Control of phase behaviour can be easily manipulated by changing the temperature or pressure. The solubility of a species in these media is governed by the density of the solvent and this allows reagents or products to be present in one phase (homogenisation) or two phases (separation) as required. This allows reactions to proceed that would otherwise be heterogeneous and hence unsuccessful.

Supercritical fluids have received considerable interest in the fields of extraction and the main examples are discussed in the following section. Supercritical carbon dioxide is particularly useful in the food industry because it has a low critical temperature, is non-toxic and is environmentally acceptable. One of the largest industrial applications of the use of supercritical carbon dioxide ($scCO_2$) is in the extraction of caffeine from coffee.[4] This compound is highly soluble in $scCO_2$ and with a decrease in the pressure, the caffeine can be precipitated and the carrier gas recycled. The overall process has to be extremely efficient as coffee is an inexpensive commodity (approximately $1 per pound[5]). It is therefore a remarkable engineering and economic achievement that full production plants are viable. There are now several large-scale plants operating within Europe and the U.S[5] and the largest plants are capable of processing 50 million lb/yr.[6] The extraction of caffeine from tea employs a similar engineering process to that in the extraction of coffee. The plant commissioned by SKW/Trosstberg in Germany is capable of processing 15 million lb/yr.[5] Supercritical CO_2 is being considered as a replacement for hexane in soybean oil extraction.[7,8] It was found that at pressures in excess of 1000 bar, the triglycerides and CO_2 became miscible.

Carbon dioxide has been tested on other materials such as corn[9] and wheat germ, grapeseed,[10] sunflower,[11] hops,[12] rice bran[13] and spearmint.[14] Some work has also been carried out on the extraction of fish oils[15] and this has received interest from

pharmaceutical companies. The solubilities of the triglycerides contained within these crops and fish products in $scCO_2$ are similar and the oils can be extracted completely if the cells are macerated.

The properties of carbon dioxide are especially attractive for extracting compounds from biological materials. Krukonis *et al.* showed that the extraction of certain chemotherapeutic agents in $scCO_2$ was appreciably more efficient than conventional methods.[5] There are several examples where SCF extraction is employed to remove biological samples including the determination of polychlorinated biphenyls levels in fish[16] and the extraction of beta blockers from liver samples.[17]

The solubility of a species is governed by the density of the solvent. This has allowed the separation of aromatic isomers which would not have been possible in liquid media. Krukonis and Kurnik[18] showed that *o*-hydroxybenzoic acid could be separated from the *para* and *meta* isomers. Chang and Morell carried out extractions on another class of aromatic isomers, the methyl nitrobenzene isomers, in $scCO_2$.[19] Another exciting development in the field of extraction is the removal of Uranium Oxide from spent nuclear fuel.[20]

Supercritical fluids can be used not only for extractions but also offer an alternative reaction medium and this allows reactions to proceed that would otherwise not be possible in liquid media. Supercritical CO_2 is relatively unreactive and most attempts to involve it in reactions have failed. An exception by Reetz[21] and co-workers is the reaction of hex-3-yne with $scCO_2$ to form cyclic esters.

One of the real advantages of supercritical solvents appears in the reactions involving gases such as H_2 and N_2. Gases are miscible in all proportions in SCF [22] and Poliakoff and co-workers [23,24] have exploited this fact to synthesise new dihydrogen and dinitrogen compounds such as $(C_5H_5)Re(N_2)_3$. They have also formed metal

complexes of Mn and Ir in $scCO_2$ which otherwise would not react in liquid solvents.[25] They were able to show that complexes of $Mn_2(CO)_{10}$ could be assembled in polyethylene and this has applications in the field of supported catalysis. Under ambient conditions, the compound is too large to diffuse into the polymer, but it can be formed after impregnation with $MnH(CO)_5$ from $scCO_2$.

Jessop *et al.*[26-29] have synthesised formic acid using the catalytic hydrogenation of $scCO_2$.

$$CO_2 + H_2 \xrightarrow{\text{Ru cat.}} HCOOH \qquad (1.1.1)$$

The solvent dissolves both the Ru catalyst, hydrogen and base which by precipitating the formate, drives the equilibrium to the right hand side of eqn. (1.1.1). This has aroused considerable interest from industry because the reaction proceeds at least an order of magnitude faster than under ambient conditions.

More recently various research groups have examined the use of SCF's in the use of polymerisation reactions. Homogeneous catalysis of the hydroformylation of supercritical propylene by $Co_2(CO)_8$ has been studied and improved yields of linear to branched chain products were found.[30] DeSimone and co-workers[31-36] have produced fluorinated polymers in $scCO_2$. Grafting of existing polymers has been carried out in a SCF at BP research.[2] Both the reagent and catalyst are dissolved in the SCF which then diffuses into the polymer where the reaction takes place.

Supercritical xenon is an extremely exciting solvent because not only is it extremely dense ($1.15 gml^{-1}$) but it is also transparent throughout the spectrum from vacuum UV to far IR. Poliakoff *et al.*[37] have demonstrated that it is a useful eluent in supercritical fluid chromatography with FTIR identification. This can be used for compounds that are too thermally labile for gas chromatography. Lawless and co-workers have used

scXe in sapphire NMR tubes to study divalent compunds of Yb which are normally too reactive in more common NMR solvents.[25]

A very important property of supercritical fluids is the high diffusion coefficient (SCF: $\approx 10^{-3}$ cm^2s^{-1}; liquids: $\approx 10^{-5}$ cm^2s^{-1}). The viscosity and density of CO_2 as a function of pressure is presented in Figure (1.1.2).[38] It is interesting to note that the viscosity of CO_2 at the critical point is 0.03cP (cf. H_2O = 0.91cP). This is beneficial in both separation methods and SCF chromatography.[39] Enzymatic reactions are another example where enhanced diffusion can produce desirable effects. Esterification reactions catalysed by lipase are important in the process of oils. In these reactions the rates are enhanced by better diffusion not only in the bulk fluid but also within the pores of the particles containing enzyme molecules.[40-43]

Supercritical water is an interesting fluid currently under investigation because its properties change more than other substances on becoming critical. As the critical temperature is reached, the hydrogen bonded structure breaks down and hence the solvent is much less polar. It is able to dissolve relatively large quantities of organic compound and it has been shown that that these can be rapidly and almost completely converted to environmentally benign species such as CO_2 and N_2.[44] There are at present over ten experimental plants operating in Germany and the US carrying out studies on the destruction of toxic organic material using scH_2O.

1.3 Electrochemistry in Supercritical Fluids

The electrochemistry of several polar fluids in the region of the critical point have been extensively studied in the past decade. The rate of an electrochemical process is often governed by the mass transport of the electroactive species to the electrode surface. It is known that the viscosity of a SCF is significantly less than in its liquid

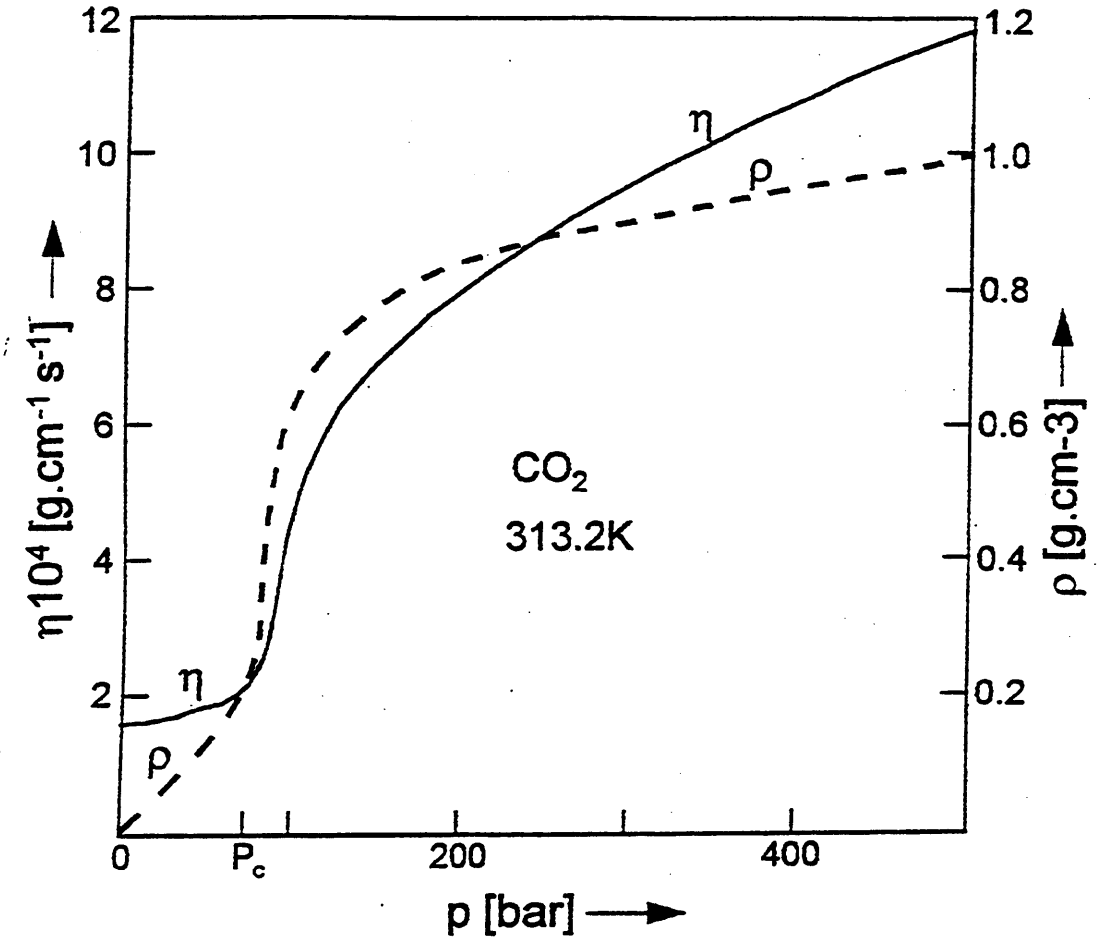

Figure (1.1.2) Density, ρ, and viscosity, η, for pure CO_2 as a function of pressure at 40°C

form and hence mass transport and ultimately process kinetics, should be enhanced. Bard and co-workers have presented a series of articles on this subject[45-53] and illustrated that the diffusion coefficients of the electroactive species were at least twice those observed in the sub-critical region. This was attributed to the decrease in solution viscosity. Of particular interest to this group is scH_2O because of its ability to dissolve organic compounds which are insoluble in this medium under ambient conditions. However, it must be stated that the critical conditions for this solvent are extreme (T_c = 374 °C, p_c = 221 bar)[48] and it is a corrosive medium (it has been reported that the solvent attacks the silica glass electrode seals). This has prompted studies into polar solvents with less extreme critical conditions such as SO_2 (T_c = 158 °C, p_c = 77.8 bar),[51] NH_3 (T_c = 113 °C, p_c = 112.5 bar)[50] and acetonitrile (Tc = 275 °C, p_c = 48 bar).[49] Although these conditions are less extreme than scH_2O, the temperatures and pressures required to obtain a SCF are still relatively high.

Little work has been carried out using less polar hydrofluorocarbon (HFC) and chloroflourocarbons (CFC's) solvents. Olsen and Tallman[54,55] investigated the behaviour of ferrocene at a microelectrode in polar halogenated solvents. It was shown that as the pressure approached the critical point, a two phase system occurred and the authors reported that the reproducibility of experimental data was poor. Abbott *et al.* have recently shown that 1,1,1,2 tetrafluoroethane (HFC134a), has an unprecedented electrochemical potential window of approximately 10V.[56]

The medium that has been of greatest interest is supercritical carbon dioxide because it has a low critical temperature and pressure, is relatively inexpensive and unreactive. The difficulty associated with voltammetry in $scCO_2$ is the negligible solubility of electrolytes resulting from the low polarity of the media. ($\varepsilon < 1.8$ at T = 50°C and P = 170 MPa).[57] Wightman *et al.*[58] attempted to measure the half wave potential of the

ferrocene oxidation in $scCO_2$ using tetrahexylammonium hexafluorophosphate ($THAPF_6$) as the supporting electrolyte. No voltammetric signal was observed at any temperature up to 80°C or pressures up to 135 bar. However, by the addition of small amounts of water (≈ 0.15 mol dm^{-3}) the sigmoidal shape voltammogram expected for a diffusion controlled process occured. The steady state current calculated was an order of magnitude greater than that observed in acetonitrile further confirming the fact that mass transport is significantly enhanced in such media. The authors went on to show[59] that a two phase system occurred in which a layer of molten electrolyte deposited on the electrode surface. Conduction was through the ionic liquid rather than the critical component. Attempts were made to coat platinum microelectrodes with ionically conducting polymer membranes for use in unmodified $scCO_2$.[60-62] However, these investigations showed that the ohmic loss distorted the voltammogram and addition of polar modifying solvents was necessary to reduce this. It is the aim of this work to assess the possibility of measuring electron transfer in unmodified $scCO_2$. The behaviour of electrolytes in non polar media is affected by the association of ions in solution. This affects not only the conductivity but also the double layer structure, both of which lead to artefacts in electrochemical measurements. It is therefore imperative to have an understanding of electrochemical investigations in non polar media prior to working in $scCO_2$. This also negates the need to perform preliminary investigations at high temperatures and pressures which have experimental difficulties associated with these conditions.

This work will compare and contrast the properties of a range of novel electrolytes in both anisole where some measurements have already been carried out[63] and cyclohexane which has many solvent properties which are similar to $scCO_2$ (cyclohexane, $\varepsilon = 2.02$ and anisole, $\varepsilon = 4.33$).[64]

1.4 Electrochemistry in Non Polar Media

Non aqueous solvents have become increasingly attractive as alternatives to aqueous media in the fields of metal deposition[65] and non-aqueous electrolyte batteries.[66] In media of low relative permittivity, voltammograms are distorted by ohmic (*iR*) loss even in the presence of excess supporting electrolyte. This has been overcome by the use of microelectrodes.[67-70] Wightman *et al.*[69] demonstrated that reversible voltammograms of ferrocene in acetonitrile could be observed even at fast sweep rates (ν = 10 Vs^{-1}). Clearly in media of high resistivity, the use of microelectrodes has enabled the electrochemist to probe electron transfer reactions that were otherwise severely distorted with ohmic loss.

It has been shown that in non-polar media, specific adsorption of ions significantly effects the kinetics of an electrochemical process. Fawcett *et al.*[70] investigated the electroreduction of nitromesitylene at a mercury electrode in propylene carbonate in the presence of tetraalkylammonium salts of varying chain length. It was shown that as the length of the alkyl chain increased the kinetics of the reduction decreased. Indeed, the standard rate constant of the process decreased by an order of magnitude when the electrolyte cation was changed from tetraethylammonium to tetraoctylammonium. This indicated that the tetraalkylammonium ions were adsorbed on the electrode forming a blocking layer whose thickness increased with alkyl chain length. Evans and co-workers[71] investigated the effects of the electrolyte cation on the kinetics of the reduction of nitroalkanes. The results supported the evidence obtained by Fawcett that the electron transfer kinetics decreased with an increase in electrolyte cation size. Abbott *et al.*[72] investigated the adsorption / desorption phenomena on an

electrochemical quartz crystal microbalance (EQCM) and showed that the desorption of tetraalkylammonium ions was a slow process.

Voltammetric studies in solutions of relative permittivity of less than ten are facilitated by the use of microelectrodes under steady state conditions. Such solutions are highly resistive as the supporting electrolyte as well as the electroactive ionic species is usually extensively ion paired. Murray *et al.*[73] showed that it was possible to observe reversible two one electron waves for the oxidation of copper tetraphenylporphrin in Toluene ($\varepsilon = 2.33$). It should be noted that such responses were only observable at very slow scan rates ($\nu < 10$ mV s^{-1}). This was thought to arise because of significant ohmic loss. Bond and co-workers[74-75] have studied the effect of ion pairing on the limiting currents in microelectrode studies in toluene. They were able to predict the limiting current of a response once the ion pair formation constants for both the electrolyte and electroactive species were known.

Abbott *et al.* have investigated conductivity and electron transfer in non-polar polyaromatic hydrocarbons. (PAH) [76,77] whose electrochemical stabilities were related to the large difference between the HOMO and LUMO. Ion pairing was shown to be prevalent in such media and this necessitated the use of microelectrodes.

REFERENCES CHAPTER I

1) L.T. Taylor, *Supercritical Fluid Extraction*, J. Wiley and Sons, New York, 1996

2) T. Clifford and K.Bartle, *Chem. Ind*, June 1996, 449

3) T. Gouw and R.J. Jentoft, *J. Chromatogr. Sci.*, 1986, **68**, 303

4) P.W. Atkins, *Physical Chemistry*, 5th Edn, Oxford University Press, 1994, 184

5) M. McHugh and V. Krukonis, *Supercritical Fluid Extraction*, 2nd Edn.,Butterworth-Heinemann, Boston, 1994

6) S.N. Katz, J.E. Spence, M.J. O'Brian, R.H. Skiff, G.J. Vogel and R. Prasad, *Method for decaffeinating coffee with a supercritical fluid,* U.S. Patent 4,911,537, 1990

7) J.P. Freidrich, G.R. List and A.J. Heaking, *J. Am. Oil. Chem. Soc.*, 1982, **61**, 223

8) M.A. Jackson and J.W. King, *J. Am. Oil. Chem. Soc.*, 1997, **74**, 103

9) D.D. Christianson, J.P. Freidrich, G.R. List, K. Warner, E.B. Bagley, A.C. Stringfellow and G.E. Inglett, *J. Food Sci.*, 1984, **49**, 229

10) A.M. Gomez, C.P. Lomez and E.M. Delaossa, *Chem. Eng. Data.*, 1996, **61**, 227

11) G.R. List, J.P. Freidrich and J. Pominski, *J. Am. Oil. Chem. Soc.*, 1984, **61**, 1847

12) C. Borchjensen and J. Mollerup, *Fluid Phase Equil.*, 1997, **138**, 179

13) J.C. Andre, M.L. Viriot and J. Villermaux, *Pure Appl. Chem.*, 1986, **58**, 907

14) A. Garcia, A. Delvias and J. Rincon., *J. Am. Oil. Chem. Soc.*, 1996, **73**,9

15) K.J. Hannigan, *Chiltons Food Eng.*, 1981, **53**, 77

16) H.B. Lee, T.E. Peart A.J. Niima and C.R. Knipe, *J. Am. Oil. Chem. Soc.*, 1995, **78**, 437

17) L. Siret, N. Bargman and M. Caude, *Chirality*, 1992, **4**, 252

18) V.J. Krukonis and R.T. Kurnik, *J. Chem. Eng. Data*, 1985, **30**, 247

19) H. Chang and D.G. Morell, *J. Chem. Eng. Data*, 1985, **30**, 74

20) N.G. Smart, C.W. Wai and C.L. Phelps, *Chem. Br.*, 1998, **34**(8), 34

21) M.T. Reetz, W. Konen and T. Strack, *Chimia*, 1993, **47**, 493

22) C.Y. Tsang and W.B. Streett, *Chem. Eng. Sci.*, 1981, **36**, 993

23) S.M. Howdle and M. Poliakoff, *J. Chem. Soc., Chem. Commun.*, 1989, 1517

24) S.M. Howdle, M.A. Healy and M. Poliakoff, *J. Am. Chem. Soc.*, 1990, **112**, 2662

25) M. Poliakoff and S.M. Howdle, *Chem. Br.*, 1995, **31**, 118

26) P.G. Jessop, Y. Hsiao, T. Ikariya and R. Noyori, *J. Am. Chem. Soc.*, 1996, **118**, 344

27) P.G. Jessop, Y. Hsiao, T. Ikariya and R. Noyori, *Nature*, 1994, **368**, 231

28) P.G. Jessop, T. Ikariya and R. Noyori, *Chem. Rev.*, 1995, **95**(2), 259

29) P.G. Jessop, T. Ikariya and R. Noyori, *J. Chem. Soc, Chem. Commun.*, 1996

30) J.W. Rathke, R.J. Klingler and T.R. Krause, *Organometallics*, 1991, **10**, 1350

31) T.J. Romack, B.E. Kipp and J.M. DeSimone, *Macromolecules*, 1995, **28**, 8432

32) D. Canelas and J.M. DeSimone, *Chem. Br.*, 1998, **34**,38

33) J.M. DeSimone, Z. Guan and C.S. Elsbernd, *Science*, 1992, **257**, 945

34) J.M. DeSimone, Z. Guan and C.S. Elsbernd, *Science*, 1994, **265**, 356

35) D. Canelas and J.M. DeSimone, *Macromolecules*, 1996, **29**, 2818

36) M.R. Clark, J.L. Kendall and J.M. DeSimone, *Macromolecules*, 1997, **30**, 6011

37) M.A. Healy, T.J. Jenkins and M. Poliakoff, *Trends Analyt. Chem.*, 1991, **10**, 92

38) G. M. Schneider, *Angew. Chem. Int. Ed. Engl.*, 1978, **17**, 716

39) Z. Balenovic, M.N. Myers and J.C. Giddings, *J. Chem. Phys.*, 1970, **52**, 915

40) T. Clifford and K.Bartle, *Chem. Br.*, 1993, 449

41) O. Aaltonen and M. Rantakyla, *Chemtech.*, 1991, 240

42) A.J. Russell and E.J. Beckman, *Enzyme Microb. Technol.*, 1991, **13**, 1007

43) T.W. Randolph, D.S. Clarj, H.W. Blanch and J.M. Prausnitz, *Science*, 1988, **239**, 367

44) R.W. Shaw, T.B. Brill, T. Clifford, C.A. Eckert and E.U. Frank, *Chem. Eng. News*, 1991, **69**, 26

45) R.M. Crooks, Fu-Ren F. Fan and A.J. Bard, *J. Am. Chem. Soc.*, 1984, **106**, 6851

46) R.M. Crooks and A.J. Bard, *J.Phys. Chem.*, 1987, **91**, 1274

47) A.C. McDonald, Fu-Ren F. Fan and A.J. Bard, *J. Phys. Chem.*, 1986, **90**, 196

48) W.M. Flarsheim, Yu-Min Tsou, I. Trachtenberg, K.P. Johnston and A.J. Bard, *J. Phys. Chem.*, 1986, **90**, 3857

49) R.M. Crooks and A.J. Bard, *J. Electroanal. Chem.*, 1988, **243**, 117

50) R.M. Crooks and A.J. Bard, *J. Electroanal. Chem.*, 1988, **240**, 253

51) C.R. Cabrera, E. Garcia and A.J. Bard, *J. Electroanal. Chem.*, 1989, **260**, 457

52) C.R. Cabrera and A.J. Bard, *J. Electroanal. Chem.*, 1989, **273**, 147

53) C. Liu, S.R. Snyder and A.J. Bard, *J. Phys. Chem. B*, 1997, **101**, 1180

54) S.A. Olsen and D.E. Tallman, *Anal. Chem.*, 1994, **66**, 503

55) S.A. Olsen and D.E. Tallman, *Anal. Chem.*, 1996, **68**, 2504

56) A.P. Abbott, C.A. Eardley, E.G. Hope and J.C. Harper, *J. Electroanal.Chem.* **in press**

57) V.A. Grinberg and V.M. Mazin, *Russian J. Elec*, 1998, **34**, 245

58) M.E. Philips, M.R. Deakin, M.V. Novotny and R.M. Wightman, *J. Phys. Chem.*, 1987, **91**, 3934

59) D. Niehaus, M.E. Philips, A.C. Michael and R.M. Wightman, *J. Phys. Chem.*, 1989, **93**, 6232

60) A.C. Michael and R.M. Wightman, *Anal. Chem.*, 1989, **61**, 2193

61) A.C. Michael and R.M. Wightman, *Anal. Chem.*, 1989, **61**, 270

62) E.F. Sullenberger and A.C. Michael, *Anal. Chem.*, 1993, **65**, 2304

63) A.P. Abbott, *Chem. Soc. Rev.*, 1993, 435

64) A.L. Horvath, *Handbook of Electrolyte Solutions*, Ellis Horwood Ltd., Chichester, 1985

65) W. Schmickler, *Interfacial Electrochemistry*, Oxford University press, 1996

66) O. Popovych and R.P.T. Tomkins, *Nonaqueous Solution Chemistry*, J. Wiley and Sons, New York, 1981

67) J.O. Howell and R.M. Wightman, *Anal. Chem.*, 1984, **56**, 524

68) P.A. Flowers, D.E. Niehaus and R.M. Wightman, *Anal. Chem.*, 1991, **63**, 1728

69) R.M. Wightman, *Anal. Chem.*, 1981, **53**, 1125

70) W.R. Fawcett, M. Fedurco and M. Opallo, *J. Phys. Chem.*, 1992, **96**, 9959

71) D.H. Evans and A.G. Gilicinski, *J. Phys. Chem.*, 1992, **96**, 2528

72) A.P. Abbott, D.C. Loveday and A.R. Hillman, *J. Chem. Soc., Faraday Trans.*, 1994, **90**, 1533

73) L. Geng and R.M. Murray, *Inorg. Chem.*, 1986, **25**, 3115

74) K.B. Oldham, T.J. Cardwell, J.H. Santos and A.M. Bond., *J. Electroanal. Chem.*, 1997, **430**, 25

75) K.B. Oldham, T.J. Cardwell, J.H. Santos and A.M. Bond., *J. Electroanal. Chem.*, 1997, **430**, 39

76) A.P. Abbott and D.J. Schiffrin, *J. Chem. Soc., Faraday Trans.*, 1990, **86**, 1453

77) A.P. Abbott and D.J. Schiffrin, *J. Electroanal. Chem.*, 1988, **256**, 477

CHAPTER II

EXPERIMENTAL

2.1 Materials
- 2.1.1 Electrolytes
- 2.1.2 Solvents
- 2.1.3 Preparation of Complexes

2.2 Instrumentation
- 2.2.1 High Pressure Apparatus
- 2.2.2 High Pressure Bulk Electrolysis
- 2.2.3 Viscosity and Density Measurements
- 2.2.4 NMR and Crystallographic Methods

2.3 Electrochemical Methods
- 2.3.1 Linear Sweep Voltammetry
- 2.3.2 Microelectrodes
- 2.3.3 Capacitance Measurements

2.1 Materials

2.1.1 Electrolytes

A range of electrolytes were studied in this work and all were rigorously purified and dried. The electrolytes were all synthesised by the same general method from the salts listed in Table (2.1.1). The quaternary ammonium bromide was dissolved in the minimum volume of methanol and this was added to a methanolic solution of the sodium tetraarylborate. The white precipitate thus formed was filtered, washed with cold methanol and recrystallised twice from acetone. The product was dried under vacuum.

Salt	Abbreviation	Source
Tetrakis(decyl)ammonium bromide	**(TDABr)**	**Fluka, > 99%**
Tetradodecylammoniumbromide	**(TDDABr)**	**Fluka, > 99%**
Sodium tetraphenylborate	**(NaTPhB)**	**Fluka, > 98%**
Potassium tetrakis(4chlorophenyl)borate	**(KTClPhB)**	**Aldrich, 98%**
Sodium tetrakis(4-fluorophenyl)borate	**(NaTFPhB)**	**Fluka, > 98%**
Sodium tetrafluoroborate	**($NaBF_4$)**	**Fluka, > 99%**

Table (2.1.1) List of compounds used in the synthesis of electrolytes (with abbreviations).

2.1.2 Solvents

The solvents used in these studies are presented in Table (2.1.2). All were used as received.

Solvent	Mol. wt.	b.p. /°C	m.p. /°C	ε	η/ cP @ 30°C	Source
cyclohexane	**84**	**81**	**6.5**	**2.02**	**0.82**	**Aldrich > 99.9%**
toluene	**92**	**111**	**-93**	**2.38**	**0.59**	**Fluka >99.5%**
butylbenzene	**134**	**183**	**-87.5**	**2.36**	**1.04**	**Aldrich A.C.S grade > 99.9%**
dichloroethane	**113**	**83.4**	**-35.6**	**10.37**	**0.73**	**Aldrich Analar > 99.5%**
anisole	**108**	**154**	**-37.5**	**4.33**	**0.79**	**Aldrich**

Table (2.1.2) The physical properties of the solvents used in this work (physical data from ref. 1)

2.1.3 Preparation of complexes

The tetradodecylammonium nickel maleonitrile complex for voltammetric investigations was prepared as follows.

i) Sodium cis-1,2-dicyano –1,2-ethylenedithiolate

$$2NaCN + 2CS_2 + 6HCON(CH_3)_2 \longrightarrow Na_2S_2C_2(CN)_2 + 6HCON(CH_3)_2 + 2S$$

Carbon disulphide (10ml) was added to a flask containing sodium cyanide (5gm) dissolved in 100ml of dimethylformamide. The green precipitate thus formed turned dark red when the mixture was stirred for 1 hour. The product was filtered and dissolved in 500ml ethanol. This was left to stand overnight and yellow crystals of the sodium complex formed. The product was washed and filtered in ethanol and dried under vacuum.

ii) Tetradodecylammonium bis(cis-1,2-dicyano-1,2-ethylenedithiolato)-nickelate (2-)

$$Ni^{2+} + 2S_2C_2(CN)_2^{2-} + 2(C_{12}H_{25})_4N^+ \longrightarrow [(C_{12}H_{25})_4N]_2[NiS_4C_4(CN)_4]$$

An excess of nickel chloride hexahydrate in 15ml water was added slowly to the cyano complex. To this, 10gm of tetradodecylammonium bromide in ethanol was added and the precipitate thus formed was washed and filtered. The product was dissolved in *iso*-butyl alcohol and left to stand until fine yellow needles of the product formed.

The preparation of Tetradecylammonium ferrocene carboxylic acid was as follows.

An excess of tetradecylammonium bromide was added to 0.5gm of ferrocene carboxylic acid (Aldrich) dissolved in methanol. The orange precipitate thus formed was washed with ethanol and filtered. The product was recrystallised twice from acetone and dried under vacuum.

2.2 Instrumentation

2.2.1 High Pressure Apparatus

The experiments using supercritical fluids were carried out in a high pressure vessel shown in Figure (2.2.1) which is rated to 2.0 kbar. Electrical feedthroughs were constructed by varnishing a nichrome rod (diameter = 2mm) and sealing it with araldite epoxy resin in an autoclave sealing plug which had been tapped to create a better seal with the resin (see inset Fig. 2.2.1). Carbon dioxide was pumped into the cell using a model 10-600 pump (Hydraulic Engineering Corp., Los Angeles). The temperature of the cell was measured using an Fe/Constantan thermocouple and was maintained at the given temperature (± 0.5 °C) using a CAL 9000 heater. The pressure was monitored using a Budenburg type 316 gauge. The experimental apparatus is shown in Fig. (2.2.2)

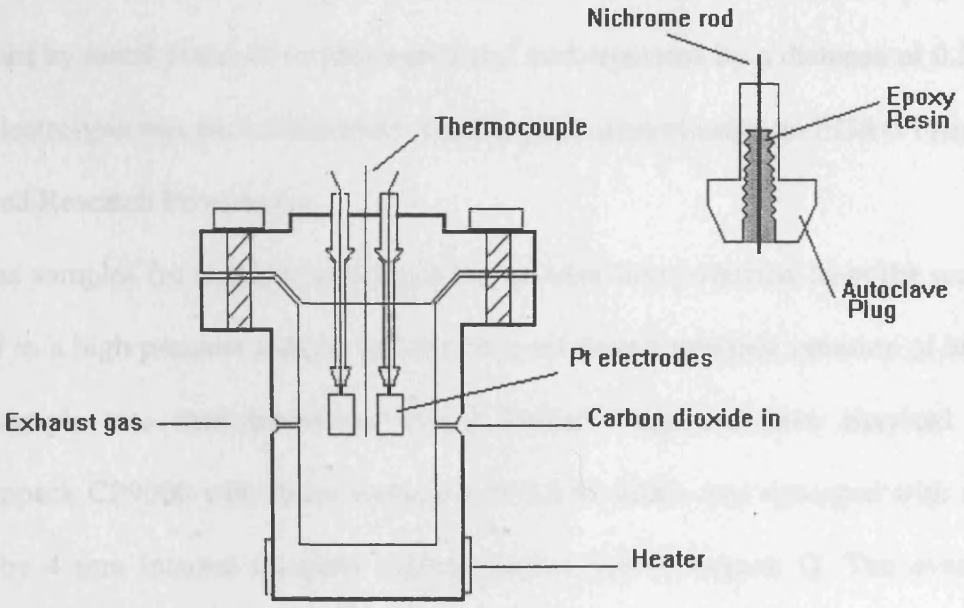

Figure (2.2.1) Schematic diagram of the high pressure cell used for supercritical fluid studies

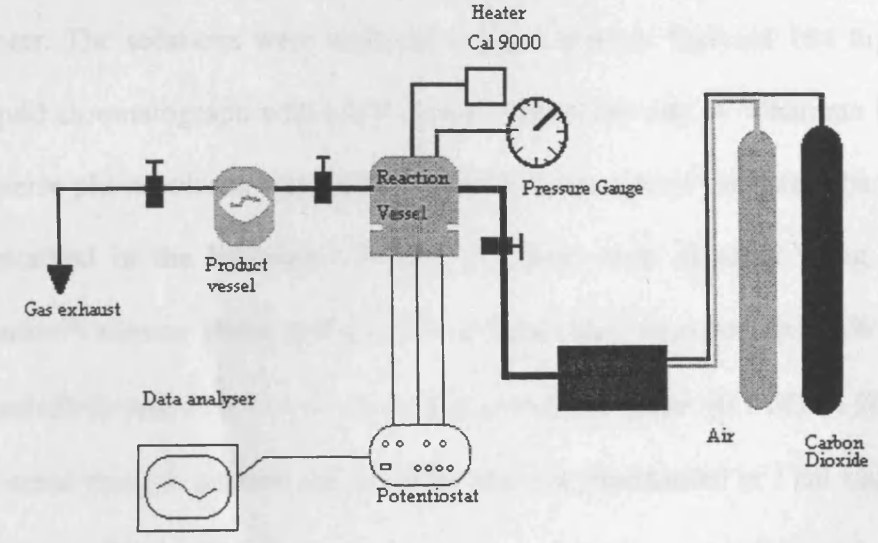

Figure (2.2.2) Diagram of high pressure apparatus.

2.2.2 High Pressure Bulk Electrolysis

The electrode arrangement was similar to that shown in Fig. (2.1.1). The Pt flags were replaced by metal plates of surface area 6 cm^2 and separated by a distance of 0.25cm. The electrolysis was performed under potentiostatic control using an EG&G Princeton Applied Research Potentiostat.

All gas samples from electrolysis experiments were first collected from the reaction vessel in a high pressure sample vessel with a maximum working pressure of 30 bar. The sample was then introduced into a Tedlar™ bag and then anaylsed on a Chrompack CP9000 with flame ionisation detection which was equipped with a 2 m long by 4 mm internal diameter column packed with Poropack Q. The oven was maintained at 30°C with nitrogen as the carrier gas.

Formate and oxalate products were analysed from the electrolyte used in bulk electrolysis experiments. The electrolyte was first dissolved in 0.1 M H_2SO_4 to liberate the acidic organic products and these were then filtered through a 20 μm glass sinter. The solutions were analysed using a Hewlett Packard 164 high performance liquid chromatograph with a UV detector set at 210 nm. A Whatman Partisphere C18 reverse phase column was used to detect the presence of formate. The mobile phase is described in the literature.[2] Oxalate products were detected using a Phenomenex *Amino*™ reverse phase column. The mobile phase incorporated 10% by vol. H_2SO_4, acetonitrile and 25% by vol. potassium phosphate buffer (0.1 M). A 20 μl sample was injected into the column and the flow rate was maintained at 1 ml min^{-1} at a constant pressure of 600 MPa.

2.2.3 Viscosity and Density Measurements

The viscosities were measured using an Ostwald viscometer and the densities were measured on a precision density meter (Anton Parr DMA 02C). Temperatures were maintained at those quoted (± 0.5° C) using a Grant W14 water bath.

2.2.4 NMR and Crystallographic Methods

X-ray crystal data were collected using an Omega scan technique. NMR spectra were recorded on a Bruker DRX-400 spectrometer at 400.13 MHz for ^{1}H, with a probehead temperature of 300 K. Samples were prepared in C_6D_6 as supplied (Cambridge Isotope Laboratories, 99.6%D). Spectra were assigned using COSY data and all chemical shift data are in ppm referenced to $Si(CH_3)_4 = 0$ ppm.

2.3 Electrochemical Methods

2.3.1 Linear Sweep Voltammetry

All voltammetry investigations were carried out using a PGSTAT 20 potentiostat (Ecochemie, Holland). Experiments carried out in the liquid phase employed three electrodes and the solutions were thoroughly degassed with nitrogen. Studies with microelectrodes employed a two electrode array.

A similar cell design as that shown in Fig. (2.2.1) was used in the voltammetric studies in the supercritical phase with one of the platinum flags replaced by either a 1mm Pt disc sealed in glass or a 10 μm Pt wire sealed in glass capillary. All potentials are quoted with respect to a Ag/AgTPhB [3] reference electrode unless stated otherwise.

2.3.2 Microelectrodes

Microelectrodes were first developed for *in vivo* electrochemical studies measuring concentrations of chemicals inside biological cells.[4-6] There are additional properties of very small electrodes which can be exploited in other areas of electrochemistry. Perhaps the most important are:

(i) high rates of steady state diffusion can be obtained and hence fast electron transfer processes and coupled chemistry can be studied without recourse to transient techniques on a short timescale,

(ii) it is possible to obtain high quality data in highly resistive media; since the currents flowing through the cell are low, ohmic drop is negligible,

(iii) charging currents are much reduced and the ratio of faradaic to non-faradaic current is greatly enhanced.

The steady state voltammograms recorded using this technique were analysed by the following method.[7] For a steady state response at fixed sampling time t,

$$E = E^{0'} + \frac{RT}{nF}\ln\frac{D_R^{1/2}}{D_O^{1/2}} + \frac{RT}{nF}\ln\frac{i_d(t) - i(t)}{i(t)} \qquad (2.3.1)$$

where D_R and D_O are the diffusion coefficients of the reduced and oxidised forms and i_d is the diffusion limiting current. When $i(t) = 1/2 i_d(t)$, the current ratio becomes unity so that the third term is zero. The potential at which this occurs is $E_{1/2}$, the *half wave potential*:

$$E_{1/2} = E^{0'} + \frac{RT}{nF}\ln\frac{D_R^{1/2}}{D_O^{1/2}} \qquad (2.3.2)$$

and (2.3.1) is often written

$$E = E_{1/2} + \frac{RT}{nF} \ln \frac{i_d - i}{i} \qquad (2.3.3)$$

When a system conforms to this equation , a plot of E vs. $\log[(i_d-i)/i]$ is a straight line with slope of 2.3RT/nF.

2.3.3 Capacitance Measurements

The low capacitance of the electrolyte solutions necessitated a novel cell design that whose main feature is a working electrode of large surface area ($1.5cm^2$) (shown in Figure (2.3.1)). The cell was constructed from a brass tube (diameter 8mm) the surface of which was coated in a thick layer of platinum black (electrodeposited by standard technique).[8] This formed the counter electrode of the cell. The working electrode was a platinum wire (Goodfellows 99.999%) of 1 mm diameter and 50 mm length. The working electrode was flamed between successive experiments to remove any adsorbed electrolyte and thus allowing reproducible results to be obtained. The reference electrode was a coil of 20 cm of silver wire between the working and counter electrodes. As with previous studies [9] a Ag/Ag^+ pseudo-reference electrode was used to preclude contamination from other ions. It was not necessary to separate the reference electrode from the working electrode compartment as the Ag^+ ions are insignificantly soluble in cyclohexane. Capacitance measurements in the supercritical phase employed two Pt electrodes of surface area 6 cm^2 (counter and working electrodes). A silver wire reference electrode was placed between the two Pt plates. Capacitances were measured via an ac impedance method. Impedance spectra were recorded using a Solartron 1254 frequency response analyser and a Solartron 1286 potentiostat with a 20 mV ac amplitude in the frequency range 65000 to 1 Hz. The data obtained were analysed using ZVIEW software.

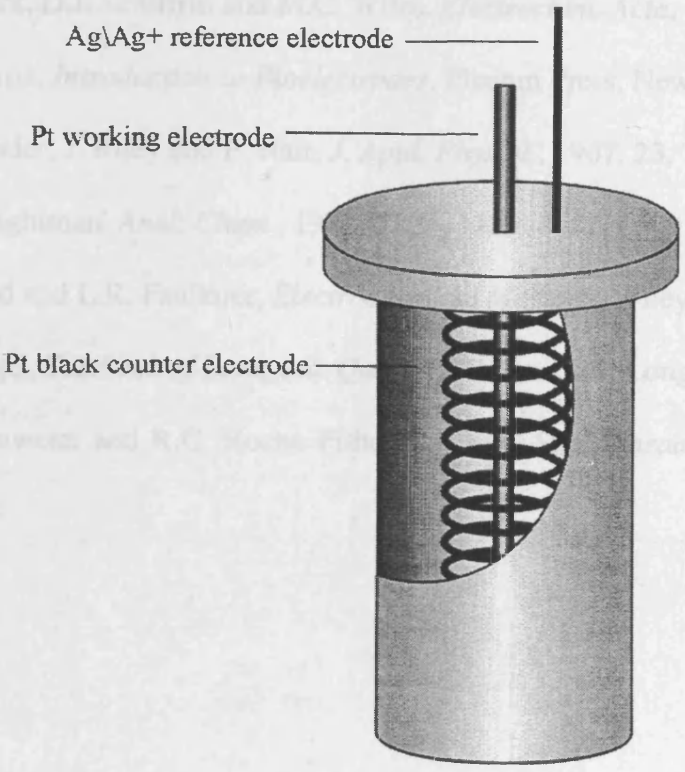

Figure (2.3.1) Diagram of the capacitance cell

REFERENCES CHAPTER II

1) A.L. Horvath, *Handbook of Electrolyte Solutions*, Ellis Horwood Ltd., Chichester, 1985

2) M.H. Khaskhali, M.I. Bhanger and F.D. Khand, *J. Chromatography B*, 1996, **675**, 147

3) D.J. Clark, D.J. Schiffrin and M.C. Wiles, *Electrochim. Acta*, 1989, **43**, 767

4) C.D. Ferris, *Introduction to Bioelectrodes*, Plenum Press, New York, 1974

5) N.J. Whaler, J. Riley and P. Nair, *J. Appl. Physiol.*, 1967, **23**, 798

6) R.M. Wightman, *Anal. Chem.*, 1981, **53**(9), 1125

7) A.J. Bard and L.R. Faulkner, *Electrochemical Methods*, Wiley, New York,1980

8) A.I. Vogel, *Textbook of Inorganic Quantitative Analysis*, Longman, London, 1978

9) W.R. Fawcett and R.C. Rocha Filho, *J. Chem. Soc., Faraday Trans.*, 1992, **88**, 1143

CHAPTER III

ION ASSOCIATION AND MOBILITY

3.1 Introduction
- 3.1.1 Ion Association
- 3.1.2 Triple Ion Formation
- 3.1.3 Conductivity in Supercritical Fluids

3.2 Results and Discussion
- 3.2.1 Conductivity Measurements in Liquid Media
- 3.2.2 Conductivity Measurements in Supercritical Carbon Dioxide

3.3 Conclusions

3.1 Introduction

In order to perform electrochemical experiments, the medium must be made sufficiently conducting. In non-polar media this can be achieved by the dissolution of tetraalkylammonium electrolytes.[1]

This work is primarily concerned with the effects of the solvent and electrolyte on the conductivity. The effects of relative permittivity and viscosity upon the association and mobility of the ions in solution is determined in this study.

3.1.1 Ion Association

In media of low relative permittivity, coulombic interactions are considerably greater than the thermal energies of the ions and as a consequence they associate in solution forming an entity which is sufficiently stable to persist through a number of collisions with solvent molecules. In the case of symmetrical electrolytes, such ion pairs will have no net charge and make no contribution to the electrical conductivity.

The phenomenon of ion association was first investigated by Bjerrum[2] in the 1920's. He postulated that ions of opposite charge within a certain distance of one another are associated. Bjerrum proposed that the critical ion capture distance, q, is given by

$$q = \frac{|z_1 z_2| e^2}{2\varepsilon k T} \qquad (3.1.1)$$

where z_1 and z_2 are the cation and anion valency respectively, e is charge on an electron, ε is the relative permittivity of the solvent, k is the Boltzmann constant and T is the temperature in Kelvin. If the distance between the two ions, r, is less than the critical capture distance then the ions can assume to be associated. On the basis of this assumption, the degree of association, $1-\alpha$, is given by the definite integral,

$$1-\alpha = 4\pi n_1 \int_a^q \exp\left(-\frac{z_1 z_2 e^2}{\varepsilon kTr}\right) r^2 dr \qquad (3.1.2)$$

where a is the distance of closest approach of the two ions. If,

$$x = -\frac{z_1 z_2 e^2}{\varepsilon rkT} \qquad \text{and} \qquad b = \frac{|z_1 z_2| e^2}{\varepsilon akT}$$

equation (3.1.2) becomes

$$1-\alpha = \frac{4\pi Nc}{1000}\left(\frac{z_1 z_2 e^2}{\varepsilon kT}\right)^3 Q(b) \qquad (3.1.3)$$

where

$$Q(b) = \int_2^b x^{-4} e^x dx \qquad (3.1.4)$$

In very dilute solutions it can be shown that

$$1/K_p \approx (1-\alpha)/c \qquad (3.1.5)$$

where K_p is the ion pair dissociation constant. Therefore equation (3.1.2) becomes,

$$\frac{1}{K_p} = \frac{4\pi N}{1000}\left(\frac{z_1 z_2 e^2}{\varepsilon kT}\right)^3 Q(b) \qquad (3.1.6)$$

The value for this integral has been given in the literature.[3]

3.1.2 Triple Ion Formation

The concept that triple ions form in media of low relative permittivity was proposed by Fuoss and Kraus in the 1930's.[3] They published a series of articles on the properties of electrolyte solutions in non-polar media. When the molar conductivity is plotted versus the square root of the concentration four distinct regions are observed;

(i) at low concentrations the conductivity decreases proportionally with the square root of concentration in accordance with Onsager's equation.

(ii) for weak electrolytes a more rapid decrease in the conductivity.

(iii) at high electrolyte concentrations in media of low relative permittivity, a minimum is obtained.

(iv) beyond this minimum the conductivity rises sharply as the electrolyte concentration increases.

The second region can be attributed to the equilibrium between single ions and neutral ion pairs and the third to the ion pair-triple ion equilibrium and the final region to the increase in concentration of triple ions. Fuoss and Kraus used these assumptions to derive a simple mathematical model in which properties of the electrolyte could be calculated.[3]

At low electrolyte concentrations the activity coefficients can be equated to unity and the limiting conductivity at infinite dilution is a sufficient approximation to the conductivity of a fully dissociated salt solution. The fraction of free ions is negligible and $(1-\alpha) \approx 1$. Thus for the equilibrium,

$$M^+ + X^- \longleftrightarrow MX \qquad (3.1.7)$$

the degree of dissociation

$$\alpha \approx (K_p/c)^{1/2} \qquad (3.1.8)$$

If there is a possibility of the further equilibria,

$$MX + M^+ \longleftrightarrow (MXM)^+ \qquad (3.1.9)$$

and

$$MX + X^- \longleftrightarrow (XMX)^- \qquad (3.1.10)$$

let

$$k_1 = \frac{[MXM^+]}{[MX][M]^+} \quad \text{and} \quad k_2 = \frac{[XMX^-]}{[XM][X]^-}$$

The approximation is made that $k_1 = k_2 = K_T$, since there is equal probability of forming $(MXM)^+$ or $(XMX)^-$ triple ions. If the ratio of the actual concentration of one of the species of triple ions to the stoichiometric concentration is defined as α_T then the equilibrium equation becomes

$$\alpha_T = (K_p c)^{1/2} / K_T \qquad (3.1.11)$$

If Λ^0 represents the limiting conductivity at infinite dilution i.e

$$\Lambda^0 = \lambda^0_{M+} + \lambda^0_{X-} \qquad (3.1.12)$$

and Λ_T that of the triple ions

$$\Lambda^0_T = \lambda^0_{MXM+} + \lambda^0_{XMX-} \qquad (3.1.13)$$

then the observed conductivity will be,

$$\Lambda = \alpha\Lambda^0 + \alpha_T\Lambda^0_T \qquad (3.1.14)$$

By substituting equations (3.1.8) and (3.1.11) into (3.1.14)

$$\Lambda = \frac{\Lambda^0 K_p^{1/2}}{c^{1/2}} + \frac{\Lambda^0_T K_p^{1/2} c^{1/2}}{K_T} \qquad (3.1.15)$$

The method of analysis proposed by Fuoss and Kraus assumes that the activity coefficient, γ, is unity. Barthel [9] suggested that in media of very low relative permittivity $(\varepsilon < 10)$ the activity coefficient would become more significant and large deviations from ideality are observed. Abbott *et. al* [10] used this assumption when analysing data in anisole/phenanthrene mixtures. It was shown that a modified Fuoss-Kraus approach was valid in which the activity coefficient could be calculated from the extended Debye-Huckel theory. The data could be fitted to the equation to obtain K_p and K_T.

$$\frac{\Lambda c^{1/2}\gamma}{\Lambda^0} = K_P^{1/2} + \frac{2K_P^{1/2} c}{3K_T} \qquad (3.1.16)$$

The degree of dissociation for the ion pair and triple ion are given by

$$\alpha = (K_p/c)^{1/2} / \gamma_{\pm} \qquad \text{and} \qquad \alpha_t = (K_p/c)^{1/2} / K_t\gamma_t \qquad (3.1.17)$$

where $\gamma\pm$ and γt are the mean activity coefficients for the single and triple ions respectively. The equivalent conductance is given by eqn. (3.1.14) and insertion of equations (3.1.17) into (3.1.14) and using the assumption that $\Lambda_t = 2/3\Lambda_s$, where Λ_t and Λ_s are the conductivities of the triple and free ions respectively, yields equation (3.1.16).

It is imperative to determine the molar conductivity of the electrolyte at infinite dilution, Λ°, so that the association constant for the electrolyte in solution can be calculated. For strong electrolytes in aqueous media, the Onsager equation is used to determine the limiting molar conductivity at infinite dilution. In media of low relative permittivity the ionic dissociation is small and there is usually insufficient data at low concentrations to analyse the systems using this approach. This problem has been overcome by the use of the Walden rule which is a consequence of the application of Stokes law to the motion of ions and has been successfully applied to data in media of low relative permittivity.[9,10]

3.1.3 Conductivity Measurements in Supercritical Fluids

Supercritical fluids have attracted much interest in the electrochemical field owing to the low viscosity and hence high mass transport properties of the solvent. Whilst the region of the critical point for aqueous systems has been extensively studied,[11-25] there are however few research articles on the conductometric properties of electrolytes in non-aqueous supercritical fluids.

Reliable values of the electrical conductance of pure water at high temperatures and pressures are useful for estimating ionic impurities in steam cycles and other processes

of industrial importance. Much of the pioneering work into the conductometric properties of electrolytes in water at temperatures from 0 to 800°C and pressures up to 400MPa was performed by Franck.[12-14] In addition to this work there are several studies of the conductivity-association behaviour in this temperature and pressure range.[15-25] These studies showed that isothermal plots of the limiting equivalent conductivity, Λ^0, for a given electrolyte *vs.* the density of the solvent yielded a straight line over the experimental range of pressures. The data could be extrapolated to zero density and it was found that for a given electrolyte a constant value of Λ^0 was obtained. Thus, the authors were able to predict the limiting molar conductivity of any given electrolyte over a range of pressures and temperatures.

As mentioned previously, the quantity of interest in conductometric studies is the limiting molar conductivities of the anions and cations. In the work of Marshall *et al.*[11] the assumption that $\lambda^0(H^+) + \lambda^0(OH^-) = \Lambda^0(H^+, OH^-)$ was employed and since limiting conductivities are additive,

$$\Lambda^0(H^+,OH^-) = \Lambda^0(HCl) + \Lambda^0(NaOH) - \Lambda^0(NaCl) \qquad (3.1.17)$$

From this, an equation for calculating the electrical conductance of liquid and supercritical water at pressures up to and including 1000MPa was proposed. Johnston *et al.*[26] used the data obtained by Marshall to predict the ion transport properties in supercritical water. A semicontinuum model was used in which the frictional coefficient was estimated from the Navier-Stokes rule.[27] From the direct application of the Stokes-Einstein law at constant viscosity, the solution of the equation provides the diffusion coefficient. It was found that in certain instances the mobilities of the ions increased ten fold above the critical point and this was verified by experimental observations. [11]

Pitzer *et al.*[28] investigated the tetra-n-butylammonium picrate-1-chloroheptane system (T_c = 414.4K) at the region below and above the critical point. It was shown that at low concentrations, a minimum followed by a sharp rise in the conductivity-concentration plots occurred and this was attributed to the formation of ion pairs and triple ions respectively. Beyond this region, a maximum appeared and this was consistent with a marked increase in solution viscosity. The data were analysed using a modified Fuoss-Kraus equation which took into account the corrections for the activity coefficients. The ion pair dissociation and triple ion formation constants were evaluated and were similar to those observed in other non-polar media.[10]

This work shows that by the dissolution of novel tetraalkylammonium electrolytes, media of relative permittivity of less than two can be made conducting. We present the conductivities of these electrolytes in non polar liquid solvents and supercritical carbon dioxide. The data were analysed in terms of the mobilities and association of the ions. Direct comparisons between the supercritical and liquid phase are made. We demonstrate that for the first time, supercritical carbon dioxide can be made conducting without the need for a polar modifying solvent.

3.2 Results and Discussion

3.2.1 Conductivity Measurements in Liquid Media

Electrochemical studies in non polar media have traditionally employed quaternary ammonium electrolytes such as tetrabutylammonium tetrafluoroborate ($TBABF_4$).[10] Whilst these are sufficiently soluble in solvents such as anisole and chloroform, they are almost totally insoluble in cyclohexane ($\varepsilon = 2.02$). It was found that longer chain quaternary ammonium salts such as tetradecylammonium tetraphenylborate (TDATPhB) were sufficiently soluble in this medium to produce conducting solutions.[29] This is a surprising observation for a solvent that has no hydrogen-bond donor or acceptor properties and is used as a standard to describe a solvent with zero electronic polarisability in solvent polarity scales.[30] The solubility of the electrolytes can be significantly enhanced by either increasing the alkyl chain length or by making the TPhB anion more hydrophobic. The solubilities for various long chain quaternary ammonium electrolytes in cyclohexane are presented in Table (3.2.1). It is interesting to note that by the addition of a fluorine atom on the *para* position on the phenyl ring (TFPhB), the solubility increases by a factor in excess of five compared to that of TDATPhB. This is a remarkable result considering the low relative permittivity of the solvent.

Electrolyte	Solubility/mol dm^{-3}
$(C_8H_{17})_4N$ $(C_6H_5)_4B$	0.015
$(C_{10}H_{21})_4N$ $(C_6H_5)_4B$	0.045
$(C_{12}H_{25})_4N$ $(C_6H_5)_4B$	0.080
$(C_{10}H_{25})_4N(p\text{-}ClC_6H_5)_4B$	0.133
$(C_{10}H_{25})_4N(p\text{-}FC_6H_5)_4B$	>0.250

Table (3.2.1) Solubilities of tetraoctylammonium tetraphenylborate (TOATPhB), tetradecylammonium tetraphenylborate (TDATPhB), tetradodecylammonium tetraphenylborate (TDDATPhB), tetradecylammonium tetrachlorophenylborate

(TDATClPhB) and tetradecylammonium tetrafluorophenylborate (TDATFPhB) in cyclohexane at 25 °C.

The molar conductivities of TDATPhB, TDDATPhB, TDATFPhB and TDATClPhB in cyclohexane at 25 °C are presented in Figure (3.2.1). It can be seen that at a concentration of about 1×10^{-3} mol dm^{-3} there is a minimum in the molar conductivity that corresponds to a change in dominant charge carriers from single ions to triple ions. These data were be fitted to a modified Fuoss-Kraus equation to obtain the equilibrium constants for ion pair dissociation, K_P and triple ion formation K_T (eqn 3.1.16). Similar studies in such media have employed the Walden rule to determine Λ^0 for a given electrolyte in a different solvent. This approach is not possible for these novel electrolytes and so the values of the limiting molar conductivity were calculated using,

$$\lambda_0 = \frac{z^2 F^2}{6 N_A \pi r \eta} \qquad (3.2.1)$$

where F is the Faraday constant, N_A is Avogadro's constant, r is the radius of the ion and η is the viscosity of the solvent. The value for $\Lambda^0 = \lambda^{0+} + \lambda^{0-}$ for a 1:1 electrolyte. The ionic radii listed in Table (3.2.2) were calculated from the work of Edward[31] and the values thus obtained were in close agreement with similar ions studied elsewhere.[32] The equilibrium constants thus obtained for the four electrolytes in cyclohexane are listed in Table (3.2.2). As expected the molar conductivity of TDDATPhB was lower than that of the corresponding TDA electrolyte due to the larger size and hence the slower migration of the TDDA cation through the solution. In previous work[10] the association of similar electrolytes in anisole has been shown to be not significantly

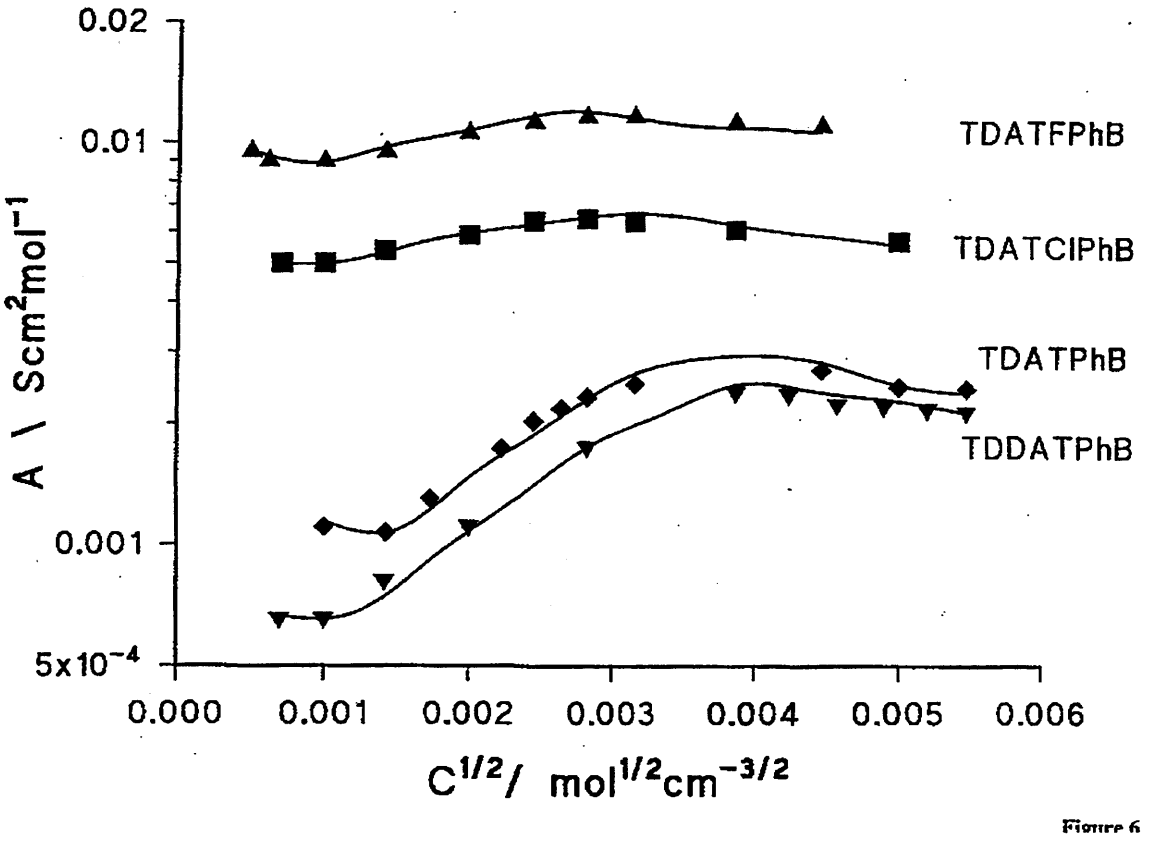

Figure (3.2.1) Plot of molar conductivity *vs.* the square root of the concentration for various electrolytes in cyclohexane at 25°C.

affected by the size of the quaternary ammonium cation in the range tetrapropyl to tetradecylammonium. This was thought to arise because the cation cannot be regarded as a hard sphere, but conversely the anion can penetrate into the space between the alkyl chain. These so-called 'penetrated ion pairs' have subsequently been shown to exist in several similar systems.[10,33,34]

Electrolyte	K_P/mol dm^{-3}	K_T/mol dm^{-3}	Λ_0/S cm^2 mol^{-1}	r^+/Å	r^-/Å
TDATPhB	$5.49x10^{-13}$	$1.05x10^{-3}$	*37.6*	*5.56*	*4.32*
TDDATPhB	$6.13x10^{-14}$	$3.61x10^{-4}$	*36.4*	*5.98*	*4.32*
TDATClPhB	$1.08x10^{-12}$	$1.65x10^{-3}$	*36.4*	*5.56*	*4.57*
TDATFPhB	$3.72x10^{-11}$	$1.89x10^{-3}$	*37.2*	*5.56*	*4.40*

Table (3.2.2) Properties of electrolytes in cyclohexane

The distance of closest approach, ***a***, for the TDATPhB salt was calculated using the theory of Bjerrum and found to be 8.51 Å. This is consistent with values measured in other non polar media.[10] This distance is less than the hard sphere radii of the ions which would give an interionic distance of 9.90 Å. This large difference is very surprising considering the bulky nature of the TPhB anion and the possibility of rotation in the decyl chains.

The X-ray crystal structure of TDATPhB was determined and is shown in Figure (3.2.2). It can be seen that, in the solid state, the boron atom is closer to the nitrogen atom (a = 6.33 Å) than the 9.90 Å suggested by the hard sphere radii. It should also be noted that the structure of the tetradecylammonium cation is not tetrahedral as would be expected.

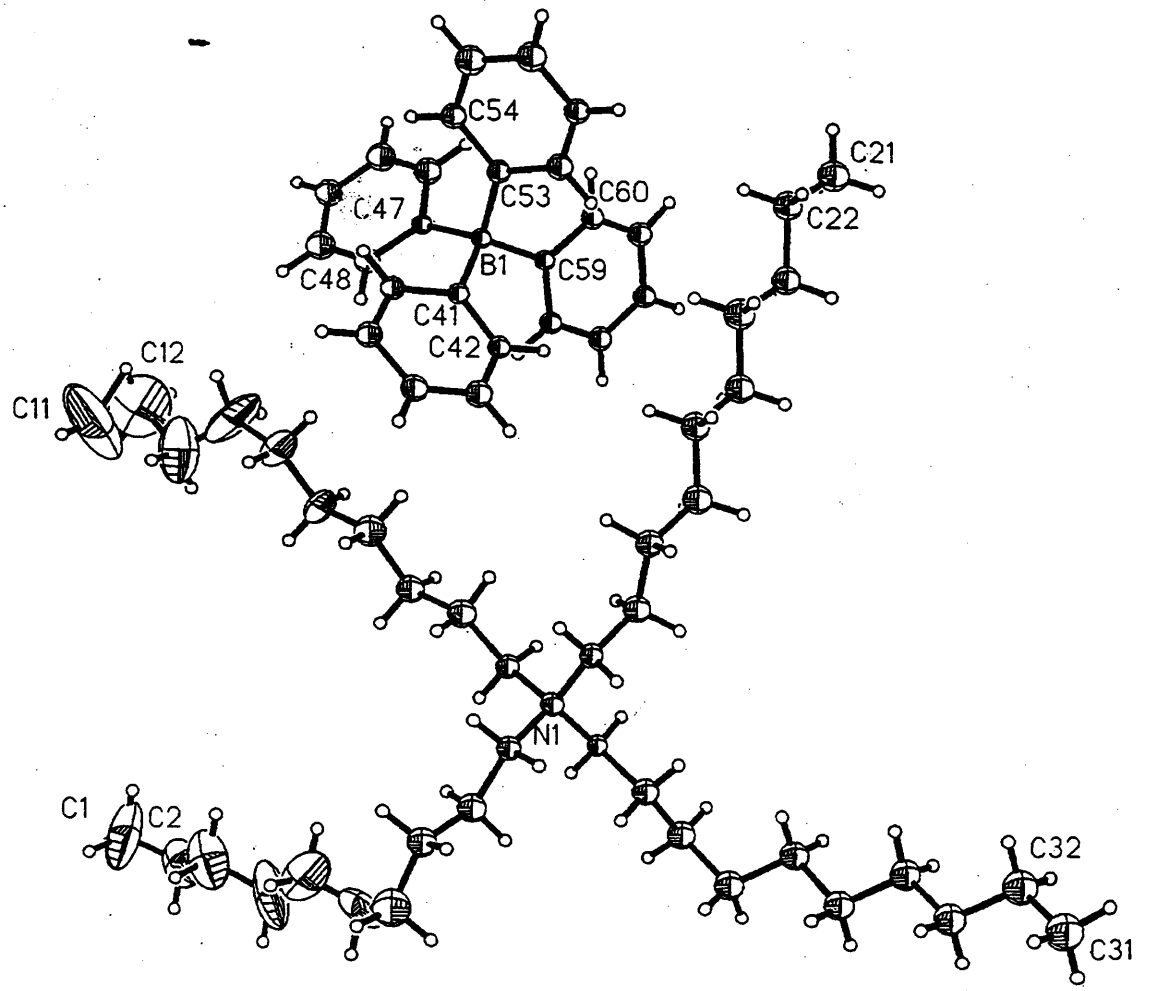

Figure (3.2.2) Thermal ellipsoid plot (SHELXTL-pc xp; Sheldrick 1991) of TDATPhB; ellipsoids represent 30% probability boundaries, H atoms are omitted for clarity

Ab initio calculations were performed to determine the minimum energy configuration of quaternary ammonium ions as a function of chain length. The first point to notice with tetraalkylammonium cations is that the geometries of lowest energy all give rise to disk-like structures. This is illustrated in Figure (3.2.3) for the triethyl-n-decylammonium cation, NEt_3Dec^+ as calculated by the *ab initio* Hartree-Fock method using a standard 3-21G basis set.[35]

It is characteristic of the lowest energy conformations from *ab initio* Hartree-Fock and density functional theory calculations on tetraalkylammonium cations, with ethyl, n-propyl and n-butyl as alkyl groups, for the closest carbon atoms to the nitrogen to be arranged tetrahedrally but for the next carbon atoms to lie approximately on a common plane containing the nitrogen atom (see Fig. 3.2.3).

Calculations were carried out on a few of the many possible conformations of Et_3DecN^+. A new conformation was obtained from the lowest energy geometry by rotation about one of the carbon-carbon bonds on the decyl chain (see inset Fig 3.2.4). The results are presented on Figure (3.2.4) where the energy (after geometry optimisation) is plotted relative to the lowest energy conformation. Since bond 9 merely rotates a methyl group at the end of the decyl chain this does not alter the energy and therefore still corresponds to the lowest energy conformation. Rotation about any bond except 1 and 9 leads to an energy increase close to 3 kJ mol^{-1}. Rotation about bond 1, that between the carbon atoms which the nearest (α) and next nearest (β) neighbours to nitrogen, leads to a much larger increase, 13 kJ mol^{-1}. This implies that the configurations of the α and β carbon atoms are probably fixed whereas the rest of the alkyl chain can adjust its conformation to suit the geometry of the environment. Nevertheless, although some modification of Fig.

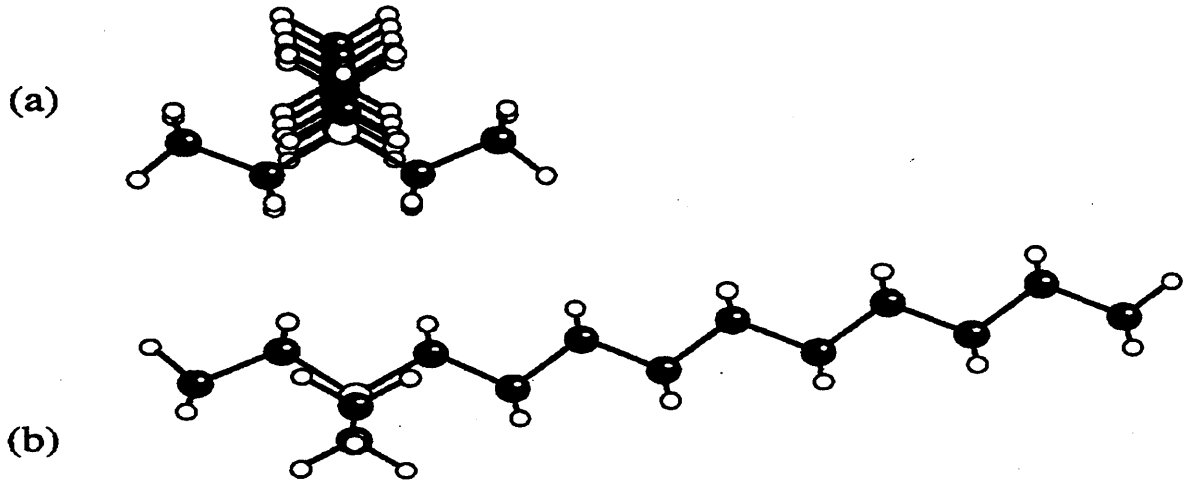

Figure (3.2.3) Two orientations [(b) is obtained by a 90° rotation of (a) about the vertical axis in the plane of the paper] of the lowest-energy conformation of the triethyl-*n*-decylammonium cation illustrating the 'disk like' nature of the ion. Carbon atoms are represented by filled circles, unfilled circles represent both nitrogen and hydrogen atoms, the former being larger.

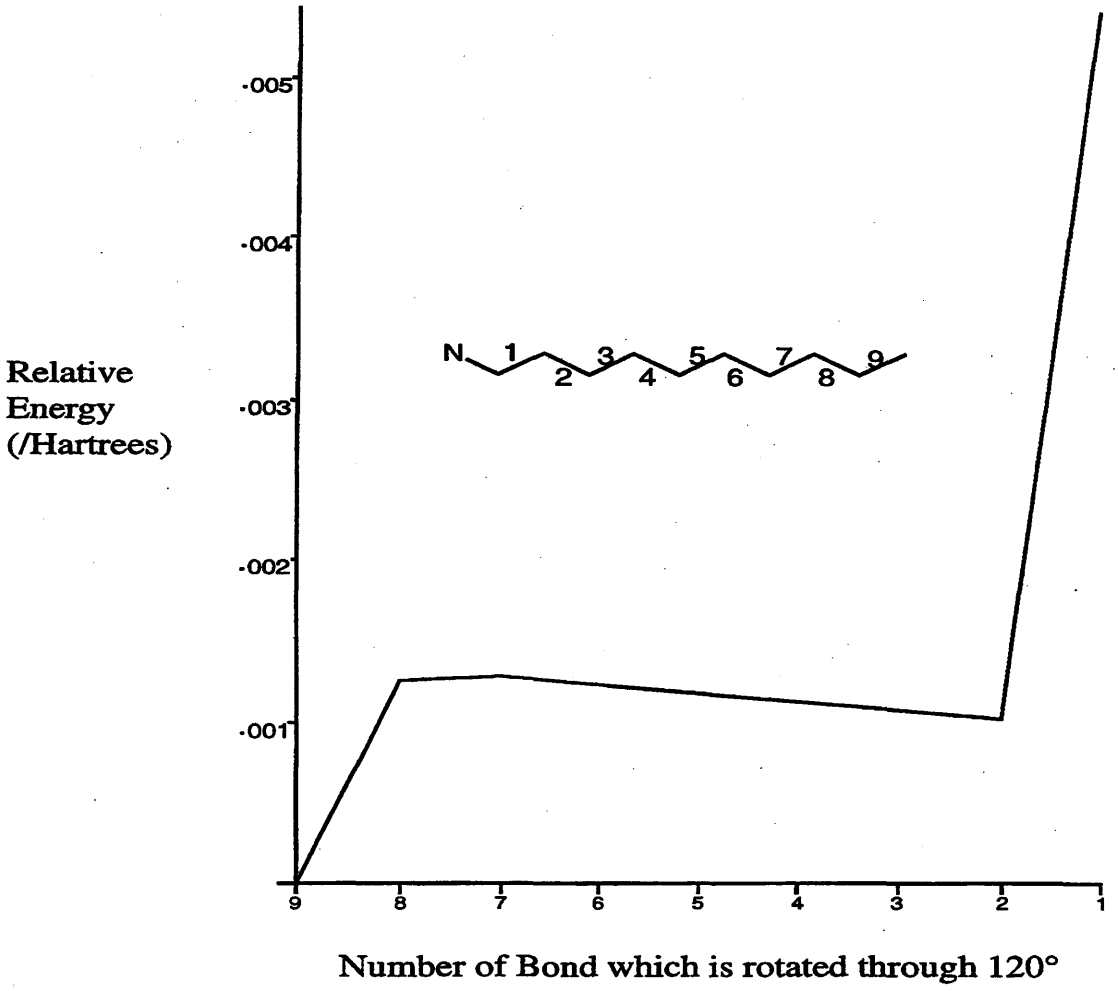

Figure (3.2.4) Change in conformational energy of the triethyl-n-decylammonium cation when one bond in the decyl chain is rotated through 120°

(3.2.4) may be in order when incorporated in a liquid phase, there will be a strong tendency for the eight closest carbon atoms to the nitrogen to form a flat disk-like arrangement. This, in turn, implies that there will be holes above and below the nitrogen atom in the random orientations of the alkyl chains, allowing small ions to penetrate. The closer the anion can approach, the more stable the ion pair, and this will reinforce the stability of the disk-like conformation leading to ion-ion distances closer than predicted assuming that the ions are hard spheres.

To investigate the ion-ion interactions further the nuclear Overhauser effects (NOE) of these electrolytes were studied in C_6D_6. The NOE is a result of dipole-dipole interactions between nuclei and as such has been used to reveal structural information of ion pairs in solution.[33,37] Interatomic NOEs were observed in the 1H NOESY spectra obtained for TDATPhB, TDDATPhB, TDATClPhB and TDATFPhB. For both TDATPhB and TDDATPhB the NOEs observed were negative and this is indicative of large correlation times (t_c). Figure (3.2.5) shows expansions of the NOESY cross-peaks between the ion pairs of TDATPhB and TDDATPhB. Strong interionic NOEs were observed between the *ortho* resonances of the phenyl rings and the $1CH_2$, 2-CH_2, 3-CH_2 and 4-CH_2 resonances of the alkyl chain of the TDA^+ cation. Weaker NOEs occur between the *meta* resonances and the same alkyl resonances, with the *para* resonances weaker still. For both the *ortho* and *meta* sites the strongest NOE is to the 1-CH_2 site, decreasing steadily in intensity to the 4-CH_2 site. For the *para* resonance NOE strengths are 2-CH_2 > 4-CH_2 > 1-CH_2 with no NOE observed to the 3-CH_2.

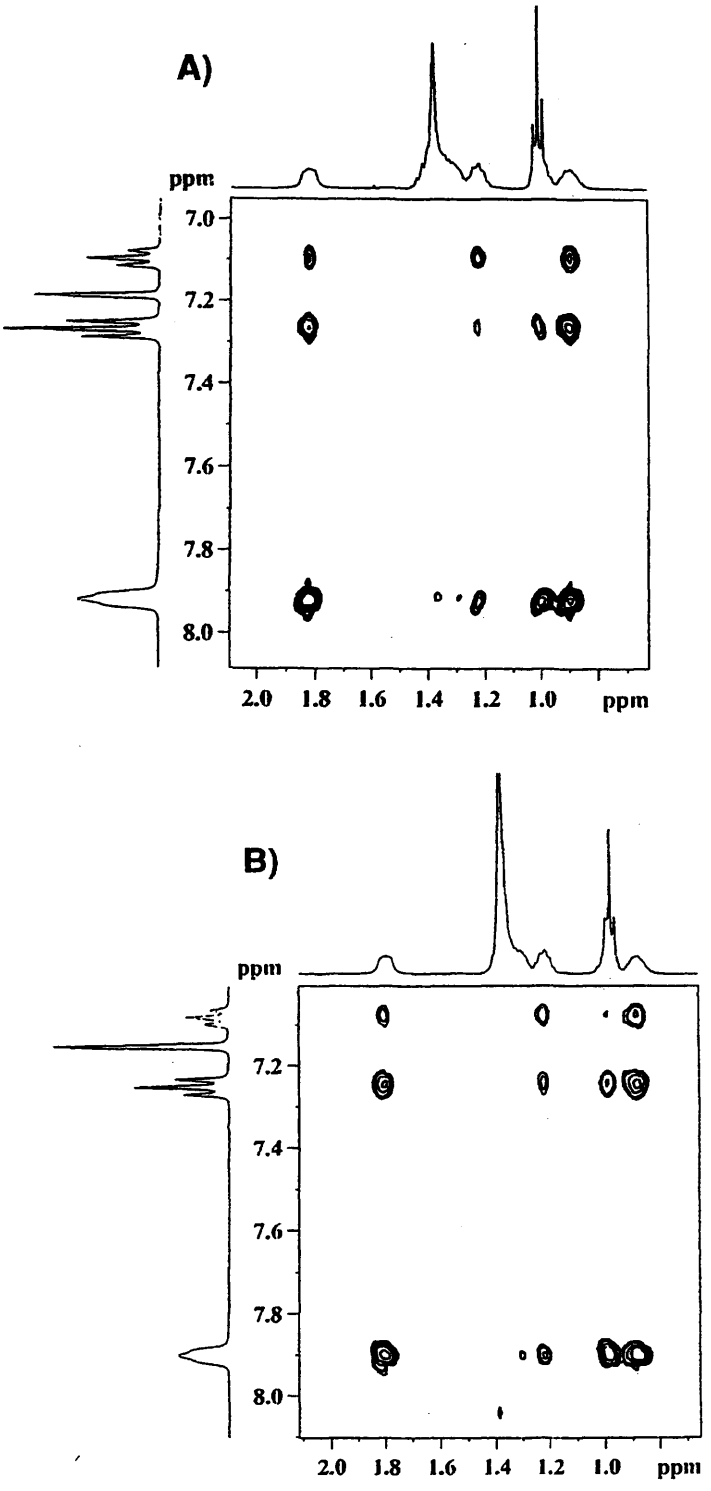

Figure (3.2.5) Expansion of two-dimensional NOESY spectra with projections of (A) TDATPhB and (B) TDDATPhB

The interionic NOEs observed for TDDATPhB follow the intensity trends seen in TDATPhB, with correlations from *ortho* > *meta* > *para*. These results suggest that for both these species in solution, the ion pair has a rigid structure whereby three of the phenyl rings of the tetrahedral anion are positioned between three of the tetrahedral cation alkyl chains, two staggered, base sharing tetrahedra. This is observed in the X-Ray crystal structure of the solid. There is clearly a discrepancy between the small interionic distances suggested by the NOEs and X-ray crystal data (about 6-7 Å) and the larger distances calculated from the conductivity data and listed in Table (3.2.1) (about 9-10 Å). This probably arises due to the simplification of the Bjerrum model used to calculate the latter value.

The NOEs observed in the chloro and fluoro-*para* substituted species (TDATClPhB, TDATFPhB) were positive. Figure (3.2.6) shows the NOESY cross-peaks between the ion pairs for TDATFPhB and TDATClPhB. A markedly different interaction is observed compared to non substituted tetraphenylborates, where the cross-peaks between the *ortho* and 1-CH_2 and 2-CH_2 resonances are very weak for TDATFPhB and unobserved in TDATClPhB. TDATFPhB shows strong NOEs from the *ortho* and *meta* resonances to alkyl resonances further along the chain, 3-CH_2 to 6-CH_2. This indicates that the bulkier *para*-fluoro substituent results in a looser positioning of the phenyl rings along the length of the cation alkyl chains. This trend increases further with the *para*-chloro substituted anion species TDATClPhB, with the *ortho* resonance showing a very weak NOE to 4-CH_2 and a strong interaction to CH_2's further along the chain from 5-CH_2. The *meta* resonance has strong cross-peaks to the 3-CH_2 increasing along to the 5-CH_2 and possibly further along the alkyl chain.

For both the TDATFPhB and TDATClPhB ion pairs the change in sign of the NOEs from negative to positive with respect to the non-substituted ion pair TDATPhB,

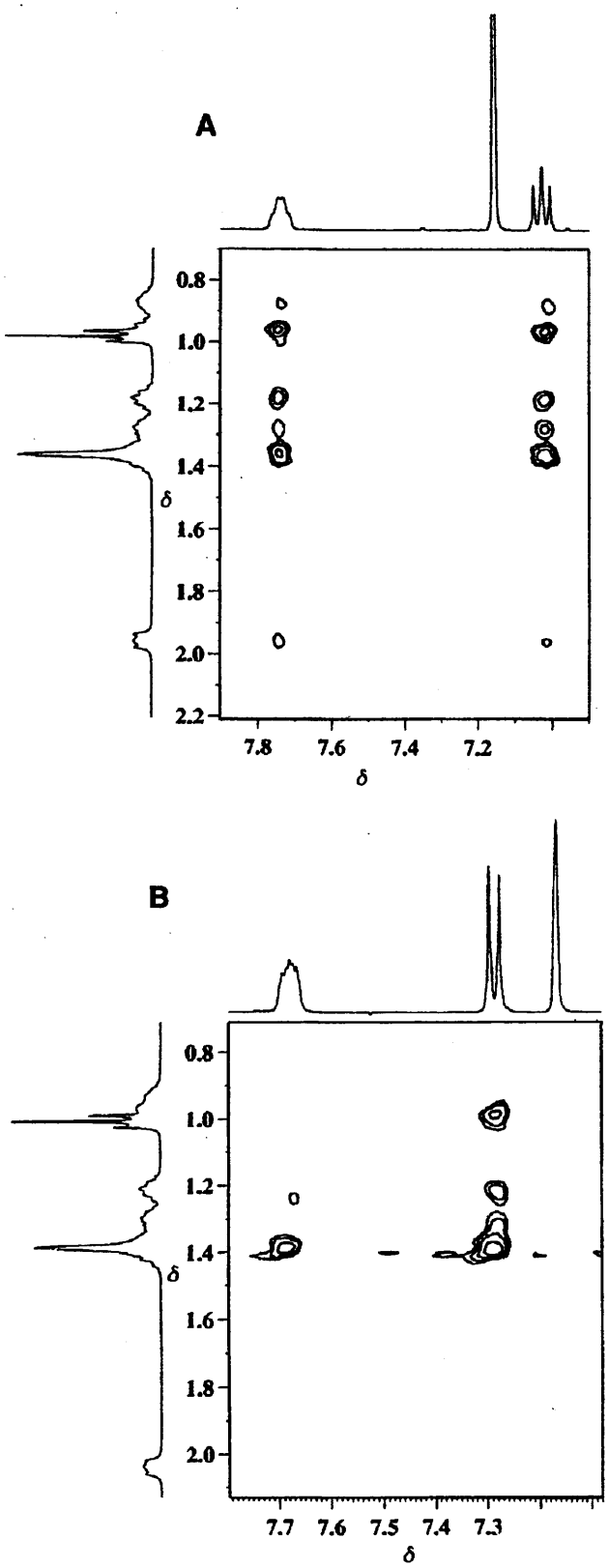

Figure (3.2.6) Expansion of two-dimensional NOESY spectra with projections of (A) TDATFPhB and (B) TDATClPhB

indicates a reduction in the correlation time (t_c) for the substituted ion pairs, despite a slight increase in molecular weight (TDATPhB = 898.81 u, TDATFPhB = 981.81 u, TDATClPhB = 1008.81 u) which would tend to make the NOEs more negative. This can best be explained if the ion pair adopts a much less rigid structure in solution with the bulkier *para* substituent, allowing for only one phenyl ring positioned between three alkyl chains, held much further out from the nitrogen centre of the cation, with considerably more degrees of freedom for both cation and anion.

There is a significant change in the conductivity for TDATClPhB and TDATFPhB solutions compared to TDATPhB which must be due to the greater hydrophobicity of the ion and hence its ability to form charge carriers. The TFPhB salt is more hydrophobic and migrates faster as it is smaller that the corresponding chloro substituted ion. The conductivities of these electrolyte solutions are comparable to those for other, more polar solvents which are routinely used for electrochemical investigations.[33]

For all of the electrolytes studied there is a decrease in the molar conductivity when the concentration increases above about 0.01 mol dm^{-3}. This is classically described as being due either to an increase in solution viscosity, hence decreasing ion mobility or the formation of quadrupoles thus decreasing the number of charge carriers. The conductivity of TDATPhB was therefore studied in a series of solvents to elucidate this observation.

The effect of the solvent upon the concentration at which the maximum molar conductivity occurs can be seen in Figure (3.2.7). The conductivity of TDATPhB in

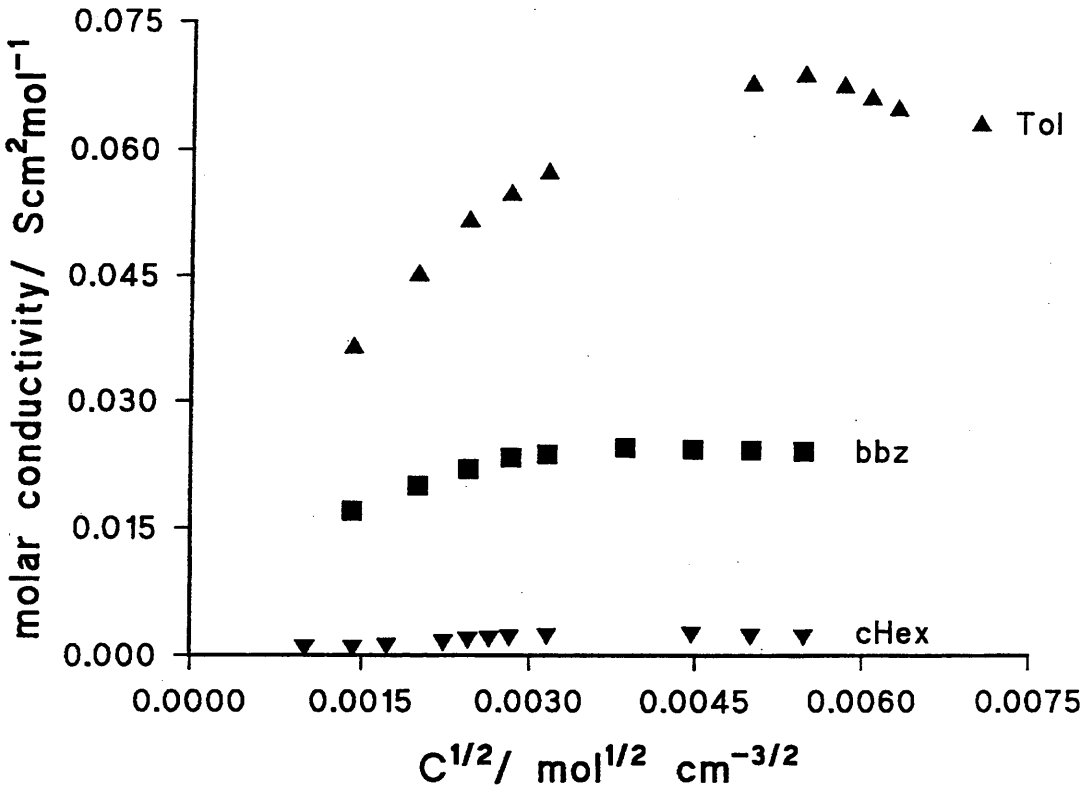

Figure (3.2.7) Plot of molar conductivity *vs.* the square root of the concentration for TDDATPhB in cyclohexane, butylbenzene and toluene at 25 °C

cyclohexane (cHex), (ε = 2.02; η = 0.898 cP) is compared with that in butylbenzene (bbz), (ε = 2.36; η = 1.04cP) and toluene (Tol), (ε = 2.38; η = 0.59) (data from ref. 38). The three solvents have been chosen because bbz and Tol have similar dielectric properties but different viscosities, while cHex and bbz have similar viscosities but different dielectric properties. If the maximum is caused by the formation of quadrupoles then it would be expected that the maximum for the least polar solvent (cHex) would occur at a lower concentration than the other two. If, however, the maximum was caused by changes in viscosity then the maximum would occur at a higher concentration for the least viscous solvent (Tol). Figure (3.2.7) shows that the maximum for cHex and bbz occur at approximately 0.01 mol dm^{-3} whereas that for toluene is about 0.03 mol dm^{-3}. This suggests that the decrease in molar conductivity with increasing concentration is caused by a subsequent increase in the solution viscosity. To analyse this trend further the viscosities of all of the solutions were measured.

Figure (3.2.8) shows the relative viscosity η_r ($\eta_r = \eta/\eta_o$) of the electrolyte solutions studied in this work as a function on electrolyte concentration. The first point to notice is that there is a large increase in the viscosity with concentration. The relative viscosity, for a solution of 0.01 mol dm^{-3} TDATPhB in cHex is equivalent to a 4 mol dm^{-3} aqueous NaCl solution.[39] Hence these large quaternary ammonium electrolytes are seen to have a dramatic effect on the viscosity. The viscosity of an electrolyte solution is classically described by the Jones-Dole equation [40]

$$\eta_r = 1 + A\sqrt{c} + Bc \qquad (3.2.2)$$

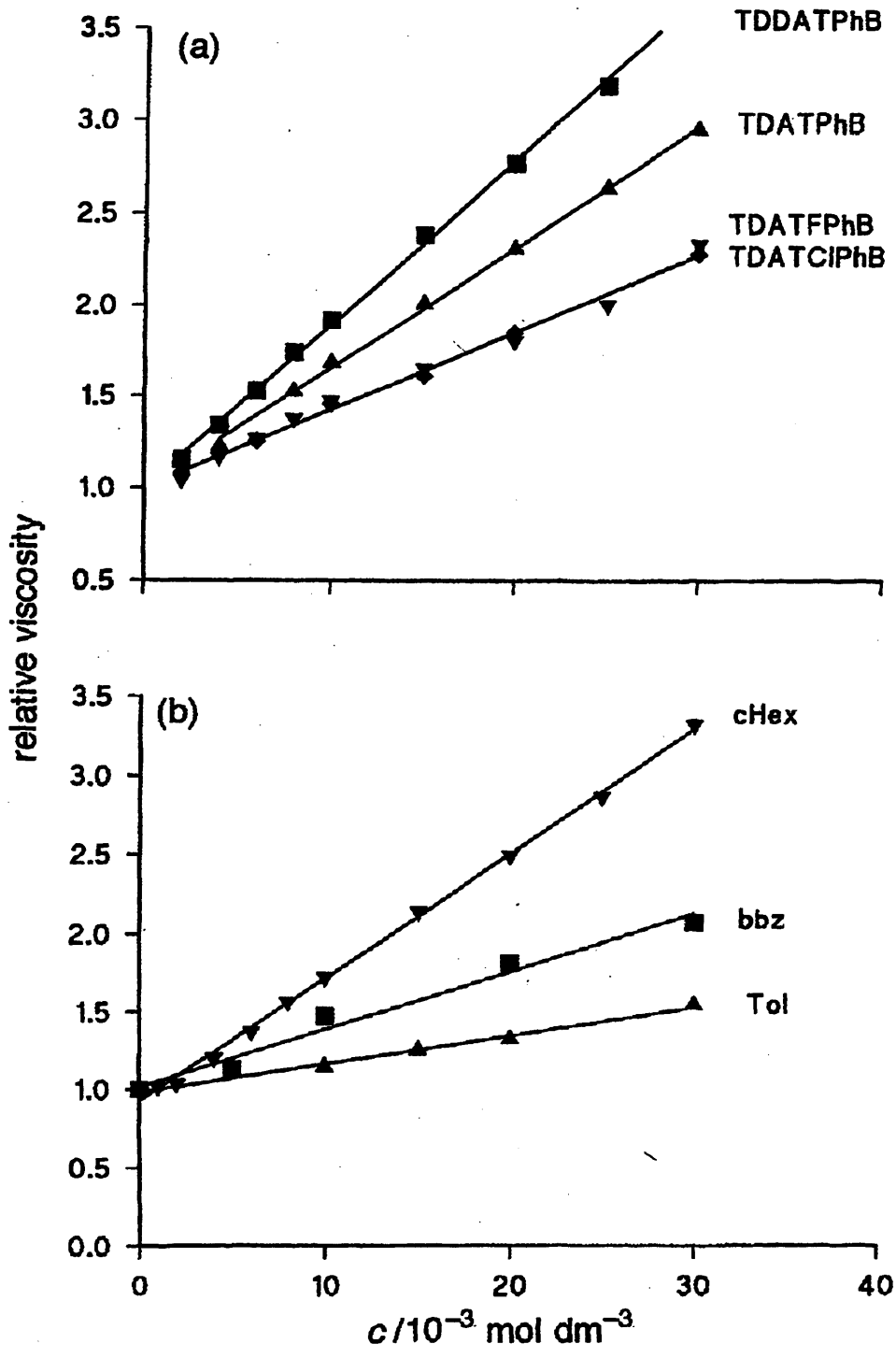

Figure (3.2.8) Plots of relative viscosity *vs.* electrolyte concentration for the solutions for (a) TDATPhB, TDDATPhB, TDATFPhB and TDATClPhB in cHex and (b) TDDATPhB in cHex, bbz and toluene at 25°C.

where A and B are constants. The constant A arises from the stiffening effect on the solution of the electric forces between the ions, which in an aqueous solution, tend to maintain a space lattice structure. The A coefficient is given by the Falkenhagen-Vernon equation.[41]

$$A=\frac{0.2577\Lambda_o}{\eta\sqrt{\varepsilon T}\lambda_o^+\lambda_o^-}\left[1-0.6863\left(\frac{\lambda_o^+-\lambda_o^-}{\Lambda_o}\right)^2\right] \qquad (3.2.3)$$

The value of A for TDATPhB in cHex is 0.15 $mol^{-1/2}$ $dm^{-3/2}$ which is much higher than for aqueous electrolytes [40] (typically 0.005 $mol^{-1/2}$ $dm^{-3/2}$) reflecting the increased ion-ion interactions in the low dielectric constant. The A factor is, however, insignificant compared to the value of the B coefficient.

The B coefficient is somewhat empirical and describes the effect of the electrolyte on the solution structure. A positive value implies that the solution is more ordered than the pure liquid whereas a negative value shows that the electrolyte is breaking up the solvent structure. The B coefficient is made up from 4 major effects: ionic solvation, structure breaking effects, steric effects and the ability of the ion field to bring about long-range order to the solvent molecules.[41] In the solutions studied in this work, it is clear that ion-solvent and solvent-solvent interactions will be negligible due to the large size of the ions and the low polarity of the solvent. Hence the controlling factor will be the size of the ions, and the flow of comparatively small cHex molecules past these large ion aggregates.

Figure (3.2.9) shows a plot of $(\eta_r-1)/c^{1/2}$ verses $c^{1/2}$ for all of the electrolytes and solvents studied in this work. All of the solutions studied fit the Jones-Dole equation

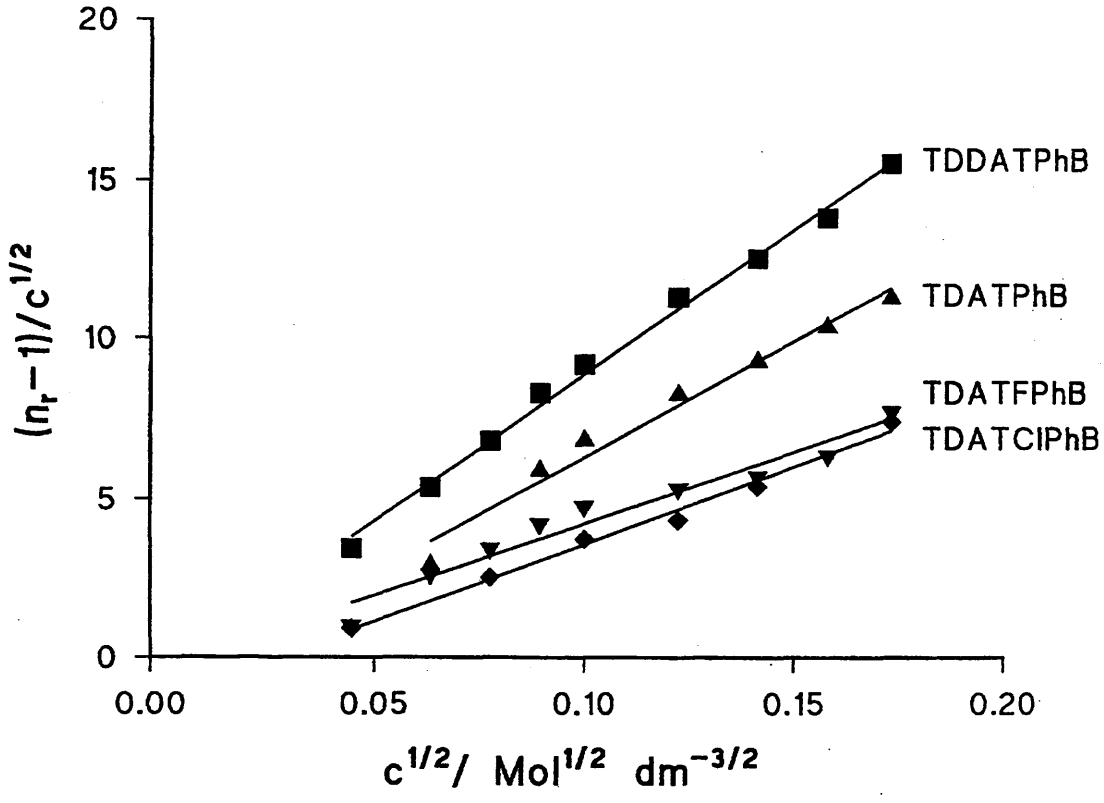

Figure (3.2.9) Jones-Dole plots for the data shown in Fig (3.2.7a)

very well. The value of B for all systems is large and positive showing that that the electrolyte solutions are highly structured compared with the pure solvent.

The very large value of B, typically 100 times larger than most aqueous electrolyte solutions, must be due to the inordinately large size of the ionic species in comparison to the solvent molecules. It has been shown that the B factor can be related to the effective rigid molar volume,[42] V_{eff}. Since K_p and K_T are so small the predominant species (about 99%) in the electrolyte solutions studied will be in the form of ion pairs. Figure (3.2.10) shows a plot of B versus V_{eff} for the four electrolytes in cHex. Values of V_{eff} were calculated from the ionic radii listed in Table (3.2.1). If all of the electrolytes are assumed to be ion pairs then a very poor correlation is obtained. If, however, TDATPhB and TDDATPhB are assumed to form quadrupoles then V_{eff} increases and a very good correlation is obtained.

Assuming that these species are evenly distributed throughout the solution then the average distance between these ion pairs in a 0.03 mol dm^{-3} solution will be 3.8 nm. Considering that the radius of a TDATFPhB ion pair is approximately 0.9 nm then there is on average 2.0 nm or about four cyclohexane molecules between each ion pair. It is immediately apparent why the viscosity of such electrolyte solutions rises so rapidly and the behaviour of such systems is probably more akin to a "dilute" molten salt than an electrolyte solution.

Figure (3.2.11) shows the molar conductivity multiplied by the relative viscosity to compensate for the decreasing ion mobility versus the square root of the concentration as a test of equation (3.1.16). Since the mole fraction of single ions is insignificant a straight line should be observed if triple ions are the major charge carriers and quadrupole formation is insignificant. This is indeed the case for TDATClPhB and TDATFPhB. There may be some curvature at higher concentrations for TDA- and

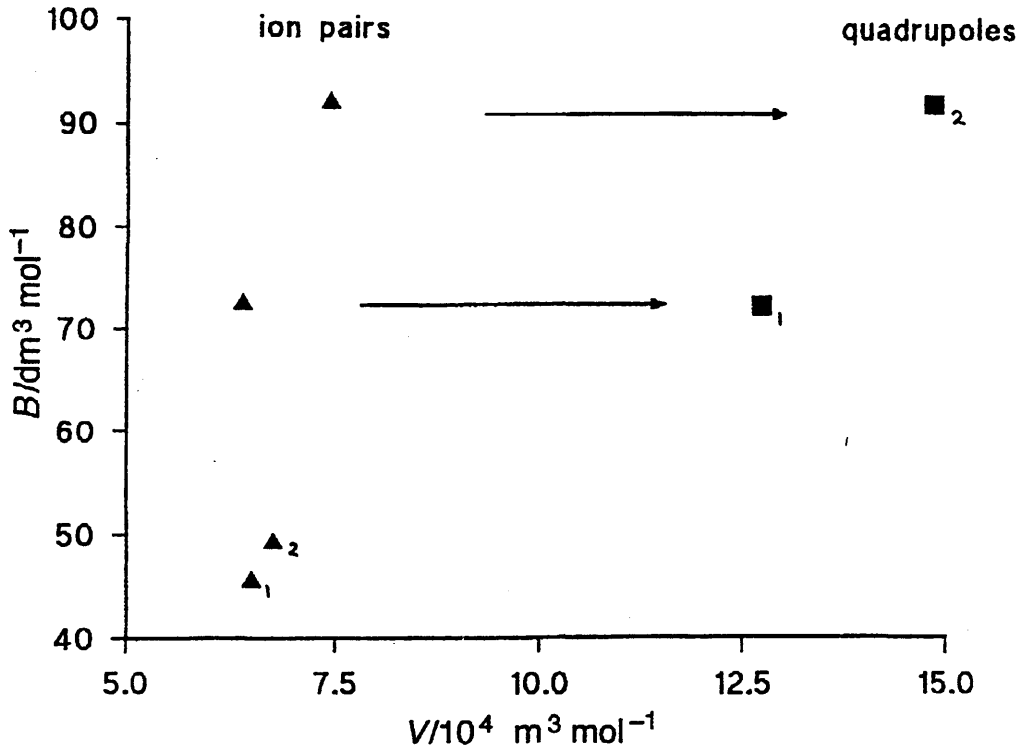

Figure (3.2.10) Plot of the effective volume *vs.* coefficient B calculated from Fig. (3.2.9) (▲1 & ▲2 = TDATFPhB and TDATClPhB respectively; ■1 & ■2 = TDATPhB and TDDATPhB respectively)

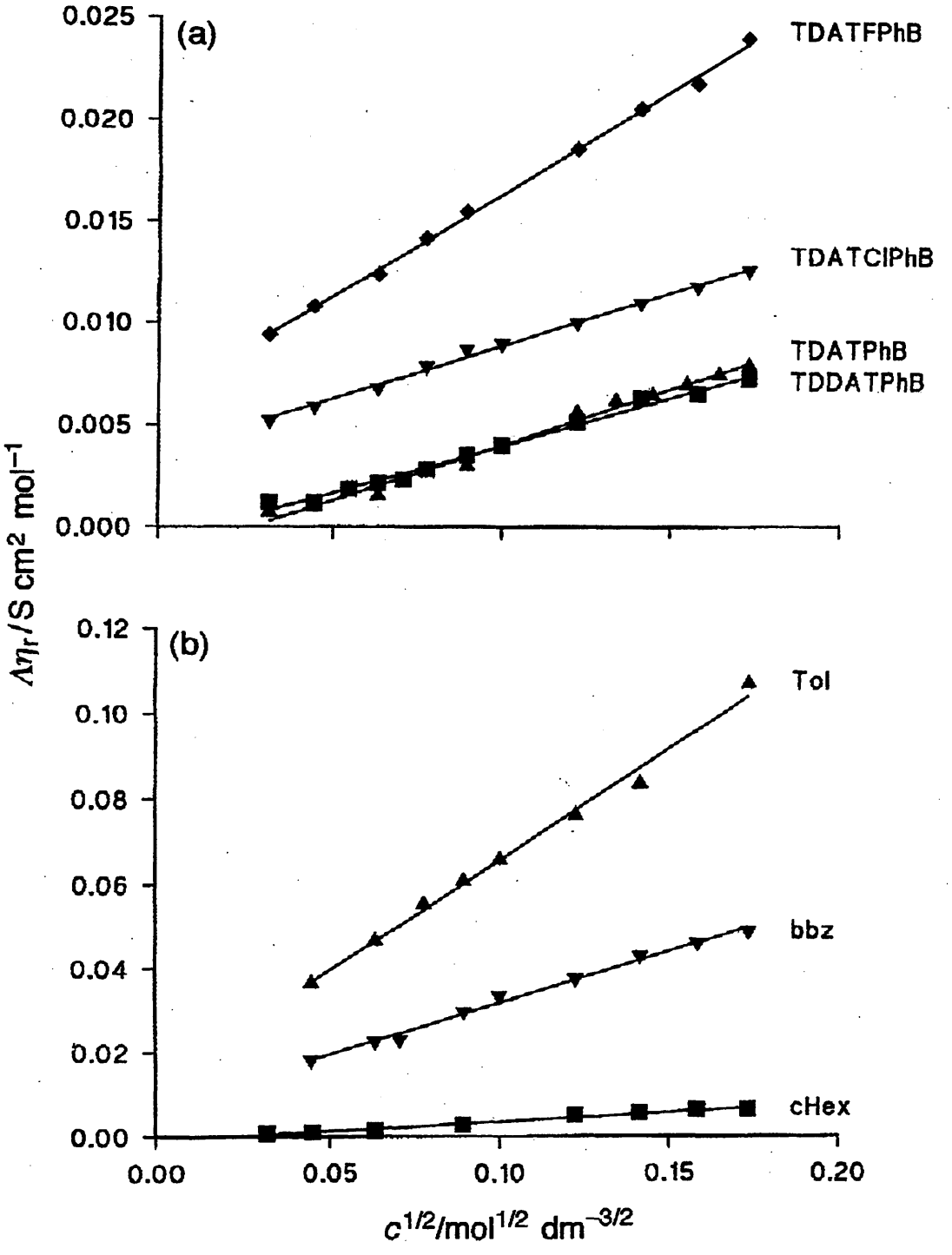

Figure (3.2.11) Plot of $\Lambda\eta_r$ *vs.* the square root of the concentration for (a) TDATPhB, TDDATPhB, TDATFPhB and TDATClPhB in cHex and (b) TDDATPhB in cHex, bbz and toluene at 25°C

TDDA- TPhB which suggests that quadrupoles are formed in solution. Likewise, Figure (3.2.11(b)) shows that for the slightly more polar solvents, Tol and bbz, the plots compensating for ion mobility show good correlation with the model whereas that in cHex shows some deviation.

3.2.2 Conductivity measurements in Supercritical Carbon Dioxide

Figure (3.2.12) shows the conductivity of 0.019 mol dm^{-3} TDATPhB in $scCO_2$ at 100 bar and cyclohexane at ambient pressure as a function of temperature. These measurements were all made when the system had reached equilibrium, starting from the highest temperature to ensure maximum solubility. As can clearly be seen, in $scCO_2$, the conductivity decreases by an order of magnitude when $T < T_c$. The values below T_c are within the noise of the measuring technique showing that the electrolyte is practically insoluble in the liquid phase. The sudden rise above T_c shows that the electrolyte is soluble in $scCO_2$ which is in itself a remarkable observation.

Comparison of these values with those for cyclohexane show that they are lower across the temperature range measured. The conductivity of an electrolyte solution will depend upon the degree of association and the migration of the charged species through the solution. For a given electrolyte, the former will be governed by the relative permittivity of the solvent, whereas the latter depends on the viscosity of the medium. Since both media have similar relative permittivity, the conductivity of the electrolyte in $scCO_2$ should be higher than cyclohexane because of the difference in viscosity (e.g. at 40°C $\eta(scCO_2(200bar)) = 8 \times 10^{-4}$; $\eta(cHex) = 7 \times 10^{-3}$ Poise).[43,44] The observed trend can only be accounted for if the electrolyte is not fully dissolved in $scCO_2$. The conductivity increases at a faster rate in $scCO_2$ than cHex which

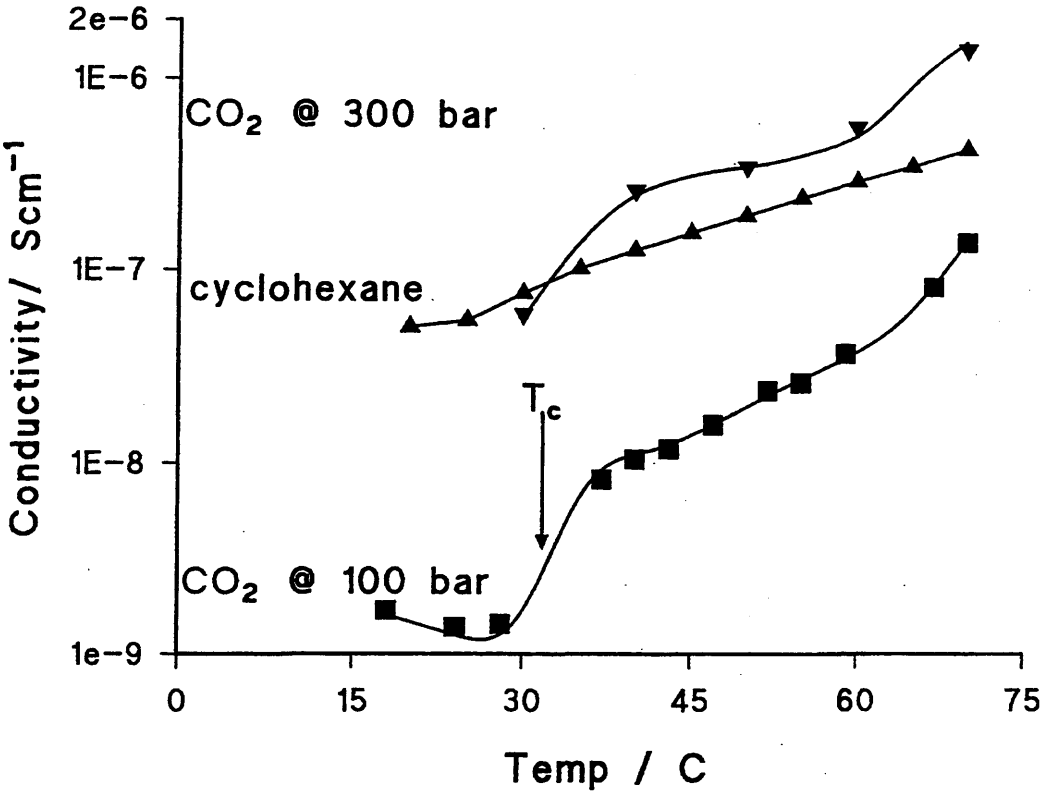

Figure (3.2.12) Effect of temperature on the conductivity of TDATPhB (19.2 mMol dm^{-3}) in cyclohexane (1 bar) and $scCO_2$ at 100 and 300 bar

suggests that the solubility of $scCO_2$ increases significantly with temperature (the electrolyte is completely soluble in cHex under the given conditions).

The conductivity of the TDATPhB/$scCO_2$ solutions at 300bar were more than an order of magnitude larger than those at 100 bar (Fig 3.2.12). This can only arise from an increase in the solubility of the electrolyte since this increase in pressure approximately doubles the viscosity[44] which should decrease the conductivity if all of the electrolyte was dissolved. In the supercritical state the solubility of the electrolyte will clearly be dependent on the ability of the solvent molecules to pack around the solute ions. The increased conductivity in $scCO_2$ suggests that the viscosity of this medium must be lower than cHex, again showing that the electrolyte is dissolved in a supercritical fluid.

The conductivity of molten TDATPhB was measured at 120°C and found to be 1.55 x 10^{-4} S cm^{-1}. This value is two orders of magnitude larger than $scCO_2$ or cyclohexane at 70°C showing that the conductivity in $scCO_2$ does not correspond to the electrolyte simply melting in the cell. Studies in which 20 mMol dm^{-3} TDATPhB was dissolved in $scCO_2$ at 300 bar and 70°C and a cell with sapphire windows showed that a single, homogeneous, supercritical phase is formed and all of the electrolyte dissolves.

Figure (3.2.13) shows the conductivity of the same TDATPhB/ $scCO_2$ solution, as shown in Figure (3.2.12), as a function of pressure. The conductivity at all temperatures is seen to increase dramatically as the pressure is raised above P_c. Again this is thought to be due to the change in solubility of the electrolyte as the density increases. Figure (3.2.16) shows the conductivity of the TDATPhB/$scCO_2$ solution at 70°C as a function of reduced density ($\rho_r = \rho/\rho_c$). The density of $scCO_2$ was calculated from previous work.[45] Three regions can be observed; where $\rho_r < 0.5$, a large increase in conductivity is observed, where $0.5 < \rho_r < 1.5$ there is little change in the

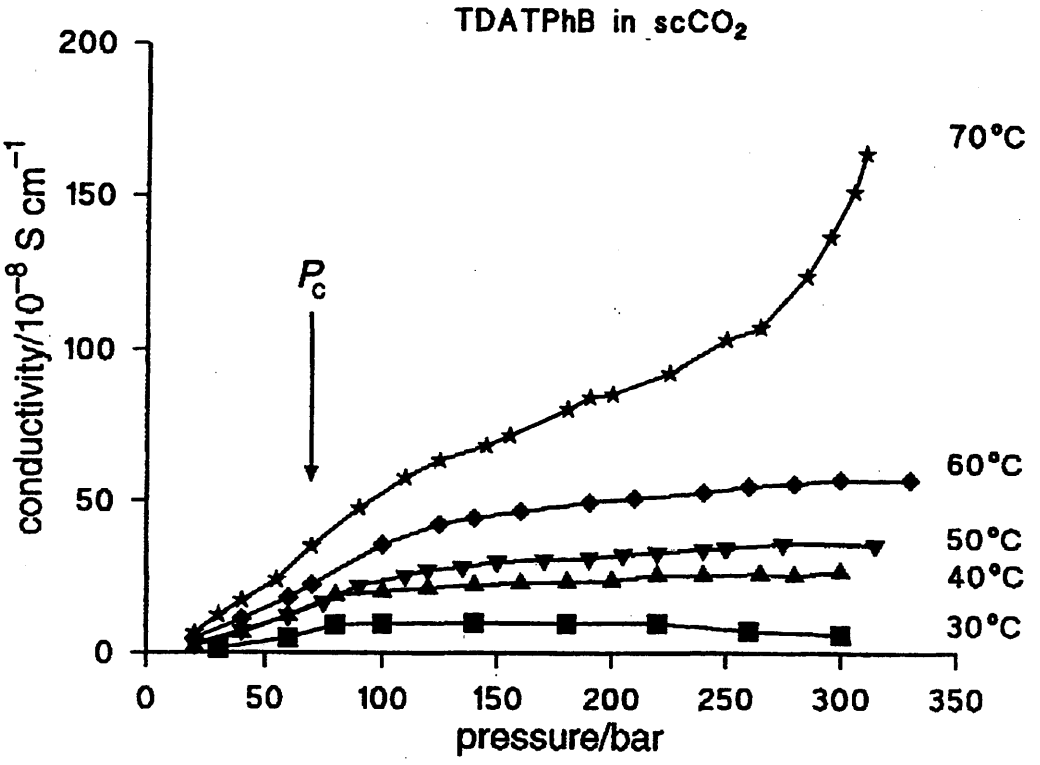

Figure (3.2.13) Effect of pressure on the conductivity of TDATPhB (19.2 mMol dm^{-3}) in $scCO_2$ at various temperatures.

conductivity and where $\rho_r > 1.5$ a large increase in conductivity is again seen. These three regions have been observed in numerous other solvent property studies of supercritical fluids[46-48] and are thought to result from changes in local solvent density. This so-called 3 density region solvation model assumes that in the subcritical region ($\rho_r < 0.5$) solvation is determined by the number of solvent molecules which can cluster around a solute ion i.e. the solvation sheath surrounding the ion is incomplete. As ρ_r increases the solvation sheath becomes complete and further increases in density cause clusters of solvent molecules and do not significantly affect solvation. The solvation process has been likened to a Langmuir adsorption equilibrium model [47-49] and a typical response can be seen in Figure (3.2.14), even though the conductivity is governed by more factors than solubility. When $\rho_r > 1.5$ there is a significant increase in solution conductivity. This region has previously been shown to produce increased clustering of solvent molecules around the solute. Since this is clearly the region in which solubility increases markedly, it can be assumed that the TDATPhB ions or clusters need to be highly solvated before significant dissolution occurs. This is expected for a charged species in a medium with a relative permittivity less than two.

The molar conductivities of TDATPhB and TDATFPhB in $scCO_2$ at 70° C and 300 bar are presented in Figure (3.2.15). Comparison of this data with that presented in Fig. (3.2.1) shows that the molar conductivity of TDATPhB in $scCO_2$ is an order of magnitude larger than that in the corresponding cHex solution. As expected this must result from the decreased viscosity and the resultant increase in the ionic mobility.

The ion pair dissociation and triple ion formation constants for the two electrolytes in $scCO_2$ are presented in Table (3.2.3). Whilst the ion pair dissociation constants are similar to those observed in cyclohexane the triple ion formation constants are smaller

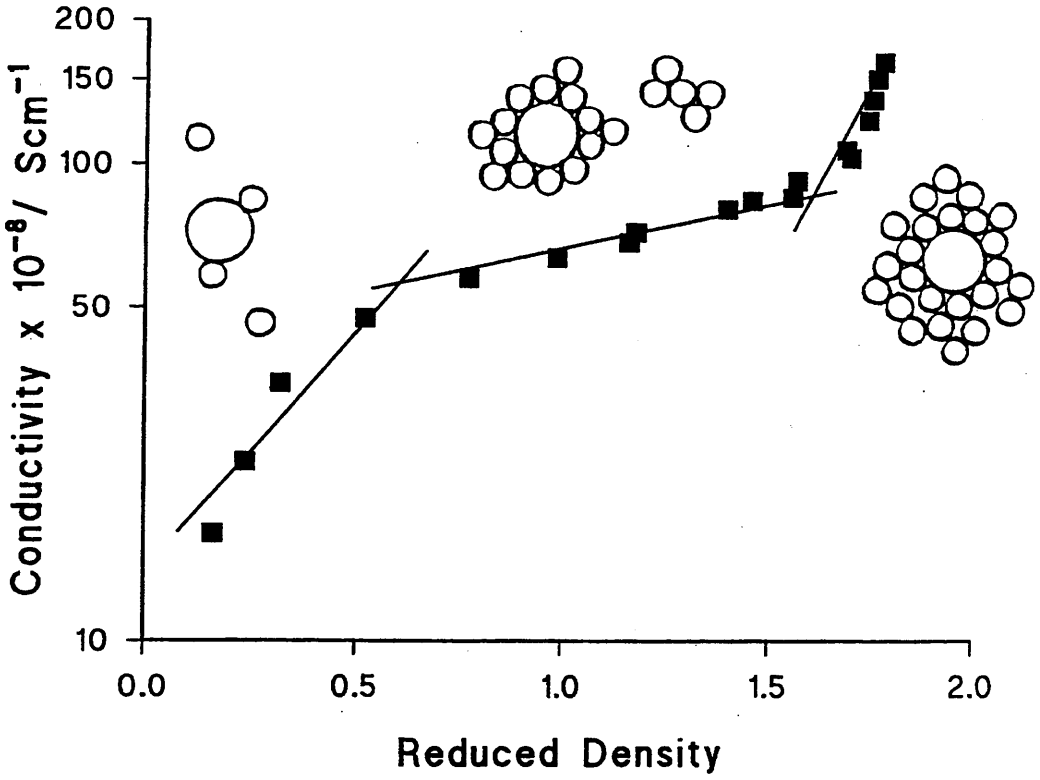

Figure (3.2.14) Conductivity of TDATPhB in $scCO_2$ at 70°C as a function of reduced density.

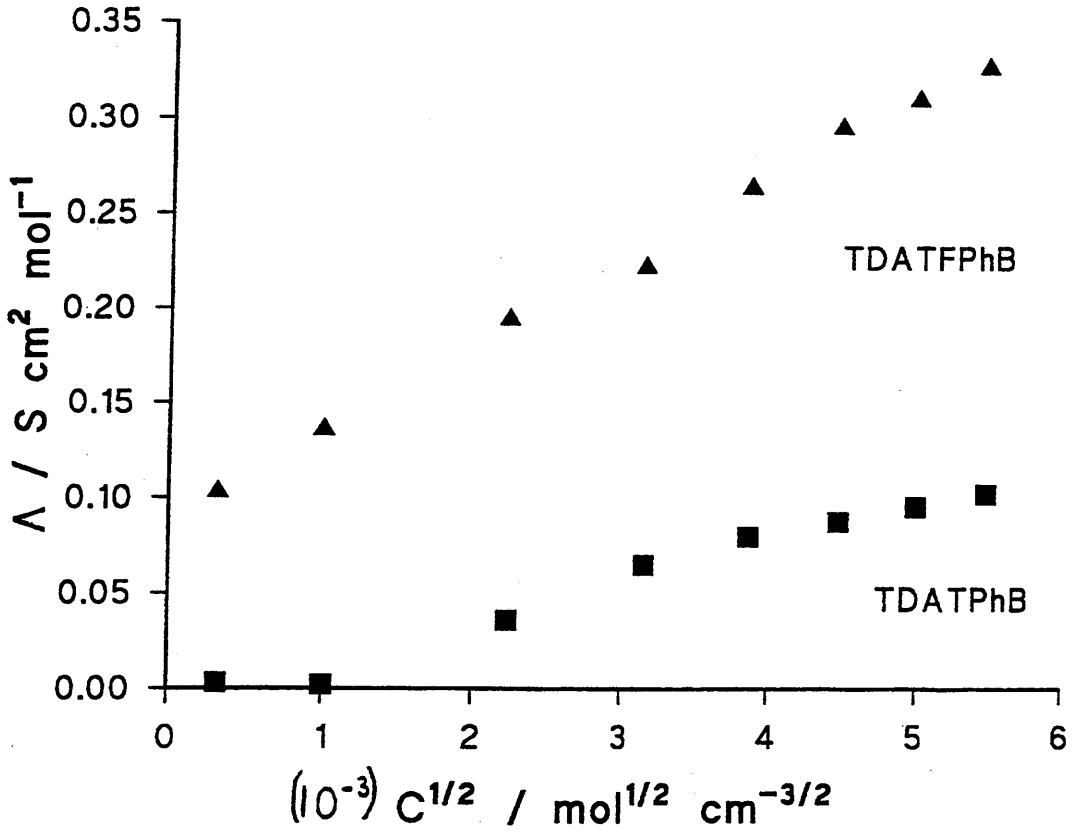

Figure (3.2.15) Plot of the molar conductivity *vs.* the square root of the concentration for TDATPhB and TDATFPhB in $scCO_2$ at 70°C and 300 bar.

in $scCO_2$. This must result from the decrease in relative permittivity. The equivalent conductivities for solutions of 10mMol TDATPhB in cHex and $scCO_2$ were calculated from equation (3.1.14). The values are given in Table (3.2.4) and are in accordance with those observed in both media. We conclude that even though the ionic strength is less in $scCO_2$, the increase in conductivity must result from the high ion mobilities in the supercritical region.

Electrolyte	K_P/mol dm^{-3}	K_T/mol dm^{-3}	Λ_0/S cm^2 mol^{-1}
TDATPhB	7.12×10^{-13}	4.27×10^{-4}	*450.2*
TDATFPhB	4.33×10^{-11}	1.05×10^{-3}	*445.4*

Table (3.2.3) Properties of electrolytes in $scCO_2$.[1]

Solvent	$\alpha \times 10^5$	$\alpha_T \times 10^5$	$\Lambda_{calc} \times 10^4$/ S cm^2 mol^{-1}	$\Lambda_{obs} \times 10^4$/ S cm^2 mol^{-1}
$scCO_2$	*0.84*	*19.70*	*6.29*	*6.50*
cHex	*0.74*	*7.05*	*0.21*	*0.20*

Table (3.2.4) Theoretical and experimental values of the molar conductivity of 10 mMol TDATPhB in $scCO_2$ and cHex solutions.

Figure (3.2.16) shows the molar conductivity of the two electrolytes multiplied by the solvent viscosity as a function of electrolyte concentration. At low concentrations the product $\Lambda\eta$ for each electrolyte in $scCO_2$ and cHex increases similarly with concentration with divergence occurring at higher concentrations. This result gives

[1] The values of the limiting molar conductivities were calculated from the Walden Rule and assuming that $\eta CO_2 = 0.075$ cP and ηcHex = 0.898 cP.

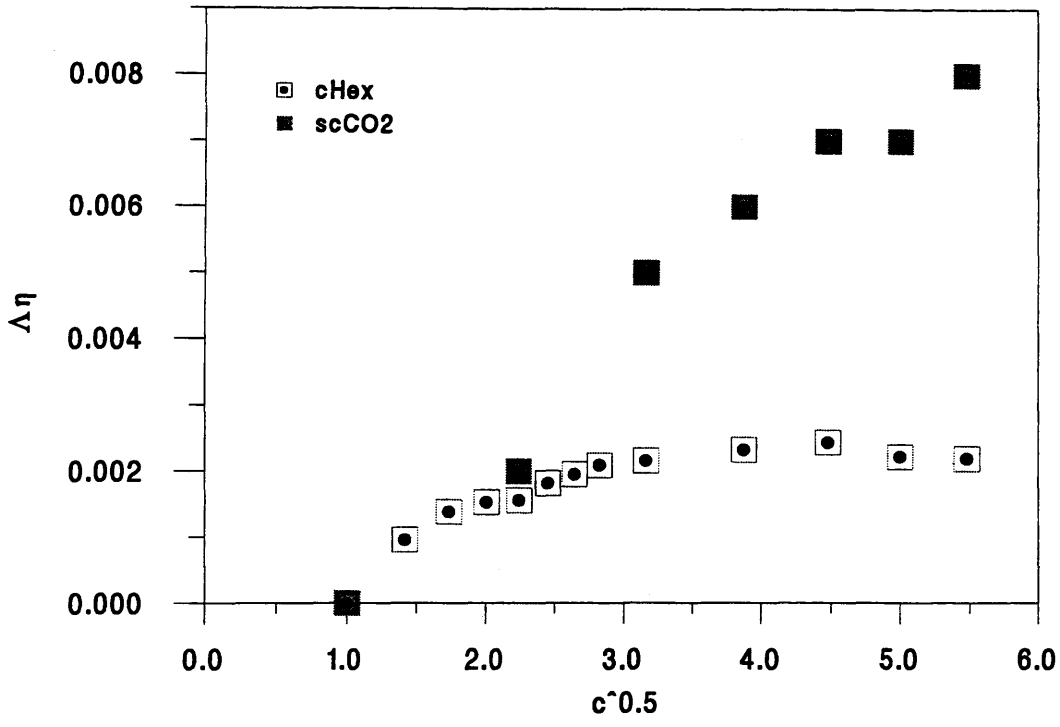

(Figure 3.2.16) Plot of $\Delta\eta_r$ *vs.* the square root of the concentration for TDATPhB in cHex (25°C) and $scCO_2$ (70°C and 300 bar).

information about the structure of electrolyte solutions in supercritical fluids. In cHex a maximum is observed which has previously been shown to result from the large increase in relative viscosity and the resulting decrease in ionic mobility. The electrolyte appears to have a different effect on the solution structure in $scCO_2$ than in cHex. In non-polar sc fluids the solute is known to cause an increase in the local density.[34] It is proposed that an increase in electrolyte concentration causes a decrease in the density of "free" solvent molecules. Hence the decrease in mobility with increasing concentration which is caused by increased ion-ion interactions is negated to some extent by the decrease in ion-solvent interactions.

3.3 Conclusions

It has been shown that by the addition of long chain tetraalkylammonium electrolytes, extremely non-polar media such as cyclohexane and supercritical carbon dioxide can be made sufficiently conducting to perform electrochemical experiments. The ions are found to be very highly associated forming penetrating ion pairs. X-Ray crystallography and minimum energy calculations have found that quaternary ammonium cations are planar in structure, rather than tetrahedral, allowing an unexpectedly small distance of closest approach in both the solid and solution states. NOE data confirm that the tetraalkylammonium tetraphenylborate electrolytes are more highly associated in solution than the corresponding halogen substituted tetraphenylborates.

The solubility of these electrolytes in $scCO_2$ are shown to be governed by the pressure and this has been ascribed to changes in density around the solute molecule. The molar conductivities in the supercritical phase are significantly greater than those observed in liquid media and this is a consequence of the extremely low viscosity of the medium.

REFERENCES CHAPTER III

1) G. Geblewicz and D.J. Schiffrin, *J. Chem. Soc., Faraday Trans.*, 1988, **84,** 561

2) N.K. Bjerrum, *Kgl. Danske Videnskab. Selskab.*, 1926, **9**, 7

3) R.M. Fuoss and C.A. Kraus, *J. Am. Chem. Soc.*,1933, **55**, 21

4) R.M. Fuoss and C.A. Kraus, *J. Am. Chem. Soc.*,1933, **55**, 476

5) R.M. Fuoss and C.A. Kraus, *J. Am. Chem. Soc.*,1957, **79**, 3304

6) R.M. Fuoss, *Chem. Rev.*, 1935, **17**, 27

7) A. D'Aprano and R.M. Fuoss, *J. Soln. Chem.*, 1975, **4**, 175

8) R.L. McIntosh, D.J. Mead and R.M. Fuoss, *J. Am. Chem. Soc.*, 1940, **62**, 506

9) J. Barthel, Angew. *Chem. Int. Ed. Engl.*, 1968, **7**, 260

10) A.P. Abbott and D.J. Schiffrin, *J. Chem. Soc., Faraday Trans.*, 1990, 86(**9**), 1453

11) W.L. Marshall, *J. Chem. Eng. Data.*, 1987, **32**, 221

12) E.U.Z. Franck, *J. Phys. Chem.*, 1956, **8**, 192

13) E.U.Z. Franck, *J. Phys. Chem.*, 1956, **8**, 107

14) E.U.Z. Franck, *J. Phys. Chem.*, 1956, **8**, 92

15) L.A. Dunn and W.L. Marshall, *J. Phys. Chem.*, 1969, **73**, 2619

16) L.A. Dunn and W.L. Marshall, *J. Phys. Chem.*, 1969, **73**, 723

17) J.D. Frantz and W.L. Marshall, *Am. J. Sci.*, 1984, **284**, 1666

18) J.D. Frantz and W.L. Marshall, *Am. J. Sci.*, 1984, **282**, 651

19) A.S. Quist and W.L. Marshall, *J. Phys. Chem.*, 1968, **72**, 3122

20) A.S. Quist and W.L. Marshall, *J. Phys. Chem.*, 1968, **72**, 2100

21) A.S. Quist and W.L. Marshall, *J. Phys. Chem.*, 1968, **72**, 1545

22) A.S. Quist and W.L. Marshall, *J. Phys. Chem.*, 1968, **72**, 684

23) A.S. Quist and W.L. Marshall, *J. Phys. Chem.*, 1966, **70**, 3714

24) L.B. Yeatts and W.L. Marshall, *J. Phys. Chem.*, 1972, **76**, 1053

25) L.B. Yeatts, L.A. Dunn and W.L. Marshall, *J. Phys. Chem.*, 1971, **75**, 1099

26) P.B. Balbuena, K.P. Johnston, P.J. Rossky and J.K. Hyun, *J. Phys. Chem. B*, 1988, **102**, 3806

27) R.B. Bird, W.E. Stewart and E.N. Lightfoot, *Transport Phenomena*, J. Wiley and Sons, New York, 1960

28) D.R. Schreiber, M. Conceicao P. de Lima, K.S. Pitzer, *J. Phys. Chem.*, 1987, **91**, 4087

29) A.P. Abbott, T.A. Claxton, J. Fawcett and J.C. Harper, *J. Chem. Soc., Faraday Trans.*, 1996, **92**(10), 1747

30) M.J. Kamlet, J.L. Abboud, M.H. Abraham and R.W. Taft, *J. Org. Chem.*, 1983, **48**, 2877

31) J.T. Edward, *J. Chem. Educ.*, 1970, **47**, 261

32) M.H. Abraham, Y. Marcus and K.G. Lawrence, *J. Chem. Soc., Faraday Trans.*, 1988, **84**, 175

33) T.C. Pochapsky and P.M. Stone, *J. Am. Chem. Soc.*, 1990, **112**, 6714

34) G. Boche, *Angew. Chem., Int. Ed. Engl.*, 1992, **31**, 731

35) Gaussian 94 (Revision B.2), M.J. Frisch, G.W. Trucks, H.B. Schlege, P.M.W. Gill, B.G. Johnson, M.A. Robb, J.R. Cheeseman, T.A. Keith, G.A. Petersson, J.A. Montgommery, K. Raghavachari, V.G. Zakrzewski, J.V. Ortiz, J.B. Foresman, J. Cioslowski, B.B. Stefanov, A. Nanayakkara, M. Challacombe, C.Y. Peng, P.Y. Ayala, W. Chen, M.W. Wong, J.L. Andres, E.S. Replogle, R. Gomperts, R.L. Martin, D.J. Fox, J.S. binkley, D.J. Defrees, J. baker, J.P. Stewart, M. Head-Gordon, C. Gonzalez and J.A. Poplo, Gaussian Inc., Pittsburgh PA, 1995

36) A.P. Abbott and T.A. Claxton, unpublished results

37) T.C. Pochapsky, A.P. Wang and P.M. stone, *J. Am. Chem. Soc.*, 1993, **115**, 11084

38) J.A. Riddick, *Organic Solvents, Physical Properties and Methods of Purification*, 4th edn., J. Wiley, Chichester, 1986

39) R.A. Robinson and R.H. Stokes, *Electrolyte Solutions*, Butterworths, London, 1959

40) C.T. Robertson, *Educ. Chem.*, 1973, **10**, 219

41) A. Sacco, A. de Giglio, A. Dell'atti and M. Petrella, *J. Chem. Soc., Faraday Trans.*, 1981, **77**, 2693

42) A.L. Horvath. *Handbook of Electrolyte Solutions*, Ellis Horwood Ltd., Chichester, 1985

43) J. A. Riddick, W.B. Bunger and T.K. Sakano, *Organic Solvents,* Wiley, New York, 1986

44) I.F. Golubev, *Viscosity of Gases and Gas Mixtures*, Israel Program for Scientific Translation, Jerusalem, 1970

45) K.S. Pitzer, D.Z. Lippmann, R.F. Curl, C.M. Huggins and D.E. Petersen, *J. Am. Chem. Soc.*, 1955, **77**, 3433

46) Y.P. Sun, C.E. Bunker and N.B. Hamilton, *Chem. Phys. Lett.*, 1993, **210**, 111

47) A. Morita and O. Kajimoto, *J. Phys. Chem.*, 1990, **94**, 6420

48) Y.P. Sun, M.A. Fox and K.P. Johnston, *J. Am. Chem. Soc.*, 1992, **114**, 1187

49) O. Kajimoto, M. Futakami, T. Kobayashi and K. Yamasaka, *J. Phys. Chem.*, 1988, **92**, 1347

CHAPTER IV

ELECTROCHEMISTRY IN SUPERCRITICAL CARBON DIOXIDE AND OTHER NON POLAR MEDIA

4.1 Introduction
- 4.1.1 The Metal-Solution Interface
- 4.1.2 Measurement of the Double Layer Capacitance

4.2 Results and Discussion
- 4.2.1 Double Layer Capacitance Measurements in Non Polar Media
- 4.2.2 Voltammetry in Dichloroethane and Anisole
- 4.2.3 Voltammetry in Cyclohexane
- 4.2.4 Voltammetry in Supercritical Carbon Dioxide

4.3 Conclusions

4.1 Introduction

Electron transfer at an electrode-solution interface is controlled by the structure of the electrical double layer. This in turn is dependent upon the relative permittivity of the solvent and the ionic strength of the electrolyte. It is therefore expected that there will be a marked difference between aqueous solutions and the non-polar fluids studies in this work.

To understand electron transfer in non-polar media it is imperative to elucidate the structure of the electrical double layer.

4.1.1 The Metal-Solution Interface

Helmholtz[1] viewed the interface as a parallel plate capacitor with a layer of ions on the solution side and a corresponding excess on the surface of the metal. We can denote these two phenomena in terms an excess charge density on the metal, q_M and an excess charge density on the solution side of the interface, q_S. The interface as a whole must be electrically neutral. It follows that we can express the charge on the interface as,

$$q_M + q_S = 0 \qquad (4.1.1)$$

The separation of the ions and the electrode surface is taken as half the diameter, a, of the solvated ion and it is clear that the double layer will behave as a capacitor with a plate separation of $a/2$. The plane passing through the centre of charge of the ions is termed the Outer Helmholtz Plane (OHP).

However, the theory predicted that the observed capacitance was independent of potential, contrary to experimental observation. Moreover, the theory does not predict

the numerical value of the capacitance at any given potential and does not take into account the effects of the concentration of the solution.

Gouy[2] and Chapman[3] devised a model in which the ions on the solution side of the interface are subject to random thermal motion that acts to equalise the concentration throughout the solution. They postulated a diffuse layer extending into the bulk of solution. However, as with the previous theory, the *diffuse double layer* model does not predict the correct experimental result. These deviations from experimental observation can be partly attributed to three assumptions;

i) the only energy involved in bringing an ion from infinity to a distance x from the surface is the electrostatic energy, neglecting ion-ion interactions which are important at higher concentrations.

ii) it is assumed that the relative permittivity is independent of the distance from the electrode (the value of ε in water falls from a value of 78 in the bulk to 6-8 in the region next to the electrode surface).

iii) the ions are treated as point charges for which the distance of closest approach to the surface is taken as zero.

When all of these corrections are taken into account they still do not explain the disagreement between theoretical and experimental observations. Stern[4] proposed that both the parallel plate capacitor and diffuse double layer models are valid and exist simultaneously. The interface could now be viewed as a system in which the bulk of potential drop occurs across the compact (Helmholtz) layer with a much smaller and more gradual change in potential across the diffuse (Gouy-Chapman) layer (see Fig. 4.1.1). This theory allowed the properties of the interface to be modelled in agreement with experimental observations.

Figure (4.1.1) Combination of Helmholtz and Gouy-Chapman layers forming the double layer at the electrode/electrolyte interface. Also shown, the potential distribution (φ) as a function of distance from the electrode surface.

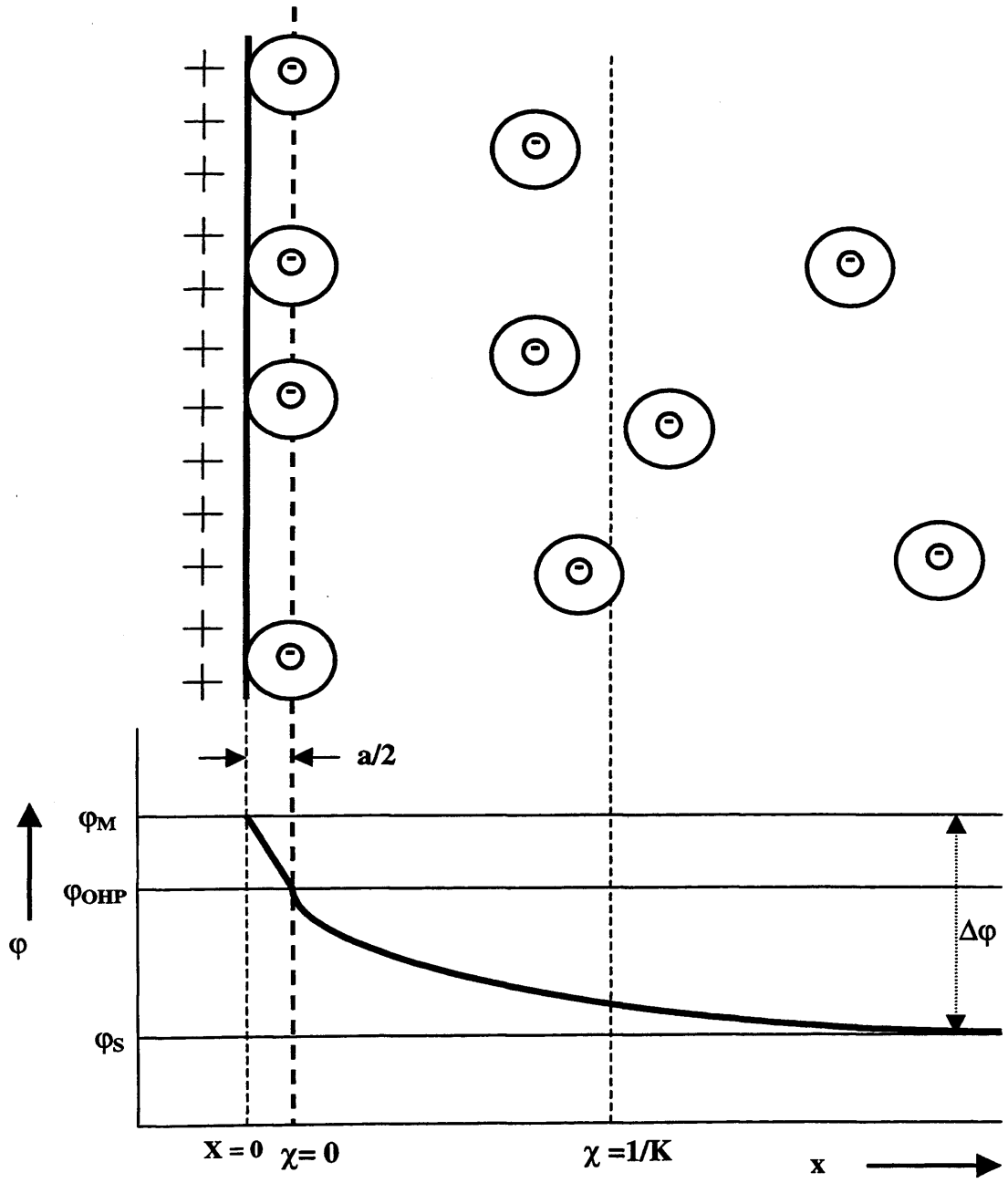

Previous experiments[5-8] have shown that certain neutral molecules and ions, particularly anions, may be adsorbed at an electrode surface. Stern proposed that these were *specifically adsorbed* with the locus of their centres defining an inner Helmholtz plane (IHP) at the interface. In order for an anion to be specifically adsorbed, it must first lose its solvation sheath in the direction towards the metal surface. Most cations are strongly hydrated and as a result, their interaction with the electrode surface is mainly electrostatic. Thus, the locus of centres of solvated ions defines the outer Helmholtz plane (OHP). The region extending beyond the OHP consists of a gradual decrease of concentration corresponding to the diffuse layer.

The interface can be thought to consist of two distinct regions. It has been stated that the interfacial region as a whole has to be electrically neutral so that the charge on the solution side is balanced by the charge on the metal. The total potential drop can be divided into an inner ($\Delta\varphi_i$) and diffuse ($\Delta\varphi_d$) contribution, i.e.,

$$\Delta\varphi\, 0 = \Delta\varphi_i + \Delta\varphi_d \qquad (4.1.2)$$

The distance, $\chi = 1/\kappa$, where χ is the outer surface potential and $1/\kappa$ is the Debye length, from the outer Helmholtz plane to the point at which the diffuse layer potential has dropped to a value $1/e$ of its total change from OHP to bulk solution is a measure of the thickness of the double layer (as shown in Fig. (4.1.1). The two charge regions are the electrical analogue of two capacitors in series. The total double layer capacitance, C, is then given by,

$$1/C = 1/C_i + 1/C_d \qquad (4.1.3)$$

Thus, the overall capacitance of the interface is predominantly determined by the smaller of the two capacitances of these regions.

Much of the work carried out in non-aqueous solvents has concentrated on media of high relative permittivity. [9,10] Solvents with lower relative permittivities (ε = 20 to 40 at r.t.p) in which the properties of the metal/solution interface have been investigated include acetone, [11-14] hexamethylphosphoramide[15,16] and acetonitrile.[17] It has been shown that ion pairing plays a significant role in determining double structure.

Some double layer studies have been made in aqueous and non-aqueous solutions containing quaternary ammonium electrolytes but very little work has been carried out in media where $\varepsilon < 10$. Long[18] investigated the capacitance of tetrabutylammonium tetrafluoroborate ($TBABF_4$) in dichloroethane and anisole at a mercury electrode in polar solutions. Dogrowska[19] studied the mercury/tetrahydrofuran electrolyte solution interface and showed that not only ion pairing but also triple ion formation has a significant effect in determining diffuse layer structure.

4.1.2 Measurement of the Double Layer Capacitance

The experimental investigation of this region has concentrated on the electrocapillary method. However this approach was not possible in the electrolyte solutions under investigation. An alternative was required which could yield reproducible data and one that was not prone to contamination effects.

When sinusoidal voltage signal ,

$$E = \Delta E \sin\omega t \qquad (4.1.4)$$

is applied to a cell, where $\omega = 2\pi f$ (f in hertz), E is the instantaneous value and ΔE is the maximum amplitude, the result is a sinusoidal current signal with the same

frequency but different in amplitude and phase. This current response can be represented by,

$$I = \Delta I \sin(\omega t + \phi) \qquad (4.1.5)$$

where ϕ is the phase shift. If the interface is ideally polarisable (behaves as a pure capacitor with negligible solution resistance), the phase angle (ϕ) will be $-\pi/2$. If the interface is ideally non-polarisable (behaves as pure resistor) then the phase angle will be zero. A real system does not behave ideally and hence the actual phase angle will be somewhere in the region $0 \leq \phi \leq 90°$. A phase sensitive voltammeter can measure the absolute value of the impedance vector $|Z|$ and the phase angle simultaneously. The impedance of a capacitor alone can be represented by an imaginary number, $Z_c = -j/\omega C$, and the impedance of a resistor is simply its resistance which is a real number. The impedance of the interface as a whole can be represented as a complex number,

$$Z(\omega) = ReZ - j(ImZ) \qquad (4.1.6)$$

where $j = \sqrt{-1}$, $\boldsymbol{ReZ}$ is the in-phase component and $\boldsymbol{ImZ}$ is the imaginary or quadrature component.

For a capacitor and a resistor in series the impedance is given by,

$$Z(\omega) = R_s - \frac{j}{\omega_c} \qquad (4.1.7)$$

and for a capacitor and resistor in parallel.

$$\frac{1}{Z(\omega)} = \frac{1}{R_f} - \frac{\omega C}{j} \qquad (4.1.8)$$

The results are often displayed in complex plane representations or as they are commonly reffered to, Nyquist plots. The X-axis is $\boldsymbol{ReZ}$ and the Y-axis is $-\boldsymbol{ImZ}$ which

is the capacitive impedance. The absolute value of the impedance vector and the phase angle are given by,

$$|Z| = [(ReZ)^2 + (ImZ)^2]^{1/2} \qquad (4.1.9)$$

and

$$\tan \phi = ImZ/ReZ \qquad (4.1.10)$$

Fig. (4.1.2) illustrates a typical Nyquist plot of a resistor and capacitor in parallel. The impedance for this circuit can be derived mathematically as a function of ω.

$$Z(\omega) = R_s + \frac{R_f}{1 + j\omega C_{dl} R_f} \qquad (4.1.11)$$

We can manipulate this expression to separate the real from the imaginary part of the impedance.

$$Z(\omega) = R_s + \frac{R_f}{1 + j\omega C_{dl} R_f} \times \frac{1 - j\omega C_{dl} R_f}{1 - j\omega C_{dl} R_f} \qquad (4.1.12)$$

Which leads to

$$Z(\omega) = R_s + \frac{R_f}{1 + (\omega C_{dl} R_F)^2} - \frac{j\omega C_{dl} R_F^2}{1 + (\omega C_{dl} R_F)^2} \qquad (4.1.13)$$

The first part of eqn. (4.1.10) is equal to ***ReZ*** and the second equal to ***ImZ***. A plot of this nature results in a semi-circle having a radius equal to $R_f/2$ and displaced from the origin by $R_s + R_f/2$. The double layer capacitance can be obtained from this plot with the assumption that

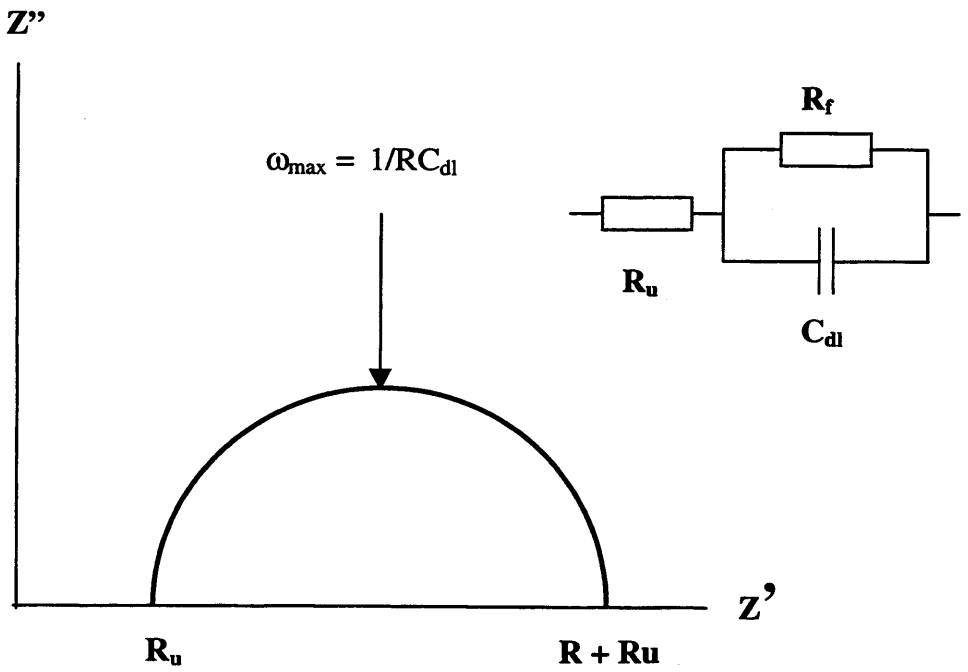

Figure (4.1.2) Complex plane impedance diagram for a parallel RC circuit with the addition of R_u, the uncompensated solution resistance. (inset: equivalent circuit)

$$R_f C_{dl} \omega_{max} = 1 \qquad (4.1.11)$$

This method of analysis is valid if the measured capacitance is independent of frequency. If this is the case, then the equivalent circuit is a good approximation of the interfacial region. [20]

In this work, we present the double layer data obtained for a variety of quaternary ammonium salts in dichloroethane (ε = 10.27), anisole (ε = 4.33) and cyclohexane (ε = 2.02). The studies were made on a platinum electrode to give a direct comparison with electron transfer data on this surface. Using Drogowska and Fawcetts analysis of the THF and MTHF data given in reference[19], the applicability of the Gouy-Chapman model to describe the variation in double layer capacity with tetraalkylammonium salt concentration in DCE is investigated. The effects of increasing anion and cation size on the measured capacity for the three solvents under investigation are shown. The first attempt to elucidate the structure of the double layer structure in media of such low relative permittivity. Unprecedented results are also presented for the capacitance at an electrode/supercritical fluid interface.

4.2 Results and Discussion

4.2.1 Double Layer Capacitance Measurements in Non Polar Media

The potential dependence of the capacitance for solutions containing 0.3 mol dm^{-3} of $TBABF_4$ in dichloroethane (DCE) and anisole at a platinum electrode are shown in Figure (4.2.1) (comparison with cHex was not possible because of the insignificant solubility of $TBABF_4$). The shape and magnitude of the capacitance-potential plots are very similar to those measured by Long[18] using a mercury electrode. Both solutions gave two peaks in the capacitance plots at ca. +0.05 and –0.6V, with a minimum occurring at ca. –0.3V. Capacitance humps are well known in capacitance studies in aqueous solutions and have been ascribed to reorientation of solvent molecules adjacent to the electrode[3] surface which is induced by the change in surface charge. The capacity maximum arises where the orientation of the solvent dipoles is minimal. Either side of the potential at which the maximum appears, the water molecules will orientate themselves with either the oxygen or hydrogen atoms directed towards the electrode surface. Such capacitance humps have also been observed in polar organic solvents such as dimethyl sulphoxide[21] and N-methyl- and dimethylacetamide.[22] Other studies using solvents such as dimethylformamide, acetonitrile and butyrolactone only observed capacitance humps at potentials positive of the potential of zero charge (pzc). Not all the data, however, is consistent with solvent reorientation and it has been suggested that specific adsorption of anions may also give a similar effect to that observed.[17] Capacitance studies in cyclohexane, discussed below also show capacitance humps. As cyclohexane has no dipole moment, the validity of the dipole reorientation model is questionable and it is envisaged that this phenomenon will not contribute towards the observed capacitance.

The capacitances at very large positive and negative overpotentials (-0.9 > E / V >

0.6), correspond well to a compact layer of ions, the capacitance of which is given by

$$C_H = \varepsilon\varepsilon_0/d \qquad (4.2.1)$$

where ε is the relative permittivity, ε_0 is the permittivity of free space and d is the distance between the centre of the ions and the electrode surface. Assuming that the value of d is the radius of the quaternary ammonium ion and using the value of capacitance at –1V, the relative permittivity close to the electrode surface can be calculated as 2.57 for DCE and 1.95 for anisole. These values are in accordance with values calculated for similar solvents on a mercury electrode.[5]

The effects of concentration on the capacitance-potential curve for $TBABF_4$ in DCE at a Pt electrode are presented in Figure (4.2.2). A decrease in the capacitance at –0.3V is observed with decreasing concentration and this is indicative of a diffuse layer minimum. The difficulty with analysing data obtained on surfaces other than mercury is the assignment of the pzc. In this work the pzc will be assumed to be at the capacitance minimum. Studies in DCE on mercury[18] have shown that this is a valid assumption and electrochemical quartz crystal microbalance studies[22] showed that there was a minimum in the mass-potential curve (i.e the pzc) at –0.3V, further validating this assumption.

In media of low relative permittivity the majority of the electrolyte solution will be in the form of ion pairs. Fawcett *et.al.*[19] used this assumption when testing the behaviour of the diffuse layer capacity data for $LiAsF_6$ and $LiClO_4$ in Tetrahydrofuran (THF). The depth of the diffuse layer minima as a function of concentration were less than that predicted by the Gouy-Chapman model of the diffuse layer. According to this model

$$1/C = 1/C_i + 1/(f\theta c_s^{1/2}) \qquad (4.2.2)$$

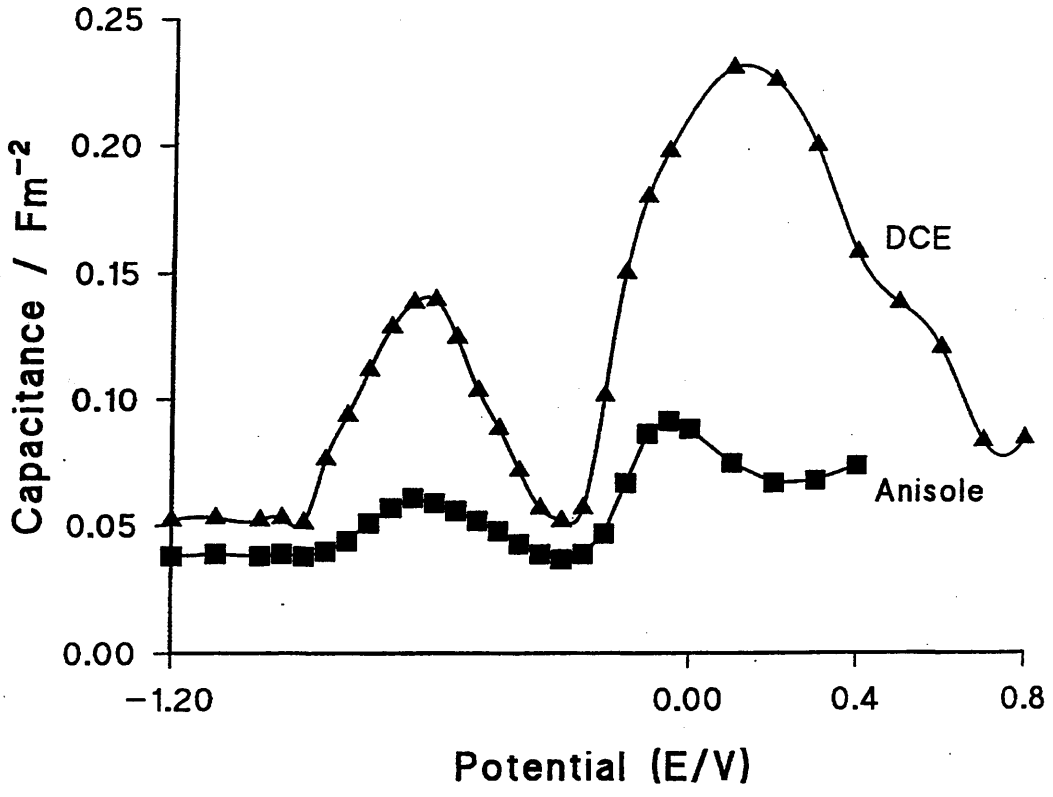

Figure (4.2.1) Capacitance of solutions containing 0.03 mol dm^{-3} of $TBABF_4$ in DCE and anisole at a platinum electrode, as a function of potential.

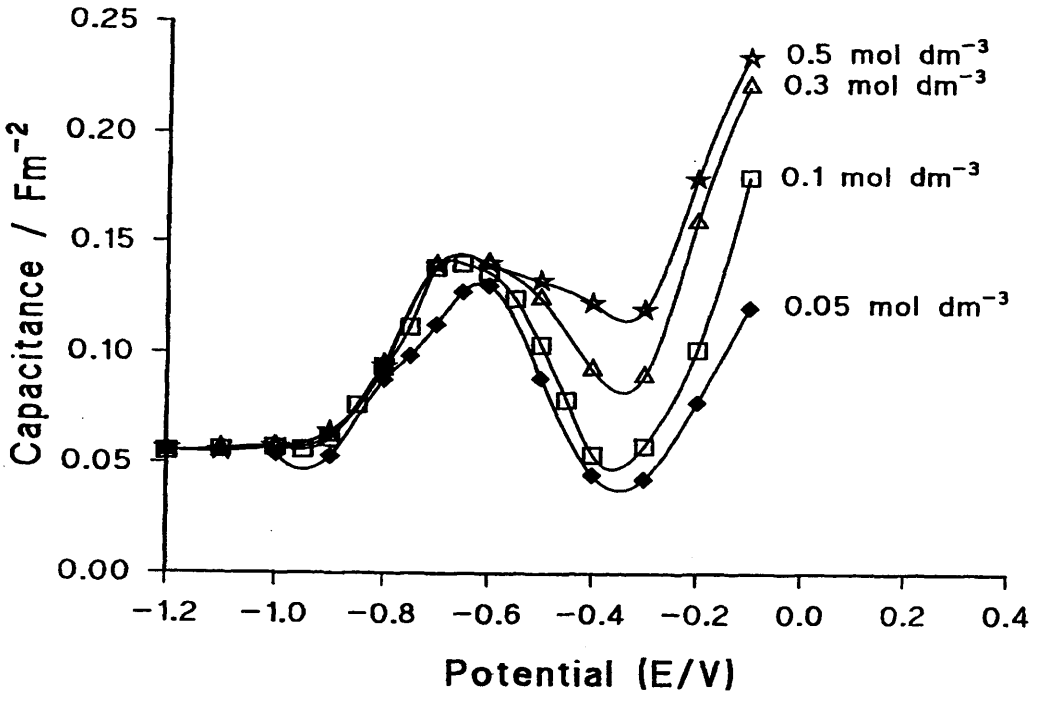

Figure (4.2.2) Effect of concentration on the capacitance-potential curve for $TBABF_4$ in DCE at a Pt electrode

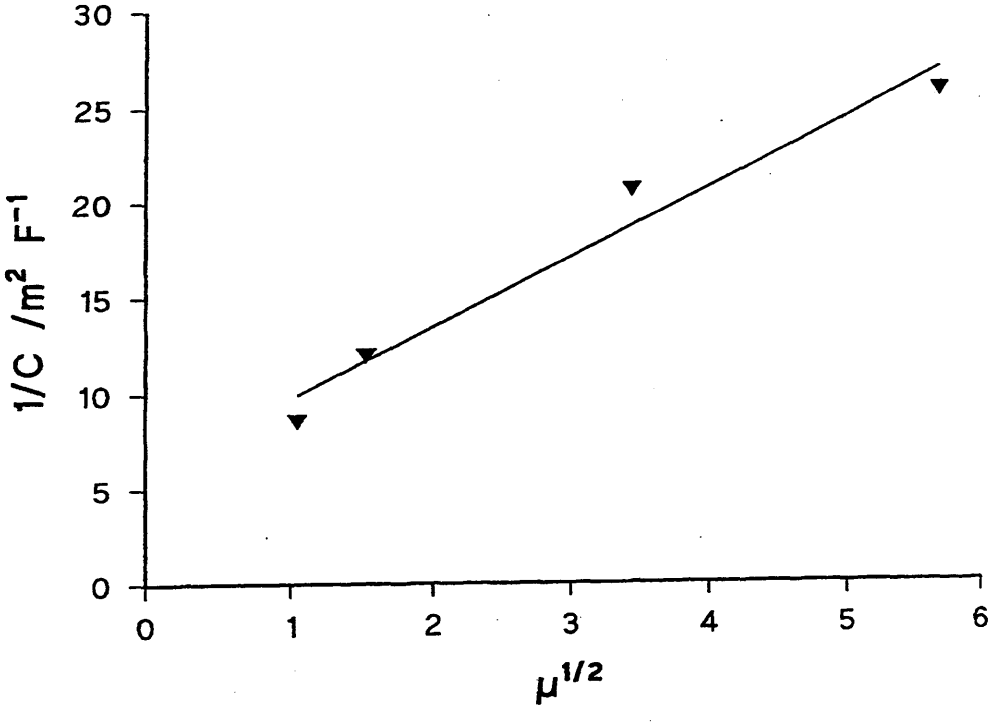

Figure (4.2.3) 1/C *vs.* $I^{1/2}$ (where $\mu^{1/2} = I^{1/2}$) at the pzc for the data shown in Fig. (4.2.2)

where C_i is the inner layer capacitance near the pzc, $\tilde{\theta}^2 = 2RT\varepsilon\varepsilon_0$ and $f = F/RT$. A plot of the inverse capacitance near the pzc, $1/C$, versus the inverse of the square root of the electrolyte concentration, $1/c_s^{1/2}$ should yield a straight line and an estimate of $f\theta$ is obtained. The values were much greater than those predicted by the Gouy-Chapman theory. Fawcett accounted for this observation by suggesting that the actual ionic strength was significantly less than the electrolyte concentration. This results from the strong ion pairing in such media. This work was supported by Damaskin[24] *et al.* who showed that the slope of the plots of experimental data would be significantly greater than the theoretical value when, as in the case of DCE, ion pairing is strong.

Fawcett proposed that if ion pairing was the only reason that actual ionic strength deviated from the theoretical concentration then a modified method of analysis can be employed. If the ion pairing process can be represented by the equation,

$$C^+ + A^- \longleftrightarrow CA \qquad (4.2.3)$$

Where C^+ represents the free cation, A^-, the free anion, CA, the ion pair and K_p, the association constant. The concentration of either ion, χ (χ=[C+]=[A-]), is given by,

$$\chi = \{(c_s - \chi)/K_p\}^{1/2} = (c_s/K_p)_{1/2} \qquad (4.2.4)$$

where $c_s > \chi$ when ion pairing is strong. The ionic strength, I, is equal to the concentration of either free ion for 1:1 electrolytes and equation (4.2.2) becomes,

$$\frac{1}{c} = \frac{1}{c_i} + \frac{K_p^{1/4}}{(f\ \theta\ c_s^{1/4})} \qquad (4.2.5)$$

A plot of $1/C$ versus $1/c_s^{1/4}$ should yield in a straight line whose slope is equal to $K_p^{1/4}/f\theta$. The intercept was found to be negative which was a meaningless result. Fawcett accounts for this by proposing that triple ion formation as well as ion pairing must be taken into account and play an important role in determining the ionic

strength of solutions in these media. This assumption has been further validated by the present work and Petrucci[25-30] and co-workers whose investigations into the properties of electrolyte solutions confirmed that triple ion formation must be taken into account when determining the ionic strength.

It can be assumed that two triple ions C_2A^+ and CA_2^- are formed with the same formation constant K_T according to the equilibria,

$$CA + C^+ \longleftrightarrow C_2A^+ \qquad (4.2.6)$$

and

$$CA + A^- \longleftrightarrow CA_2^- \qquad (4.2.7)$$

then

$$[C_2A^+] = [CA_2^-] = K_T[CA][C^+] = K_T[CA][A^-] = K_TK_p[C^+]_2[A^-]$$

$$= K_TK_p[C^+][A^-]_2 \qquad (4.2.8)$$

The formation constants for the two triple ions are the same, $[C^+] = [A^-] = \chi$, and

$$[C_2A^+] = [CA_2^-] = K_TK_p\chi^3 \qquad (4.2.9)$$

(4.2.12)

By mass balance,

$$C_s = [C^+] + [CA] + 2[C_2A^+] + [CA_2^-]$$

$$= [A^-] + [CA] + [C_2A^+] + 2[CA_2.]$$

$$= \chi + K_p\chi + 3K_TK_p\chi^3 \qquad (4.2.10)$$

The ionic strength of the solution is given by,

$$I = [C^+] + [C_2A^+] = [A^-] + [CA_2^-] = \chi + K_tK_p\chi \qquad (4.2.11)$$

The ionic strength was calculated from equation (4.2.11) where $\chi = (c/K_p)^{1/2}$. The values for the inner layer capacitance were derived using

$$\frac{1}{C}=\frac{1}{C_i}+\frac{1}{f\theta\sqrt{I}}\left(1+\frac{\sigma^2}{4\theta^2 I}\right)^{-1} \qquad (4.2.12)$$

Where σ is the charge density. Figure (4.2.3) shows that a plot of *1/C vs.* $I^{1/2}$ yields a reasonable linear correlation, showing that the data fits a modified Gouy-Chapman model for the diffuse layer, assuming that triple ions are the major charge carriers.

Figure (4.2.4) shows the capacitance of solutions containing 0.3 mol dm^{-3} of various electrolytes in DCE at a Pt electrode. Tetrabutylammonium tetraphenylborate (TBATPhB) gives results similar to the $TBABF_4$ electrolyte solutions. Long[18] suggested that the peak at –0.6V was caused by the adsorption of the cation on the electrode surface, but if this were the only cause then the peaks for $TBABF_4$ and TBATPhB would be of the same magnitude. This difference cannot be accounted for by differences in ionic strength as TBATPhB[31] has a smaller association constant and hence a higher ionic strength. The capacitance for the TBATPhB solution should therefore be larger than the corresponding value for $TBABF_4$, whereas the opposite is observed. Analysis of Figure (4.2.2) also shows that there is little change in the capacitance maximum at –0.6V, as a function of ionic strength, further confirming that the decrease in the capacitance for TBATPhB with respect to $TBABF_4$ is due to the anion. This anion effect can also be seen in the data presented by Drogowska[19] for $LiAsF_6$ and $LiCLO_4$ in THF although it is not noted by the authors (cf. Fig. 1 and 5 in ref. 19).

The capacitance humps at potentials positive of the pzc show a marked anion, but not a marked cation effect. This shows that the equilibria between positively and negatively charged ion aggregates are different in these non polar media and suggests that the aromatic anions are more stable than solvated aliphatic cations i.e. 2CA ↔

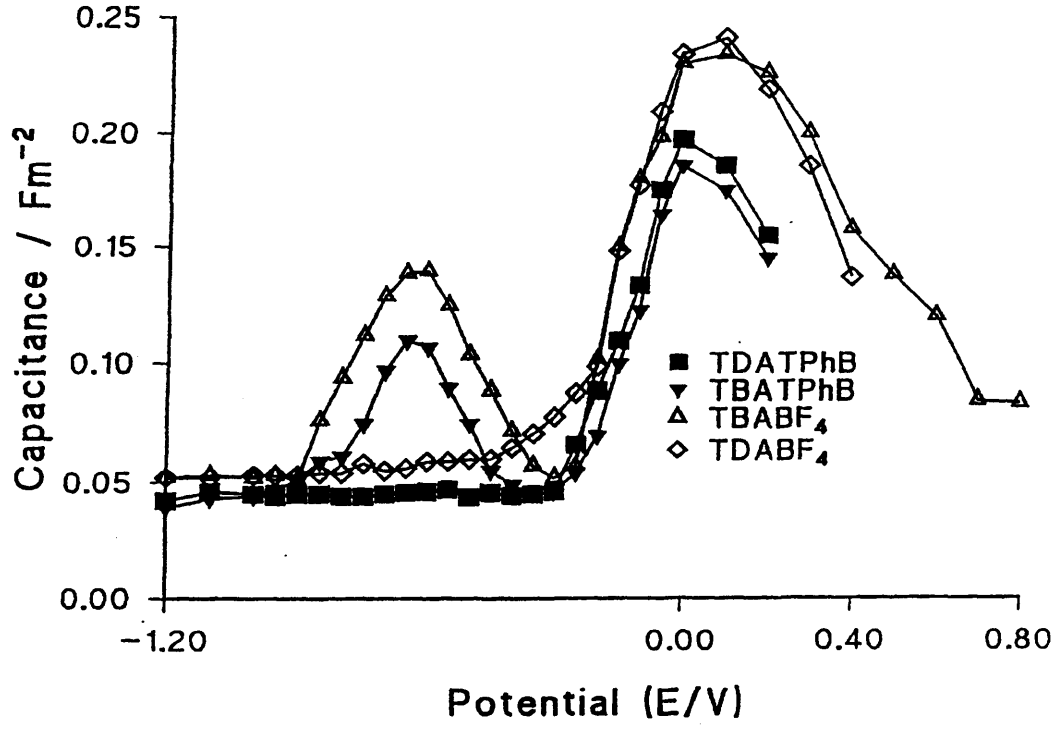

Figure (4.2.4) Capacitance of solutions containing 0.03 mol dm^{-3} of various electrolytes in DCE at a Pt electrode

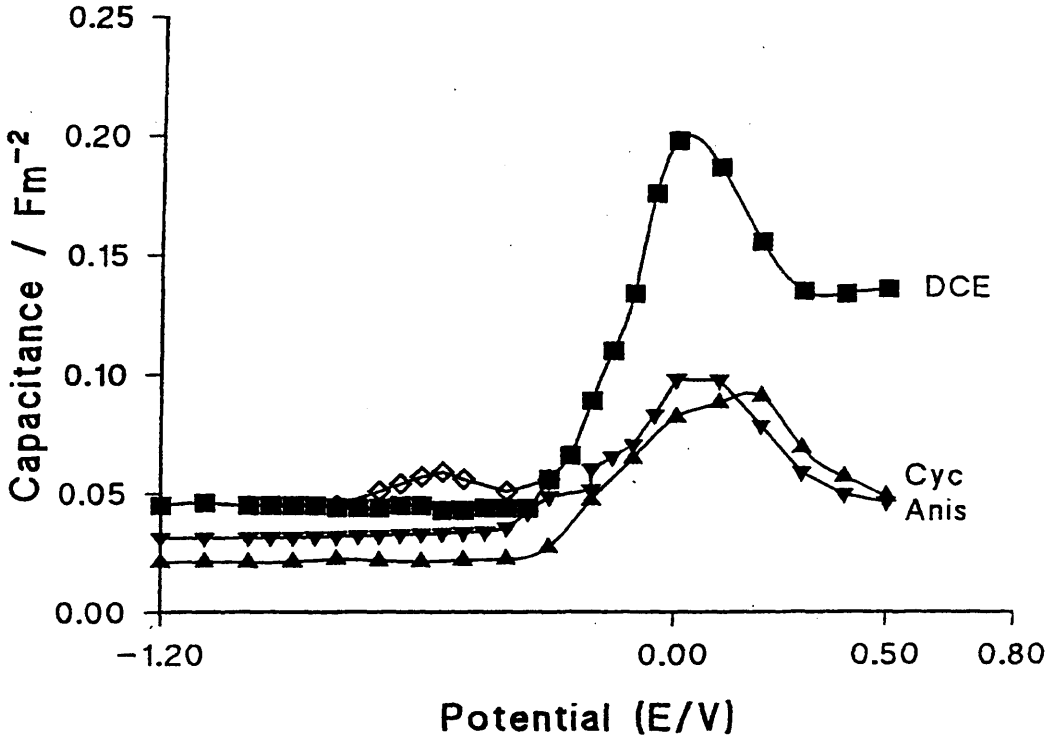

Figure (4.2.5) Capacitance *vs.* potential plot for DCE, anisole and cHex containing TDATPhB (c = 0.03 mol dm^{-3}) at a platinum electrode. Direction of potential steps for DCE: (◇) negative, (■) positive.

$C_2A^+ + A^-$.

The capacitance humps are clearly electrolyte dependent and cannot be due to the reorientation of the solvent dipole in the electric field. An alternative explanation for the occurrence of capacitance humps is that the solvent is strongly adsorbed at potentials close to the pzc and is displaced by the specific adsorption of electrolyte Work by Gambert *et. al.*[6] investigated the influence of alkanes and benzene derivatives on the double layer properties of Hg/CH_3CN electrolyte interfaces. It was found that non-polar molecules adsorbed at potentials close to the pzc and their desorption at larger overpotentials caused peaks in the capacitance-potential plots which are similar in magnitude and position to those observed in Figure (4.2.4). This simple desorption of the solvent and adsorption of the ions from solution does not, however, explain the apparent anion effect on the peak at –0.6V. This observation can only be explained if the adsorbing species is not a single ion but an ion pair or a triple ion. In non-polar media such as these, ion aggregates are considerably more stable than single ions and their reticence to dissociate may even be marked within the double layer. The capacitances observed could arise from the complex process of ion aggregates in solution being adsorbed on the electrode surface and then ions of opposite charge desorbing from the electrode surface. The desorption of a quaternary ammonium ion has been previously shown to be a very slow process[17] as the solvation of a charged species will be difficult in such a non-polar medium.

Figure (4.2.5) shows the capacitance-potential plot of DCE, anisole and cHex containing TDATPhB at a platinum electrode. For all the solutions, only one peak was observed at ca. +0.1V. A similar response was observed previously by others investigating the double layer properties of long chain quaternary ammonium electrolytes.[18,32] However, Fig. (4.2.5) also shows that the capacitance in DCE is

dependent on the experimental conditions. When the measurements were made starting at negative dc potentials and stepping positive, then no peak was observed at –0.6V i.e. cations are specifically adsorbed and only desorb when a sufficiently large overpotential is applied. However, when the dc potential steps were made stepping negative from the pzc then a small peak is observed at –0.6V. This is consistent with the adsorption of an ion aggregate, followed by the desorption of the TPhB anion. The presence of mixed charged species on an electrode surface was proposed previously by Devanathan and Fernando for the adsorption of tetraalkylammonium iodides at the mercury water interface.[11]

Figure (4.2.6) shows the capacitance of a 0.3 mol dm^{-3} TDATPhB-DCE solution at a Pt electrode at –0.6V as function of time. The capacitance increases with time, reaching a constant value after about 30 min. This is compatible with the slow equilibria between ion aggregates in solution and on the electrode surface in these non-polar media. The slow desorption of ions will also lead to electrochemical artefacts when dynamic studies are made. Fast potential sweep rates will not allow the desorption of ions from the surface and hence the process will appear irreversible. This will manifest itself as an apparent *iR* artefact, even when microelectrodes are used. It is for this reason that voltammetric studies can only be made at very slow potential sweep rates ($\nu < 1 mV\ s^{-1}$) in media of ultra low relative permittivity such as supercritical CO_2 and cHex.

Figure (4.2.7) shows the capacitance-potential plot for various tetrakis(decyl)ammonium electrolytes (c = 0.03 mol dm^{-3}) in cHex at a platinum electrode. This is the first double-layer capacitance measurement in an apolar medium. As with the results in DCE and anisole a hump is observed at +0.2V. This cannot be due to a dipolar rearrangement, since cHex has no dipole or quadrupole

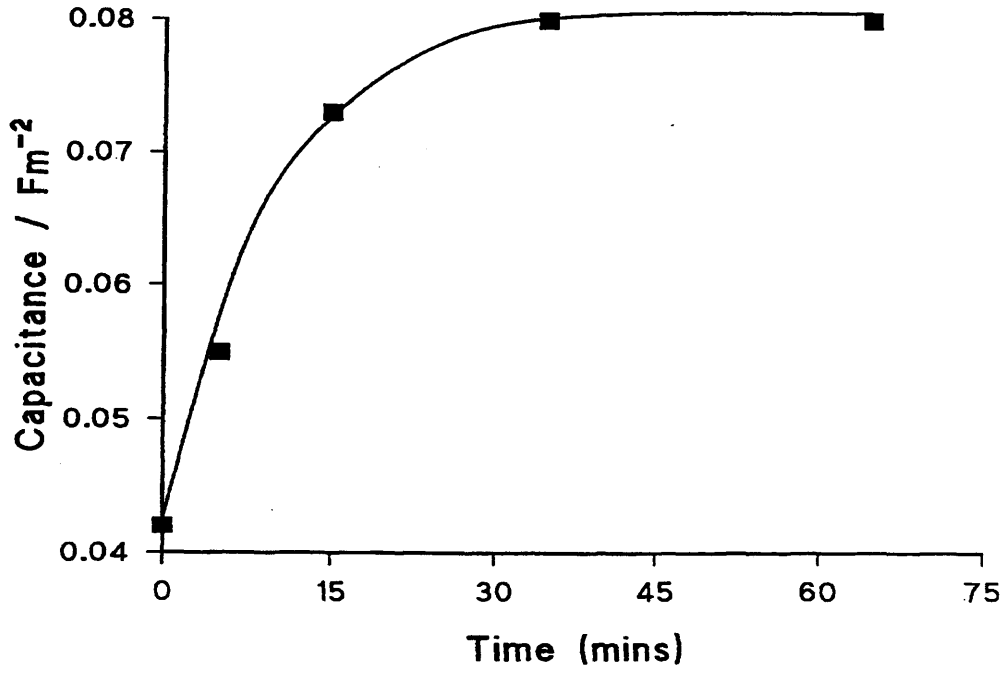

Figure (4.2.6) Capacitance of a 0.3 mol dm^{-3} TDATPhB-DCE at a Pt electrode at -0.6V, as a function of time

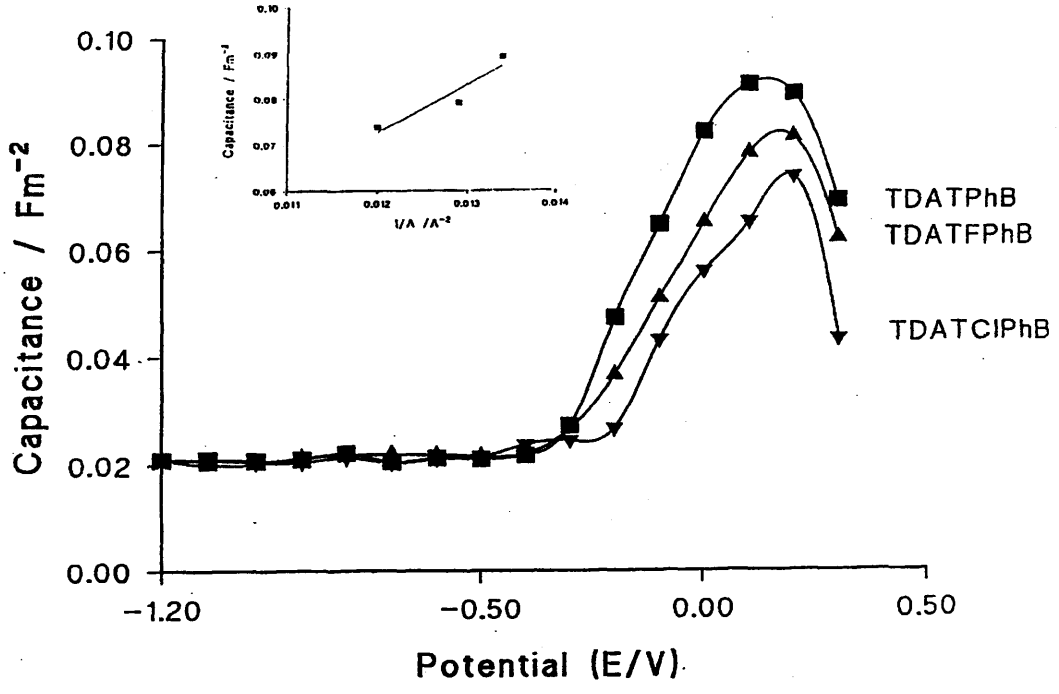

Figure (4.2.7) Capacitance *vs.* potential for various tetrakis(decyl)ammonium electrolytes (c = 0.03 mol dm^{-3}) in cyclohexane at a platinum electrode.
Inset: peak capacitance *vs.* the inverse of the area occupied by the anion on the surface.

moment. Neither is this change in capacitance due to the difference in ionic strength as the association constants for these electrolytes are in the order TDATPhB > TDATClPhB > TDATFPhB,[33] clearly different to the trend shown in Fig. (4.2.7). The peak capacitance is inversely proportional to the area occupied by the anion on the surface (see inset Fig. (4.2.7) which shows that it arises from an adsorption phenomenon.

Figure (4.2.8) shows the double layer capacitance of 0.03 mol dm^{-3} TDATPhB at a Pt electrode in $scCO_2$ at 70° C and that previously reported in cyclohexane. The capacitance peak observed in cHex at +0.1V is absent in $scCO_2$. It has been proposed that this peak originated from the adsorption of triple ions on the electrode surface and the magnitude of the peak capacitance was due to the size of the ion rather than the ionic strength. If this is indeed the case then the difference in capacitance for TDATPhB in cHex and $scCO_2$ can only arise from a change in the structure of the double layer. In $scCO_2$ the double layer capacitance resembles that of a parallel plate capacitor and can be described by the Helmholtz model (see eqn (4.2.1)). The lack of a diffuse layer minimum at c.a. 100mV despite the low ionic strength ($I = 1.04 \times 10^{-5}$ mol dm^{-3}) could result from either slow ion desorption or the collapse of the diffuse layer.

Niehaus[34] reported that in non-polar SCF such as $scCO_2$, voltammetric measurements are impossible because the diffuse region is so large. However, it has been shown in this work that at potentials greater and less than the pzc, specific adsorption of ions occurs. Assuming that the electrode is covered by a layer of ions approximately 10Å thick, the potential profile as a function of distance from the electrode surface can be calculated as follows.

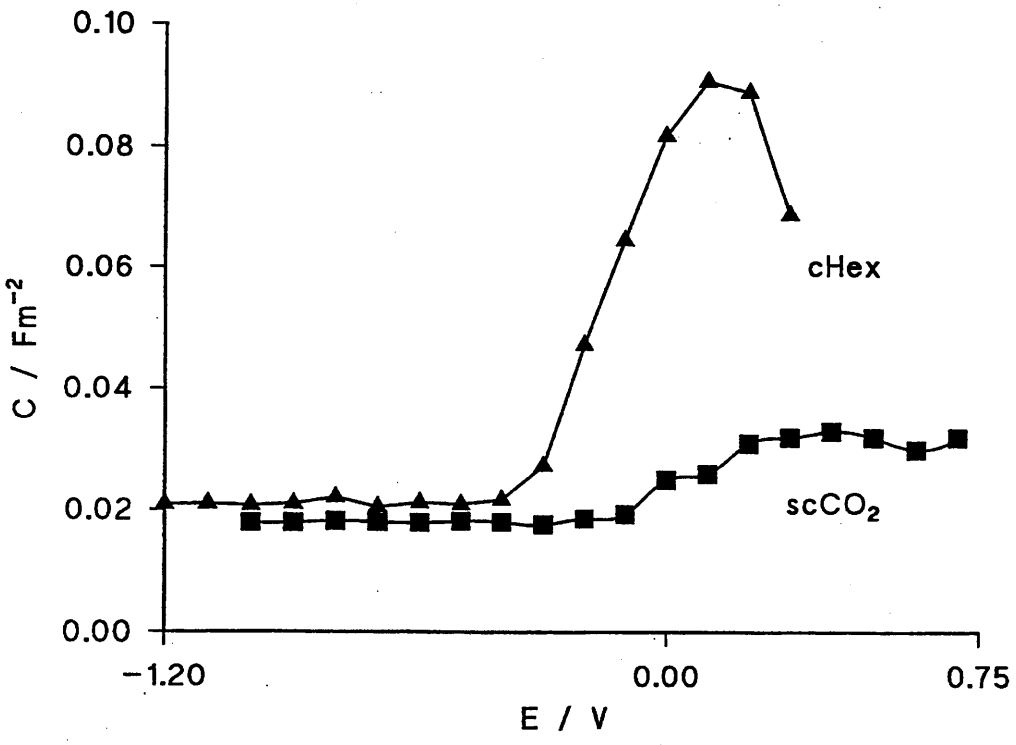

Figure (4.2.8) Double layer capacitance measurements in (i) cHex and (ii) $scCO_2$ (220 bar 70°C) containing 0.03 mol dm^{-3} TDATPhB

The field strength at the OHP , x_2, can be calculated from

$$\left(\frac{d\varphi}{dx}\right)_{x=x_2} = -\left(\frac{8kTn^0}{\varepsilon\varepsilon^0}\right)^{1/2} sinh\left(\frac{ze\varphi_2}{2kT}\right) \qquad (4.2.13)$$

The potential profile in the diffuse layer of a 1:1 electrolyte is given by

$$\frac{tanh(ze\varphi/4kT)}{tanh(ze\varphi_2/4kT)} = e^{-\kappa(x-x_2)} \qquad (4.2.14)$$

where, φ_2 is the potential at x_2 with respect to the bulk solution and κ is defined by

$$\kappa = (2n_0z^2e^2/\varepsilon\varepsilon_0kT)^{1/2} \qquad (4.2.15)$$

where e is the charge on an electron, n_0 is the number concentration of each ion in the bulk solution, ε_0 is the permittivity of free space, ε is the bulk permittivity, z is the charge, k is the Boltzmann constant and T is the absolute temperature. Using this, the potential drop, $(d\varphi/dx)$, was calculated as a function of distance from the electrode surface for 0.04 mol dm^{-3} solutions of a 1:1 electrolyte in cHex and water for a surface potential of 0.16V and the results are shown in Figure (4.2.9). As can clearly be seen in cHex, the bulk of the potential drop occurs across the compact layer which extends approximately 8 Å from the electrode surface. The potential drop across the diffuse layer is negligible due to the low ionic strength. An ion close to the electrode surface will experience the potential, φ_2, and this value is significantly less than the applied potential at the electrode surface. Therefore, double layer corrections must be taken into account when measuring reaction kinetics in these media.

The kinetics of the desorption/adsorption of an ion have been shown to be slow in these media .[23] Therefore the potential, φ_2, experienced by an electroactive species will be governed by the surface coverage of the electrolyte at the electrode surface. This will manifest itself as an artefact in the voltammetric responses in non-polar

media.

The potential profile in the compact layer is dependent upon the extent of surface coverage by an adsorbed species. Two possible extremes exist,

i) if the surface is completely covered then the profile is similar to that shown in Fig. (4.2.9)

ii) in the absence of specific adsorption, the potential profile decays in accordance with the Gouy-Chapman model of the diffuse layer.

Because the kinetics of desorption are slow, at fast sweep rates the outer potential experienced by an electroactive species is significantly less than the applied potential and hence the kinetics of a process will appear to be slow. This may manifest itself in what appears to be an *iR* artefact. It was previously suggested that increasing the cationic radius led to a decrease in electron transfer kinetics because the electrolyte blocked the electrode surface and extended electron transfer occurred.

4.2.2 Voltammetry in Dichloroethane and Anisole

To determine whether the electrolyte blocks electron transfer at an electrode/solution interface or simply leads to an artefact im the voltammetry at fast sweep rates, a series of experiments were carried out in non-polar solvents with a range of electrolytes. Figure (4.2.10) shows a cyclic voltammogram of tetracyanoquinodimethane (TCNQ) on a 75 μm Pt microelectrode in anisole containing 0.1 mol dm^{-3} $TBABF_4$. The two waves at *ca.* 0.0 and –0.6V are well known to be due to the reduction of TCNQ to form the TCNQ anion radical and anion respectively,[36]

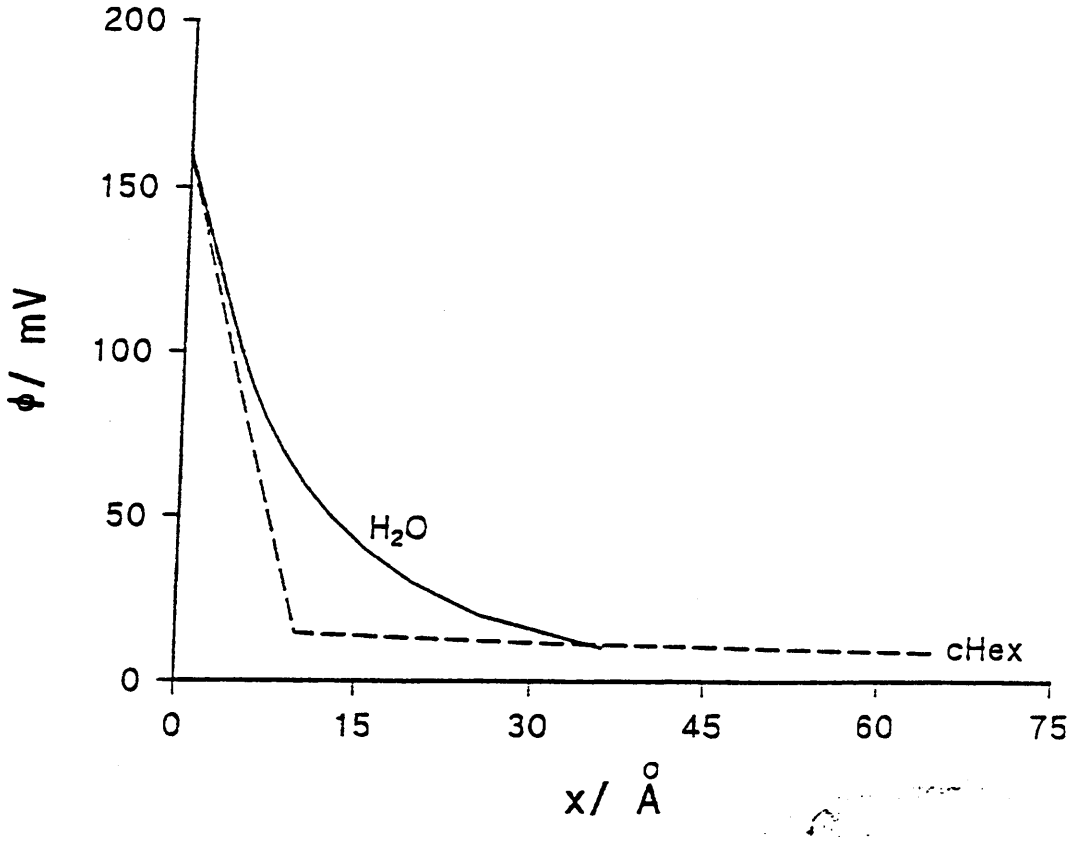

Figure (4.2.9) Potential profiles through the compact and diffuse layer model calculated for a 1:1 electrolyte (0.1 mol dm^{-3}) at 25°C, where $\varphi_0 = 0.16V$

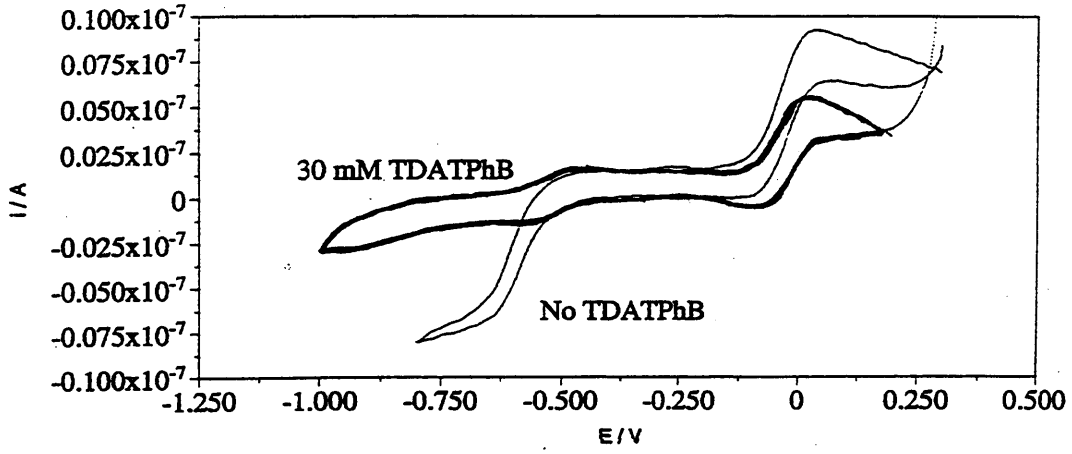

Figure (4.2.10) Cyclic voltammograms of TCNQ in anisole at a platinum microelectrode (75 μm) containing 0.1 mol dm^{-3} $TBABF_4$ and 0.1 mol dm^{-3} $TBABF_4$ plus 0.03 mol dm^{-3} TDATPhB . (current axis corrected to read 0 A at –0.3V for ease of comparison). Sweep rate = 10 mV s^{-1}

$TCNQ + e^- \longleftrightarrow TCNQ^{\cdot -}$

$TCNQ^{\cdot -} + e^- \longleftrightarrow TCNQ^{2-}$

This compound was chosen as a model system as the two redox processes are known to be reversible and the half wave potentials coincide with the humps in the capacitance curves. The slopes of $\log[(i_d - i)/i]$ *vs.* E for both redox couples were calculated for solutions containing $TBABF_4$ and those to which TDATPhB had been added. When $TBABF_4$ is used as an electrolyte, both the reduction to the anion radical and the dianion are reversible. The addition of TDATPhB (30mMol) causes a marked reduction in the current and the reversibility of both processes (slopes = 75 and 77 mV respectively). These cannot be *iR* artefacts since there is an increase in the conductivity of the solution following the addition of TDATPhB.

To investigate this trend further, a series of voltammograms were recorded for the TCNQ redox couples in dichloroethane and anisole with a variety of tetraalkylammonium electrolytes on a 10 μm Pt electrode. The data were analysed by plotting E *vs.* $\log[(i_d - i/)i]$ and the results are presented in Tables (4.2.1) and (4.2.2).

	$TCNQ + e^-$ $\leftrightarrow TCNQ^{\cdot -}$	$TCNQ^{\cdot -} + e^-$ $\leftrightarrow TCNQ^{2-}$
Electrolyte	**αnF/2.303RT / mV**	**αnF/2.303RT / mV**
$TBABF_4$	**61**	**60**
$TDABF_4$	**82**	**83**
TBATPhB	**66**	**69**
THATPhB	**67**	**69**
TOATPhB	**70**	**72**
TDATPhB	**89**	**89**
TDATClPhB	**81**	**80**
TDATFPhB	**82**	**81**

Table (4.2.1) Table of the slopes of the plots described in the literature[36] of the TCNQ two electron reduction in Anisole (TBA=tetrabutylammonium, THA=tetrahexylammonium, TOA=tetraoctylammonium, TDA=tetradecylammonium)

	$TCNQ + e^- \leftrightarrow TCNQ^{\cdot-}$	$TCNQ^{\cdot-} + e^- \leftrightarrow TCNQ^{2-}$
Electrolyte	**αnF/2.303RT / mV**	**αnF/2.303RT / mV**
$TBABF_4$	**59**	**60**
$TDABF_4$	**75**	**71**
TBATPhB	**64**	**62**
THATPhB	**65**	**63**
TOATPhB	**65**	**66**
TDATPhB	**74**	**76**
TDATClPhB	**72**	**72**
TDATFPhB	**71**	**71**

Table (4.2.2) Table of the slopes of the plots described[36] of the TCNQ two electron reduction in DCE.

Analysis of the data shows that nature of the electrolyte has a marked effect upon the reversibility of the reduction process. Comparison between the results for $TBABF_4$ and $TDABF_4$ show that the reduction waves deviate significantly from the Nerstian value of 59 mV in the presence of $TDABF_4$. It has been shown in this work that specific adsorption of ions occurs at the potentials of the reduction waves and the data from the voltammetry further confirms that the large TDA cation is adsorbed at these potentials.

Comparison of the data for TBATPhB, THATPhB and TOATPhB show that the values of the slopes do not significantly change. However, there are large deviations for both $TDABF_4$ and TDATPhB in DCE and anisole. Fawcett *et al.*[37] noted that the length of the alkyl chain of the electrolyte significantly affected the kinetics of the reduction of nitromesitylene. It was proposed that extended electron transfer took place in which the electron tunnelled through the film. The rate of reaction depended upon the thickness of the film size which is controlled by the size of the ion adsorbed on the electrode. A sliight decrease is observed in reversibility for both processes in the series TBA > THA > TOA > TDA for both solvents. The same , however is not

observed for the effect of the anion. For the TDA salts the reversibility of both processes is in the order BF_4 = TFPhB > TClPhB > TPhB. Therefore, the apparent reversibility of the process in these media must be governed by the desorption of an ion rather than by extended electron transfer.

The observation that both anion and cation affect processes either side of the pzc further confirms that mixed ionic films are present at the electrode surface. To demonstrate the effect of this slow desorption artefact a series of voltammograms of TCNQ (1 mMol) in DCE in the presence of 0.1 mol dm^{-3} $TDABF_4$ at sweep rates of (a) 50 mV s^{-1} and (b) 10 mV s^{-1} and (c) 1 mVs^{-1} were recorded. The results of the analysis are presented in Table (4.2.3).

	$TCNQ + e^- \leftrightarrow TCNQ^{\cdot-}$	$TCNQ^{\cdot-} + e^- \leftrightarrow TCNQ^{2-}$
Sweep rate / mV s^{-1}	**αnF/2.303RT**	**αnF/2.303RT**
50	**82**	**79**
10	**74**	**76**
1	**61**	**60**

Table (4.2.3) Table of the slopes of the plots described[36] of the TCNQ two electron reduction in DCE.

The voltammogram at a sweep rate of 10 mV s^{-1} was also recorded when the concentration of the TCNQ species was reduced to 0.5 mMol dm^{-3} and no change in the Nerstian slope was observed.. Therefore the apparent decrease in the slopes of the plots cannot be as a result of *iR* loss. The kinetics of desorption of ions has been shown to be a slow process (Fig (4.2.6) and hence fast sweep rates yield electrochemical responses which appear irreversible. The importance of this result

cannot be underestimated as it affects all voltammetric studies in non-aqueous media that use quaternary ammonium electrolytes. It also questions the validity of all rate constant data obtained by fast sweep rates in such media.

4.2.3 Electrochemical Investigations in Cyclohexane.

Figure (4.2.11) shows cyclic voltammograms of $TDDA_2Ni(mnt)_2$ (a), ferrocene carboxylic acid (b) and ferrocene (c) in cyclohexane containing TDATPhB (0.04 mol dm^{-3}) on a platinum microelectrode (10μm). At slow scan rates (ν = 1mVs^{-1}) a reversible one electron wave is observed for the oxidation of the nickel complex.

The observed response for

$$[Ni(mnt)_2]^{2-} - e^- \longleftrightarrow [Ni(mnt)_2]^-$$

does not however follow classical diffusion. Calculation of the diffusion coefficient for this process yields a value of 3.6×10^{-11} cm^2 s^{-1} which is five orders of magnitude smaller than that predicted by the Stokes-Einstein equation (4.9×10^{-6} cm^2 s^{-1}). An irreversible response is recorded for the ferrocene carboxylic acid and no response is observed for ferrocene oxidation. The slow ion desorption and the low value of φ_2 preclude the oxidation of ferrocene close to the electrode surface. Anionic $FcCOO^-$ and $[Ni(mnt)_2]^{2-}$ can compete for adsorption sites with electrolyte ions as they are electrostatically attracted to the electrode surface and hence electron transfer can be observed.

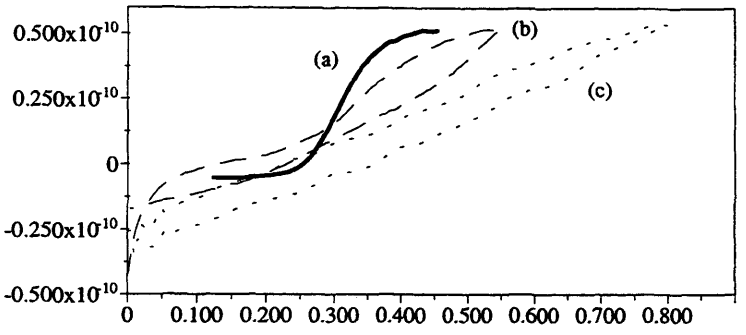

Figure (4.2.11) cyclic voltammograms of (a) $TDDA_2Ni(mnt)_2$, (b) ferrocene carboxylic acid and (c) ferrocene in cyclohexane containing TDATPhB (0.04 mol dm^{-3}) on a platinum microelectrode (10μm). Sweep rate = 1 mV s^{-1}.

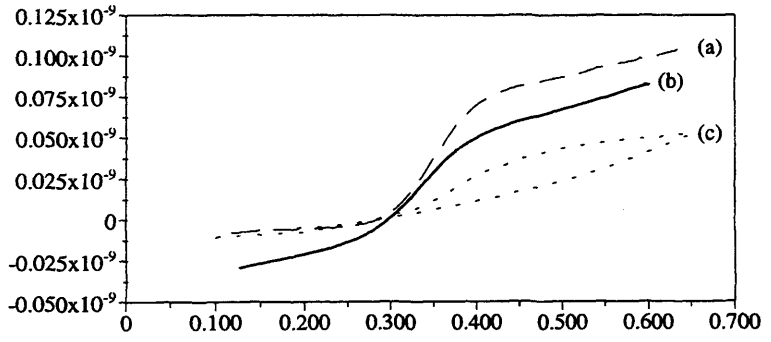

Figure (4.2.12) cyclic voltammograms of (a) $TDDA_2Ni(mnt)_2$, (b) ferrocene carboxylic acid and (c) ferrocene in cyclohexane containing TDATClPhB (0.04 mol dm^{-3}) on a platinum microelectrode (10μm). Sweep rate = 1 mV s^{-1}.

Figure (4.2.12) shows voltammograms of $TDDA_2Ni(mnt)_2$ (a), ferrocene carboxylic acid (b) and ferrocene (c) in cyclohexane containing TDATClPhB (0.04 mol dm^{-3}) on a platinum microelectrode (10μm). Reversible responses are recorded for both the nickel and ferrocene carboxylic acid complexes. The oxidation of the ferrocene to the ferrocinium cation was observed but the reverse process was irreversible. This suggests that as the cation is formed, it diffuses away from the electrode surface and hence no reduction wave is observed. At potentials positive of the pzc we have shown that a layer of anions are present at the electrode surface. These ions may form ion pairs with the ferrocinium cation and hence can diffuse into the bulk of solution. Wightman *et al.*[38] illustrated that the cation was insoluble in similar media and a diffusion controlled peak was observed on the reverse scan. No such response was observed in cHex further suggesting that the ion or ion pair diffuses away from the electrode surface.

The results with the TClPhB derivative suggest that the kinetics of desorption of the halogenated ions are faster than the TPhB anion confirming the explanation of the values observed in Table (4.2.1) and (4.2.2). Since the outer potential depends upon the extent of surface coverage and hence on the kinetics of ion desorption, its value would be greater than that in TDATPhB solutions. This effect has also been observed in the responses of TCNQ in DCE and anisole with a variety of electrolytes. Therefore, electron transfer can be observed for an uncharged species in solutions containing the TClPhB and TFPhB anions.

Figure (4.2.13) shows cyclic voltammograms of $TDDA_2Ni(mnt)_2$ in cyclohexane in the presence of 0.4 mol dm^{-3} (a) TDATFPhB, (b) TDATClPhB) and (c) TDATPhB at a sweep rate of 1 mV s^{-1}. For all three processes, reversible one electron waves were

recorded. The current decreases in the order of TDATFPhB > TDATClPhB > TDATPhB. This must arise from the decrease in the kinetics of desorption in the order TDATFPhB > TDATClPhB > TDATPhB.

4.2.4 Electrochemical Investigations in $scCO_2$

Ferrocene was selected as the initial test substance for voltammetric studies in $scCO_2$ because it has been shown to be soluble in this medium.[39] No electron transfer response was observed even at the very slow sweep rates employed (ν = 1 mV s^{-1}) No signal for the oxidation of ferrocene in $scCO_2$ at 300 bar and 70 °C was observed even at a 10 μm Pt and 0.04 Mol TDATClPhB as the supporting electrolyte.

Figure (4.2.14) shows a cyclic voltammogram for $TDDA_2Ni(mnt)_2$ in $scCO_2$ at 70 °C and 300 bar using TDATPhB as a supporting electrolyte. The observed response for the redox process is similar to that shown in Fig. (4.2.10) using cyclohexane as the solvent. However, it must be noted that the voltammogram is distorted. Since the relative permittivities of cHex and $scCO_2$ are similar it would be expected that the two voltammograms should be similar. The current in $scCO_2$ is approximately the same as that observed in cHex. Double layer capacitance data in both media suggest that the structure at a supercritical / electrode interface is different to a solution / electrode interface. Therefore, the similarities in the currents between the two media must result from the desorption kinetics of adsorbed ions.

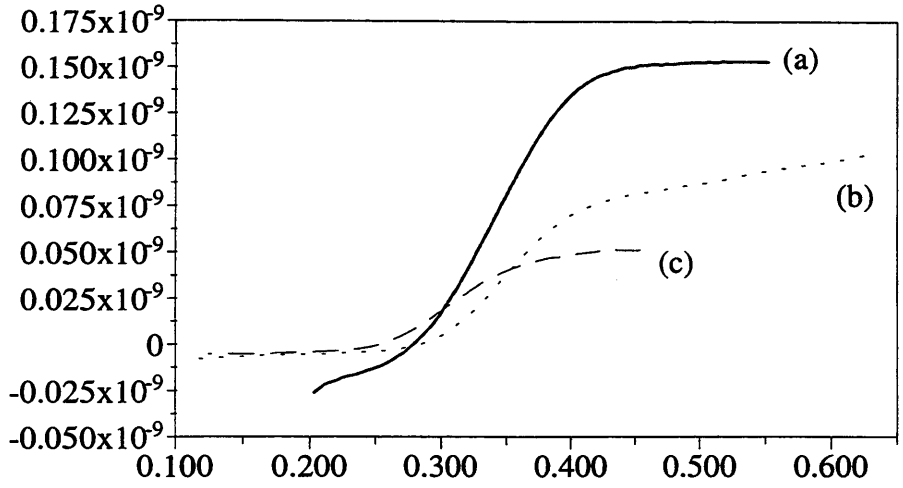

Figure (4.2.13) cyclic voltammograms of $TDDA_2Ni(mnt)_2$ in cyclohexane in the presence of 0.4 mol dm^{-3} (a) TDATFPhB, (b) TDATClPhB) and (c) TDATPhB at a sweep rate of 1 mV s^{-1}.

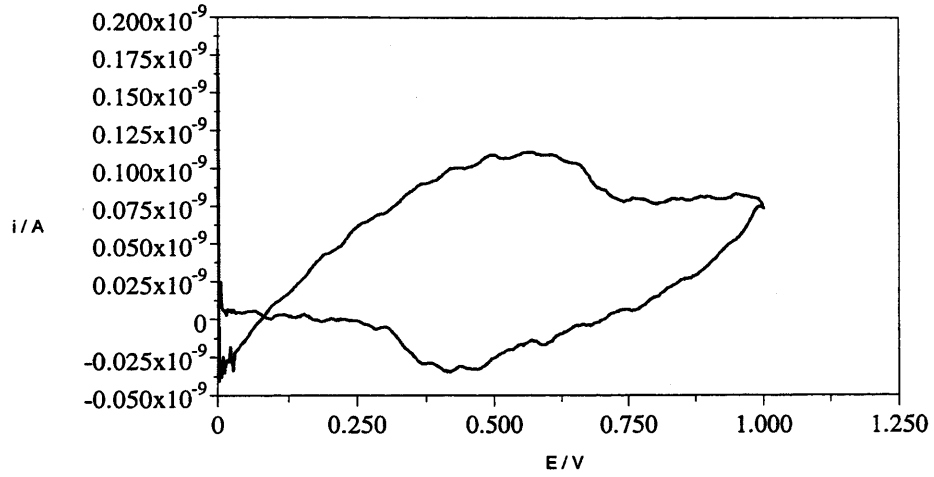

Figure (4.2.14) Cyclic voltammogram of $TDDA_2Ni(mnt)_2$ (1 mMol dm^{-3}) in $scCO_2$ containing TDATClPhB (0.04 mol dm^{-3}) at 300 bar and 70°C , sweep rate = 1 mVs^{-1}

4.3 Conclusions

Electron transfer and double layer capacitance studies have been carried in non-polar media such as $scCO_2$ and cyclohexane. An electrochemical response can only be measured at slow sweep rates due to the slow kinetics of ion desorption. This has important ramifications to all voltammetry in non-polar fluids containing quaternary ammonium electrolytes, invalidating a large amount of kinetic data in the literature.

CHAPTER IV REFERENCES

1) D.M. Mohilner, *Electroanal. Chem.*, 1966, **1**, 241

2) R. Parsons, *Adv. Electrochem. Electrochem. Eng.*, 1961, **1**,1

3) D.C. Grahame, *Ann. Rev. Phys. Chem.*, 1955, **6**, 337

4) O. Stern, *Z. Elektrochem.*, 1924, **30**, 508

5) R. Gambert and H. Baumgaertel, *J. Electroanal. Chem.*, 1985, **183**, 315

6) R. Gambert and H. Baumgaertel, *J. Electroanal. Chem.*, 1985, **185**, 147

7) B. Damaskin, S. Karpon and S. Dyatkina, *J. Electroanal. Chem.*, 1985, **189**, 183

8) D.C. Grahame, *Chem. Rev.*, 1947, **41**, 441

9) J.R. Macdonald and C.A. Barlow Jr., *J. Chem. Phys.*, 1962, **36**(11), 3062

10) R. Parsons, *Chem. Rev.*, 1990, **90**, 813

11) M.A.V. Devanathan and M.J. Fernando, *J. Chem. Soc., Faraday Trans.*, 1961, **58**, 368

12) S.H Kim, T.N. Anderson and H. Eyring, *J. Phys. Chem.*, 1970, **74**, 4555

13) R. Payne, *Physical Chemistry of Organic Solvent Systems*, Plenum Press, London and New York, 1973

14) M. Jurkiewicz-Herbich, *Pol. J. Chem.*, 1978, **52**, 1063

15) M. Jurkiewicz-Herbich, *Pol. J. Chem.*, 1976, **50**, 515

16) M.D. Mackey and R. Peat, *J. Electroanal. Chem.*, 1983, **137**, 321

17) R. Payne, *J. Phys. Chem.*, 1967, **71**, 1548

18) E.E. Long, *Ph.D Thesis*, Liverpool University, 1992

19) M.A. Drogowska and W.R. Fawcett, *J. Electroanal. Chem.*, 1987, **222**, 293

20) E. Gileadi, *Electrode Kinetics*, VCH, New York, 1993

21) R. Payne, *J. Am. Chem. Soc.*, 1967, **89**, 489

22) R. Payne, *J. Phys. Chem.*, 1967, **73**, 3598

23) A.P. Abbott, D.C. Loveday and A.R. Hillman, *J. Chem. Soc. Faraday Trans.*, 1994, **90**, 1533

24) M.D. Levi, A.V. Shlepkov, B.B. Damaskin and I.A. Bagotskaya, *J. Electroanal. Chem.*, 1982, **138**, 1

25) P. Jagodzinski and S. Petrucci, *J. Phys. Chem.*, 1974, **78**, 917

26) H. Farber and S. Petrucci, *J. Phys. Chem.*, 1975, **79**, 1221

27) H. Farber and S. Petrucci, *J. Phys. Chem.*, 1976, **80**, 327

28) D. Saar, J. Brauner, H. Farber and S. Petrucci, *J. Phys. Chem.*, 1978, **82**, 545

29) D. Saar, J. Brauner, H. Farber and S. Petrucci, *J. Phys. Chem.*, 1978, **82**, 1943

30) S. Onishi, H. Farber and S. Petrucci, *J. Phys. Chem.*, 1980, **84**, 2922

31) A.P. Abbott and D.J. Schiffrin, *J. Chem. Soc. Faraday Trans.*, 1990, **86**, 1453

32) W.R. Fawcett, M. Fedurco and M. Opallo, *J. Phys. Chem.*, 1992, **96**, 9959

33) A.P. Abbott and J.C. Harper, *J. Chem. Soc., Faraday Trans.*, 1996, **92**, 3895

34) C.H. Hamann, A. Hamnett and W. Vielstich, *Electrochemistry*, Wiley-VCH, New York, 1997

35) D. Niehaus, M.E. Philips, A.C. Michael and R.M. Wightman, *J. Phys. Chem.*, 1989, **93**, 6232

36) A.J. Bard and L.R. Faulkner, *Electrochemical Methods*, Wiley, New York, 1980

37) W.R. Fawcett, M. Fedurco and M.Opallo, *J. Phys. Chem.*, 1992, **96**, 9959

38) M.E. Philips, M.R. Deakin, M.V. Novotny and R.M. Wightman, *J. Phys. Chem.*, 1987, **91**, 3934

CHAPTER V

ELECTROCHEMICAL REDUCTION OF CARBON DIOXIDE IN SUPERCRITICAL FLUIDS

5.1 Introduction
- 5.1.1 Electrochemical Reduction of CO_2
- 5.1.2 Mechanism of CO_2 reduction
- 5.1.3 Reduction of CO_2 at Elevated Temperatures and Pressures

5.2 Results and Discussion
- 5.2.1. Voltammetry
- 5.2.2 Bulk electrolysis of supercritical CO_2/H_2O mixtures

5.3 Conclusions

5.1 Introduction

The many thousands of compounds produced worldwide are derived from a few very basic raw materials, the source of carbon being almost exclusively from fossil fuels. The limited reserves of crude oil and coal has necessitated increased scientific efforts to discover alternative sources of carbon. Carbon dioxide is one of the major waste products from industrial processes and therefore is found in large quantities in the environment. It was estimated that anthropogenic CO_2 emissions in the year 1989 exceeded 7×10^9 tons [1] and even with the emission guidelines agreed at the World Summit for the Environment in 1997, this figure is estimated to rise by a 15% annually by the year 2015.[2] If an efficient and cheap means could be found, the reduction of CO_2 offers a rich source of carbon for the production of industrial feedstocks.

5.1.1 Electrochemical Reduction of CO_2

Carbon Dioxide is a thermodynamically stable compound with an enthalpy of formation of –396kJ mol^{-1}.[3] It is recognised that the most difficult step of the reduction process is the activation of the molecule itself. This can be achieved either by reaction with inorganic and organometallic catalysts[4-13] or via electrochemical methods. The latter of these processes has been extensively studied over the past century in aqueous and non-aqueous electrolyte solutions at cathodes made of various materials.[14] The most common reactions are:

$$CO_2 + H^+ + 2e^- \longrightarrow HCOO^- \qquad (5.1.1)$$

$$CO_2 + 2H^+ + 2e^- \longrightarrow CO + H_2O \qquad (5.1.2)$$

$$CO_2 + 6H^+ + 6e^- \longrightarrow CH_3OH + H_2O \qquad (5.1.3)$$

$$CO_2 + 8H^+ + 8e^- \longrightarrow CH_4 + 2H_2O \qquad (5.1.4)$$

$$2CO_2 + 2e^- \longrightarrow (COO^-)_2 \qquad (5.1.5)$$

The reaction products often comprise of a mixture of various substances and the reduction of CO_2 in aqueous media at cathodic potentials invariably results in the evolution of hydrogen.[14] Therefore it is necessary to describe the reaction selectivity in terms of the faradaic yield for each of the above processes.

Faradaic yields and the distribution of the reaction products depend upon the nature of the cathode used and the reaction conditions employed. In aqueous solutions the majority of organic products have a single carbon atom (C_1 products). Metal electrodes used in this medium are grouped into categories depending on the nature of the major reaction product:

Group I (Hg, Pb, Sn) :	$HCOO^-$ formed,
Group II (Au, Ag, Zn) :	CO formed,
Group III (Cu, Mo) :	CH_3OH, CH_4 etc. formed,
Group IV (Ni, Fe, Al) :	CO_2 does not reduce.

This classification is somewhat misleading as alternative reaction products may form on the same cathode material under a different set of conditions.

Much of the recent work carried out in aqueous media has concentrated on those materials that have a high hydrogen overpotential. These include zinc alloys, tin, mercury and lead electrodes.[15-20] The major reaction product at ambient temperature and pressure is formate with small amounts of CO detected. Bandi *et. al.* obtained yields of formate in excess of 80%,[21-23] however, the rate of conversion and efficiencies of the processes were generally poor. Formate is perhaps the least desirable of C_1 products because its

separation from the reaction mixture is a labour consuming process and its value as a feedstock is low.

The concurrent production of hydrogen in the reduction of CO_2 can be minimised in two ways:

(i) in aqueous solutions by employing metals with large hydrogen overpotentials

(ii) by employing non-aqueous solvents.

The latter approach was first adopted by Haynes and Sawyer [24] who studied the reduction process at Au and Hg in dimethylsulphoxide (DMSO). On both of these materials at the potentials employed (-2.0 V vs NHE) CO and formate were the major products. It was proposed that the distribution of reaction products was closely linked to the amount of water present in the solvent. There have been reports that high yields of oxalate can be obtained on both Hg and stainless steel particularly at lower overpotentials. This has created a great deal of interest because it provides a potentially cheap source of C_2 products. This work was further confirmed by Gressin *et.al.* [16] who demonstrated that yields of oxalate in excess of 80% could be obtained in dimethylformamide (DMF) and DMSO. Ikeda *et.al.* [15] studied the selectivity of reduction products in both aqueous and non-aqueous media at lead and indium electrodes and found that oxalate was the major product at lead electrodes in propylene carbonate. A careful series of additions of water were added to the reaction mixture and a reduction in the amount of oxalate was observed. This was coupled with a subsequent increase in the amount of formate obtained and this has been attributed to a change in reaction pathway.

Christensen *et al.* have reported that oxalate formed on a modified platinum surface in acetonitrile.[25] The consumption of CO_2 was monitored during the reaction and it was found that the conversion of the gas to oxalate was approximately 90%.

5.1.2 Mechanism of CO_2 reduction.

The conditions and solvent employed greatly affect the reaction pathway of the reduction process. Therefore, considerable attention has been given to elucidate the mechanism of CO_2 reduction. Much of the initial work was performed by Haynes and Sawyer [24] who employed controlled potential coulometry and galvanostatic methods to study the reaction at Au and Hg in DMSO. A series of chronopotentiometric experiments were recorded at different CO_2 concentrations. The net cathodic current I_c is given by:

$$I_c = nFAk_c[CO_2]_0 \qquad (5.1.5)$$

which can be written:

$$I_c = nFA[CO_2]_0 k^0 \exp(-\beta n_c f[E - E_0]) \qquad (5.1.6)$$

where n is the number of electrons, β is the transfer coefficient, f = F/RT, k^0 is the heterogeneous rate constant and n_c is the number of electrons in the rate determining step. In order to determine the concentration of CO_2 at the electrode surface, the authors used the concept of the transition time, τ. This is the time taken for the concentration of the species to fall to zero at the electrode surface and is marked by a rapid change in the potential of the working electrode. The change of potential is often quite large and hence τ can be measured with a high degree of precision. By incorporating the transition time into equation (5.1.6) it can be shown that:

$$I_c = nFA[CO_2^*]k^0(1-[t/\tau^{1/2}])\exp(-\beta n_c f[E - E^0]) \qquad (5.1.7)$$

where $[CO_2^*]$ is the concentration of the bulk solution and t is the time from the start of the experiment. The authors were then able to calculate βn_c and k^0 from a series of plots. The value of βn_c obtained from the various experiments on the different metal surfaces were close to 0.5 and they proposed that the first step, the formation of the anion radical, was rate limiting. This observation was supported by the work of Aylmer-Kelly [26] *et al.* and Lamy [27] *et al.*

The main product of the reaction in aprotic media was oxalate and based upon this fact Aylmer-Kelly *et al.* postulated two possible reaction mechanisms:

$$CO_2 + e^- \longrightarrow CO_2^{\bullet -}{}_{ads} \quad (5.1.8)$$

$$2CO_2^{\bullet -}{}_{ads} \longrightarrow C_2O_4^{2-} \quad (5.1.9)$$

and:

$$CO_2^{\bullet -} + CO_2 \longrightarrow {}^-O_2C\text{-}CO_2^{\bullet} \quad (5.1.10)$$

$${}^-O_2C\text{-}CO_2^{\bullet} + e^- \longrightarrow C_2O_4^{2-} \quad (5.1.11)$$

The reaction (5.1.9) is second order in $CO_2^{\bullet -}$ while (5.1.11) is first order with respect to the radical anion. The authors found evidence that suggested the solution coupling reaction (5.1.11) was the most probable mechanism. Gressin and colleagues were able to expand on these findings and produced a reaction scheme which is now widely accepted. Fig. (5.1.1) shows a summary of the processes involved during the electrochemical reduction of CO_2 in aprotic media.

5.1.3 Reduction of CO_2 at Elevated Temperatures and Pressures

The poor solubility of CO_2 in aqueous media at 25°C (0.033 mol dm^{-3})[18] has limited the efficiency of the reduction process and it is generally recognised that it is necessary to increase the mass transport of CO_2 to the electrode surface. It has been proposed that a large partial pressure of CO_2 should make it possible to increase the mass transfer owing to an increase in solubility of CO_2 in the electrolyte solution. Ito *et al.* reported the effects of increasing the pressure on the electrochemical reduction of CO_2 using Zn, In, Pb and

Figure (5.1.1) Mechanism of the reduction of CO_2 in aprotic media

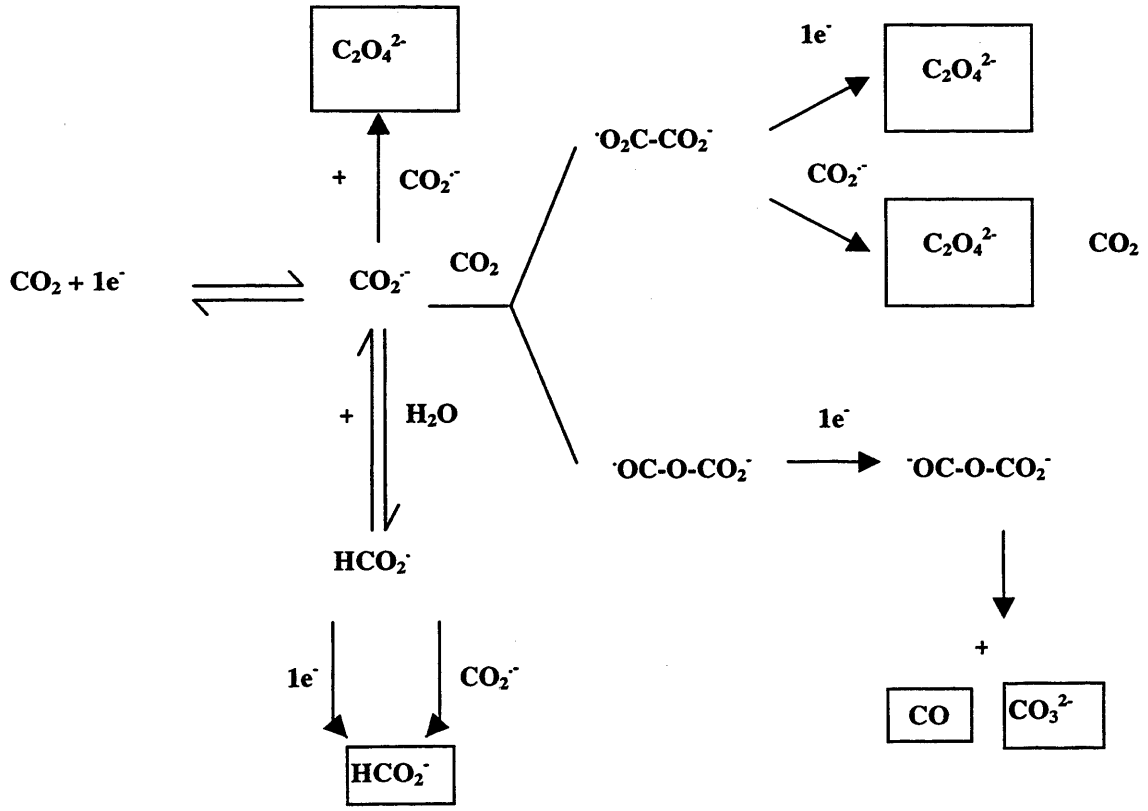

Sn electrodes whose hydrogen overpotential is large.[19] They showed that the Faradaic efficiency and the current density were increased by increasing the pressure to 20 atm. Various authors have since shown that CO_2 was reduced with fairly high Faradaic efficiencies (16-62%) under high pressures (50-60 atm) of CO_2 on Group VI metals (Fe, Co, Ni, Pd, Pt), on which CO_2 does not reduce at 1 atm.[20,21] The main products of the reaction were formate and carbon monoxide with small quantities of C_4 products detected.

The concurrent production of hydrogen during the reduction of CO_2 in aqueous media has limited the product distribution to formate and CO. Several groups have proposed that supercritical CO_2 offers a potentially more selective means of obtaining C_2 products. Recent work has been carried out to reduce CO_2 in the supercritical state using Ru, Mn and Rh complexes and relatively high yields have been achieved.[22-24] Bandi *et al.* have carried out work in liquid CO_2 at 60 bar and 50° C using Pd-Fe alloy electrodes. The only product obtained was CO, however no attempts were made to analyse the electrolyte.

The work presented here is an investigation into the catalytic properties of Pt and Pb in the reduction of CO_2 in the supercritical state. The advantages of carrying out such a process in $scCO_2$ is that transport to and from the electrode surface is rapid and gaseous reactants are miscible in all proportions. Product distributions and efficiencies are presented at two electrode surfaces with varying water content. This is the first such study of the electrochemical reduction of CO_2 in the supercritical state.

5.2Results and Discussion

5.2.1 Voltammetry

Figure (5.2.1) shows current potential curves obtained at a Pt electrode (0.1cm diameter) in 0.1 mol dm^{-3} $TBABF_4$ aqueous solution under 1, 60 and 200 atm CO_2. The onset potential for the cathodic current shifts more negatively under increasing CO_2 pressure compared with that observed for the current under 1 atm CO_2. Such a negative shift has also been observed on metals such as Ni, Co and Pd.[28-30] This significant shift in potential is believed to be caused by the adsorption of intermediates (e.g. adsorbed CO formed on the electrode surface by the reduction of CO_2) and has been reported by Enyo and co-workers.[31]

Hara *et. al.*[32] carried out studies on Rh and Ag electrodes in aqueous solutions. They observed that although the total cathodic current was independent of the pressure, the partial current density for CO_2 reduction increased substantially as a function of CO_2 concentration (pressure). It was proposed that the enhancement of CO_2 reduction is accompanied by the suppression of hydrogen evolution from the reduction of water. It was shown that under a pressure of 30 atm. with a Pt electrode, the faradaic efficiency for the reduction of CO_2 was approximately 50% compared to trace amounts formed under 1 atm. Therefore at high pressures, the suppression of hydrogen evolution results in a change in product selectivity.

Figure (5.2.2) shows the current-potential curve at a Pt microelectrode (10μm) at various pressures of CO_2. Comparison of the potential at which reduction occurs in the supercritical and liquid states at a Pt electrode at the same pressure shows that the potential has shifted positively in $scCO_2$ by almost 1V. This suggests that the mechanism in $scCO_2$ / H_2O mixtures is different to that of carbon dioxide in water mixtures. Ito[29] and

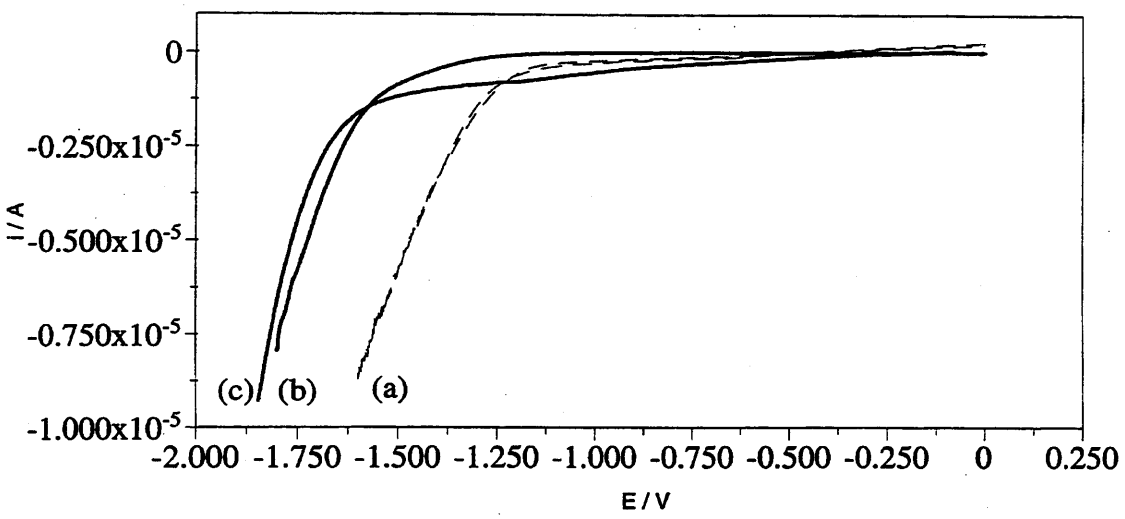

Figure (5.2.1) Current potential characteristics of the electrochemical reduction of CO_2 at a Pt electrode in water at 70° C containing 0.1 Mol $TBABF_4$ under (a) 1 atm, (b) 60 atm and (c) 200 atm. Scan rate = 10 mV s^{-1}

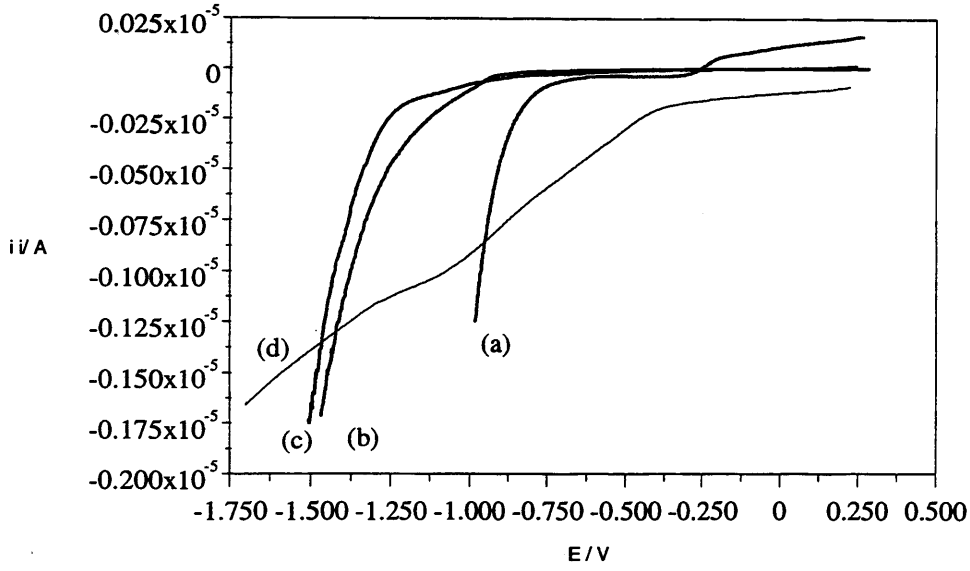

Figure (5.2.2) Current potential characteristics of the electrochemical reduction of CO_2 at Pt microelectrodes (d) at 120 bar and 70° C containing 0.1 Mol $TBABF_4$ and 0.5M H_2O. Also shown is the reduction process under 1 atm pressure (a), 60atm (b) and 200 atm(c) in water at a Pt microelectrode. Scan rate = 10mV s^{-1}.

co-workers observed a similar response in aqueous media on a Zn electrode at a pressure of 30 atm. They suggested that the substantial positive shift of the cathodic current was due to an increase in the concentration of CO_2 in solution. An additional explanation is that there is a change in mechanism of the reduction process in $scCO_2$. It is known that in aqueous systems on Pt surfaces, the reduction of CO_2 occurs by the virtue of the interaction with adsorbed carbon dioxide with adsorbed hydrogen.[34] This reaction will only proceed if the centres of the two adsorbed species are adjacent and the rate of the process is governed by θ_H and θ_{CO2}, where θ_H and θ_{CO2} are the fractional surface coverage of H_{ads} and CO_{2ads} respectively. The chemisorption of H_{ads} on Pt is favourable and the interaction of CO_2 with Pt is weak. Therefore under ambient conditions, the electrode is almost completely covered with a layer of hydrogen atoms and hence this precludes the reduction of CO_2. At high pressures of CO_2 it is known that CO_2 adsorbs on Pt and hence the reduction process proceeds. In the supercritical system, the voltammograms suggest that at low overpotentials, the formation of H_2 is favoured, and conversely at high overpotentials, CO_2 reduction proceeds. It has also been noted that at ambient pressures, the electrode is poisoned by the adsorption of CO. A change in the reaction mechanism could preclude this step and hence make CO2 reduction easier.

Figure (5.2.3) shows the voltammogram of $scCO_2$ / water at 120 bar at Pt and Pb microelectrodes. As can clearly be seen, there is a significant difference in the potential of the cathodic wave on Pb compared to Pt. This must be due to a difference in the mechanism of the two processes.

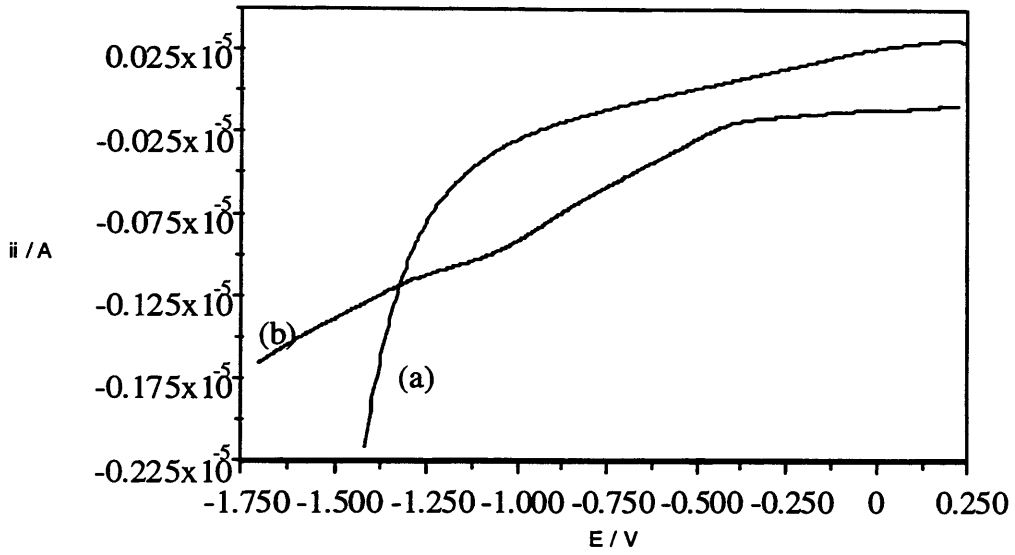

Figure (5.2.3) Current potential characteristics of the electrochemical reduction of CO_2 at Pt (b) and Pb (a) microelectrodes at 120 bar and 70° C containing 0.1 Mol $TBABF_4$ and 0.5M H_2O. Scan rate = 10mV s^{-1}.

5.2.2 Bulk Electrolysis in Supercritical Carbon Dioxide / Water Mixtures

The results of the electrolysis experiments are shown in Table 5.2.1.

Electrode	Pressure /atm	Water content	Faradaic Efficiency/%			
			CO	HCOOH	CH_4	HC_2O_4H
$Pt^{(a)}$	**120**	**0.5M**	**tr**	**28.8**	**tr**	**-**
$Pt^{(b)}$	**120**	**0.1M**	**tr**	**22.1**	**tr**	**-**
$Pb^{(a)}$	**120**	**0.5M**	**tr**	**-**	**tr**	**15.6**

Table (5.2.1) Key: tr; trace
a: constant potential –4V
b: galvanostatic control (10μA cm^{-2} - 1μA cm^{-2})

It is assumed that the remaining current was used for the production of hydrogen. The detection of hydrogen was not possible because of the permeability of the sample bags. From the voltammetric responses in $scCO_2$/water mixtures, we have assumed that the majority of product for all three processes was hydrogen. This is in accordance with other work.[15] The first point to note is that there is clearly a change in mechanism when Pt is replaced by a Pb electrode. Ikeda *et al.*[15] reported that in nonaqueous media on Pb electrodes the following mechanism occurred,

$$2CO_2 + 2e^- \longrightarrow 2CO_2^{\cdot-} \longrightarrow (COO)_2^{2-} \qquad (5.2.1)$$

It was also reported that as the water content increased, the quantity of oxalate produced decreased dramatically and the formation of formate increased according to the following reaction.

$$CO_2^{\cdot-}{}_{ads} + H_2O \longrightarrow HCOO^- + OH^- \qquad (5.2.2)$$

In the present studies no formate was formed and it is as yet unclear why the conditions of the experiment prevent the formation of the salt. Vassiliev *et al.*[35] proposed that on Pb electrodes, adsorbed CO_2 molecules participate in reaction (5.2.1),

$$CO_2^{\cdot-}{}_{ads} + CO_{2ads} \xrightarrow{k_1} (CO_2)_2^{\cdot-}{}_{ads} \qquad (5.2.3)$$

$$(CO_2)_2^{\cdot-}{}_{ads} + e^- \xrightarrow{k_2} (CO_2)_2^{2-} \qquad (5.2.4)$$

where $k_1 >> k_2$. Under such extreme pressures, the concentration of CO_2 in the region of the electrode would be expected to be significantly greater than that of water and reaction (5.2.2) would be less favourable.

Comparison of the two results at a Pt electrode show that as the water content decreases, the production of formate decreases and that of hydrogen increases. It should be noted that the conditions employed were different between the two experiments. It has been shown that the mechanism and product distribution is greatly affected by the current density.[36-38] Hara *et al.*[39] illustrated that under galvanostatic control, the production of hydrogen could be significantly enhanced by the application of high current densities. The absence of CO from the reduction products obtained using Pt further confirms the idea that there is a change in mechanism from the reduction in aqueous solutions.

5.3 Conclusions

We have demonstrated for the first time that CO_2 can be electrochemically reduced in the supercritical state and that mass transport is enhanced in this media. It has been shown that the reduction potential shifts significantly positive under supercritical conditions and

this has been ascribed to the increase in CO_2 concentration at the electrode and that CO does not poison the electrode surface. This is further validated by the bulk electrolysis analysis where only trace amounts of CO were detected.

The nature of the electrode material affects the reaction mechanism and we have shown that formate is the major product on Pt and oxalate on Pb. It has been proposed that at high pressures, the reaction of water with the radical anion is precluded and hence formate does not form on Pb electrodes in $scCO_2/H_2O$ mixtures. The efficiencies of the reduction of CO_2 are similar to those reported in the literature but the process kinetics are probably greatly enhanced due to the increased rate of mass transport in the supercritical state.

REFERENCES CHAPTER V

1) W. Leitner, Angew. *Chem. Int. Ed. Engl.*, 1995, **34**, 2207

2) New Scientist, Nov. 1997, No. 2106, 5

3) Physical Chemistry 5th Edt., P.W. Atkins, Oxford University Press, Oxford, 1995

4) M.M. Ali, H. Sato, T. Mizukawa, K. Tsuge, M. Hagi and K. Tanake, *Chem. Commun.*, 1998, 249

5) M. Hirano, T. Akano, T. Imai and K. Kuroda, *Energy Convers. Mgmt.*, 1995, **36**, 585

6) A.F. Cherashev and A.P. Khruscch, *Russian Journal of Electrochemistry*, 1997, **33**, 196

7) H. Tanaka and A. Aramata, *J. Electroanal. Chem.*, 1997, **437**, 29

8) Y. Kohno, T. Tanaka, T. Funabiki and S. Yoshida, *Chem. Lett*, 1997, 993

9) F. Saladin and I. Alxneit, *J. Chem. Soc. Faraday Trans.*, 1997, **93**(23), 4159

10) Y. Chen, K. Tomishige and K. Fujimoto, *Chem. Lett*, 1997, 999

11) C. Caix, S.C. Noblat and A. Deronzier, *J. Electroanal. Chem.*, 1997, **434**, 163

12) K. Tanaka, *Bull. Chem. Soc. Jpn.*, 1998, **71**, 17

13) S. Yanagida, M. Kanemoto, K. Ishihara, Y. Wada, T. Sakata and H. Mori, *Bull. Chem. Soc. Jpn.*, 1997, **70**, 2063

14) V.S. Bagotzky and N.V. Osetrova, *Russian Journal of Electrochemistry*, 1995, **31**(5), 453

15) S. Ikeda, T. Takagi and K. Ito, *Bull. Chem. Soc. Jpn.*, 1987, **60**, 2517

16) J.C. Gressin, D. Michelet, L. Nadjo and J.M. Saveant, *Nouveau Journal de Chemie*, 1979, **3**(8-9), 545

17) Y. Hori, K. Kikuchi, A. Murata and S. Suzuki, *Chem. Lett.*, 1985, 1695

18) Y. Hori, K. Kikuchi, A. Murata and S. Suzuki, *Chem. Lett.*, 1986, 897

19) P.G. Rusell, N. Kovac, S. Srinivasan and M. Steinberg, *J. Electrochemical Soc.*, 1977, **124**, 1329

20) A.F. Cherashev and A.P. Khrushch, *Russian Journal of Electrochemistry*, 1997, **33**(2), 181

21) A. Bandi. *J. Electrochem. Soc.*, 1990, **137**, 2157

22) A. Bandi. *J. Electrochem. Soc.*, 1991, **141**, 1342

23) A. Bandi, M. Specht, T. Weimer and K. Schaber, *Energy Convers. Mgmt.*, 1995, **36**(6-9), 899

24) L.V. Haynes and D.T. Sawyer, *Anal. Chem.*, 1967, **39**, 332

25) P.A. Christensen and S.J. Higgins, *J. Electroanal. Chem.*, 1995, **387**, 127

26) A.W. Aylmer-Kelly, A. Bewick, P.R. Cantrill and A.M. Tuxford, *Faraday Disc. Chem. Soc.*, 1974, **56**, 96

27) E. Lamy, L. Nadjo and J.M Saveant, *J. Electroanal. Chem.*, 1977, **78**, 403

28) A. Kudo, S. Nakagawa, A. Tsuneto and T. Sakata, *J. Electrochem. Soc.*, 1993, **140**(6), 1541

29) K. Ito, S. Ikeda and M. Okabe, *Denki Kagaku*, 1980, **48**, 247

30) K. Ito, S. Ikeda and M. Okabe, *Denki Kagaku*, 1981, **49**,106

31) S. Taguchi, A. Aramata and M. Enyo, *J. Electroanal. Chem.*, 1994, **372**, 161

32) K. Hara, A. Kudo and T. Sakata, *J. Electroanal. Chem.*, 1995, **386**,

33) O. Krocher, R.A. Koppel and A. Baiker, *Chem. Commun.*, 1996, 1497

34) Y.B. Vasiliev, V.S. Bagotsky, O.A. Khazova and N.A. Mayorova, *J. Electroanal. Chem.*, 1985, **189**, 311

35) Y.B. Vasiliev, V.S. Bagotsky, O.A. Khazova and N.A. Mayorova, *J. Electroanal. Chem.*, 1985, **189**, 295

36) Y. Hori, A. Murata and R. Takahashi, *J. Chem. Soc. Faraday Trans.*, 1989, 85, 2309

37) Y. Hori and A. Murata, *Electrochim. Acta.*, 1990, **35**, 1777

38) Y. Hori, A. Murata and R. Takahashi, *J. Chem. Soc. Faraday Trans.*, 1991, **87**, 127

39) K. Hara, A. Kudo and T. Sakata, *J. Electroanal. Chem.*, 1995, **391**, 141

CHAPTER VI

SUMMARY AND FUTURE WORK

6.1 Summary
- 6.1.1 Conductivity
- 6.1.2 Double Layer Structure and Electrochemistry
- 6.1.3 Electrochemical Reduction of Carbon Dioxide

6.2 Future work
- 6.2.1 Electrical Double Layer and Electrochemistry
- 6.2.2 Electrolysis

6.1 Summary

This work has shown that novel electrolytes can be synthesised which are highly soluble in extremely non-polar media such as cyclohexane and supercritical carbon dioxide. The conductivity of a range of electrolytes has been quantified in a range of solvents. The effect of these electrolytes on electron transfer of standard redox species has been measured and these results have been reasoned by characterising the double layer properties.

Electrochemical reduction of CO_2 in the supercritical phase has also been demonstrated for the first time.

6.1.1 Conductivity

It has been shown that novel tetraalkylammonium electrolytes are soluble in cyclohexane and supercritical carbon dioxide ($scCO_2$). Conductivity measurements in these media have shown that the ions are highly associated forming penetrated ion pairs and higher ion aggregates. This has been confirmed by NMR and X-Ray crystallographic measurements. Minimum energy calculations have found that the quaternary ammonium cations are planar in structure, rather than tetrahedral, allowing an unexpectedly small distance of closest approach in both the solid and solution states.

The conductivity of the electrolytes can be significantly affected by fluorination or chlorination of the tetraphenylborate anion. The solutions are highly structured and this is reflected in the marked increase in the viscosity of the pure solvent by the addition of small amounts of the electrolytes.

It has been demonstrated for the first time that conducting solutions in unmodified $scCO_2$ can be achieved and the molar conductivities are an order of magnitude greater

than those in liquid media with similar dielectric properties. This is due to the low viscosity of the supercritical fluid.

6.1.2 Double Layer Structure and Electrochemistry

The results from the capacitance measurements in the non-polar media employed suggested that specific adsorption of ions occurred in all of the solution/electrolyte systems studied. Capacitance humps were observed at potentials negative of the pzc for $TBABF_4$ and TBATPhB in anisole and dichloroethane. These were ascribed to the adsorption of a cation. It was also shown that at these potentials, inclusion of an anion occurred and this was confirmed by altering the direction of the potential sweep.

The length of the carbon chain on the tetraalkylammonium cation had a significant effect on the capacitance-potential curves. It was demonstrated that as the chain length increased from C_4 to C_{10}, the humps negative of the pzc disappeared. This suggested that the desorption/adsorption of an ion is extremely slow in such non-polar media. This was further confirmed by measuring the capacitance as a function of time at the potential at which the hump occurred. It was found that the capacitance reached a maximum after approximately 25 mins. thus confirming the slow process kinetics.

The double layer structure of a supercritical fluid/electrode interface was measured for the first time and the capacitance potential curve showed that the electrode was completely covered by a layer of electrolyte. The magnitude of the capacitance at potentials positive of the pzc were markedly smaller than those observed in cyclohexane.

Voltammetric measurements in dichloroethane proved that the nature of the electrolyte significantly affected the reversibility of a process. As the length of the tetraalkylammonium chain on the cation was increased from C_4 to C_{12}, the reduction

processes of TCNQ became more irreversible. This was further proof that the desorption of the novel electrolytes is a slow process.

It has been shown for the first time that electron transfer is possible in non-polar media such as cyclohexane and supercritical carbon dioxide. However, it was only possible to observe a response at very slow sweep rates for a charged electroactive species. The electroactive species competes for electron transfer sites with the electrolyte and as the desorption process is slow, voltammograms can only be recorded at sweep rates $\nu < 2$ mVs^{-1}. The electrochemical responses in $scCO_2$ were significantly different than those observed in other non-polar media. This was ascribed to the extremely slow desorption of electrolyte from the surface of the electrode.

6.1.3 Electrochemical Reduction of Carbon Dioxide

The electrochemical reduction of CO_2 in the supercritical phase was performed at 120 bar and 70°C and it was shown that the nature of the reduction products depended upon the electrode material employed. Formate and hydrogen were primarily formed on a Pt electrode. The voltammograms of the reduction in $scCO_2$/water mixtures showed that the onset of the cathodic potential was approximately 1V positive of that observed in aqueous media. It was proposed that there is a change in mechanism of the reduction process between supercritical-water emulsions and high pressure aqueous systems.

Oxalate and hydrogen were the main products on a Pb surface and this has been observed in other non-aqueous media.

6.2 Future Work

6.2.1 Electrical Double Layer and Electrochemistry

Previous experiments have shown that the adsorption/desorption of an electrolyte/electrode surface can be measured using the electrochemical quartz crystal microbalance (EQCM). However, the adhesives used to bond the electrode to the quartz crystal are chemically unstable in media such as cyclohexane. If a mechanical means could be found to overcome this problem, the mass potential curves obtained would allow the calculation of an adsorption isotherm. From this, information regarding the nature of interactions can be elucidated.

Future work involving supercritical carbon dioxide would require the addition of polar modifying solvents. The ideal co-solvent should be polar and electrochemically stable. Potential candidates include hydrofluorocarbon solvents such as HFC 134A. These are chemically stable solvents and it has been shown in this laboratory that they are extremely resistant to oxidation and reduction.

6.2.2 Electrolysis

In aprotic media on lead electrodes, the reaction product is usually oxalate and the efficiency of the process is high. Supercritical carbon dioxide is an extremely non-polar medium and it is necessary to modify it with polar solvents such as water. It would be advantageous to avoid protic modifying solvents as these can affect the reaction pathway. It has been shown that an inert solvent HFC 134A can be made sufficiently conducting by the addition of tetraalkylammonium electrolytes. Supercritical CO_2/HFC 134A mixtures potentially offer an excellent reaction medium because it is more polar than unmodified $scCO_2$ and is an aprotic medium. Therefore

the products of an electrolysis experiment would not include unwanted material such as hydrogen and water.

APPENDIX

Table 1 Crystal data

Formula	$C_{64}H_{104}BN$
M_r	898.29
Temperature/K	190
Crystal system	Triclinic
Space group	P1
A/*A*	10.157 (4)
B/*A*	11.387 (5)
C/*A*	27.943 (11)
α/degrees	82.47 (1)
β/degrees	82.74 (1)
γ/degrees	67.40 (1)
U/A^3	2948 (2)
Z	2
ρ_{calc}/g cm^{-3}	1.012
μ/mm^{-1}	0.056
crystal size/mm	0.72 × 0.37 × 0.06
Data collection diffractometer	Siemens P4
Radiation	Mo
λ/*A*	0.71073
$2\theta_{max}$/degrees	45
reflections collected	8066
independent reflections	7308
R_{int}	0.0641
Structure refinement	
$R_1[F > 4\sigma(F)]$	0.0996
wR_2[all data]	0.3061
S	0.982
Parameters refined	595
$\Delta\rho_{max}$; $\Delta\rho_{min}$/e A^{-3}	0.317; -0.363

NMR Data

^{1}H NMR of TDATPhB

ortho-H (δ 7.92), *meta*-H (δ 7.27), *para*-H (δ 7.09), 1-CH_2 (δ 1.83), 2-CH_2 (δ 0.88), 3-CH_2 (δ 0.98), 4-CH_2 (δ 1.21), 5-CH_2 (δ 1.31), 6-9 CH_2 (δ 1.37), CH_3 (δ 0.99)

^{1}H NMR of TDDATPhB

ortho-H (δ 7.90), *meta*-H (δ 7.25), *para*-H (δ 7.08), 1-CH_2 (δ 1.80), 2-CH_2 (δ 0.88), 3-CH_2 (δ 0.99). 4-CH_2 (δ 1.21), 5-CH_2 (δ 1.31), 6-11 CH_2 (δ 1.36), CH_3 (δ 0.98)

^{1}H NMR of TDATFPhB

ortho-H (δ 7.74), *meta*-H (δ 7.03), 1-CH_2 (δ 1.96), 2-CH_2 (δ 0.87) 3-CH_2 (δ 0.95), 4-CH_2 (δ 1.18), 5-CH_2 (δ 1.28), 6-9 CH_2 (δ 1.37), CH_3 (δ 0.99)

^{1}H NMR of TDATClPhB

ortho-H (δ 7.68), *meta*-H (δ 7.29), 1-CH_2 (δ 1.99), 2-CH_2 (δ 0.89), 3-CH_2 (δ 0.96), 4-CH_2 (δ 1.19), 5-CH_2 (δ 1.29), 6-9 CH_2 (δ 1.38), CH_3 (δ 0.99)